

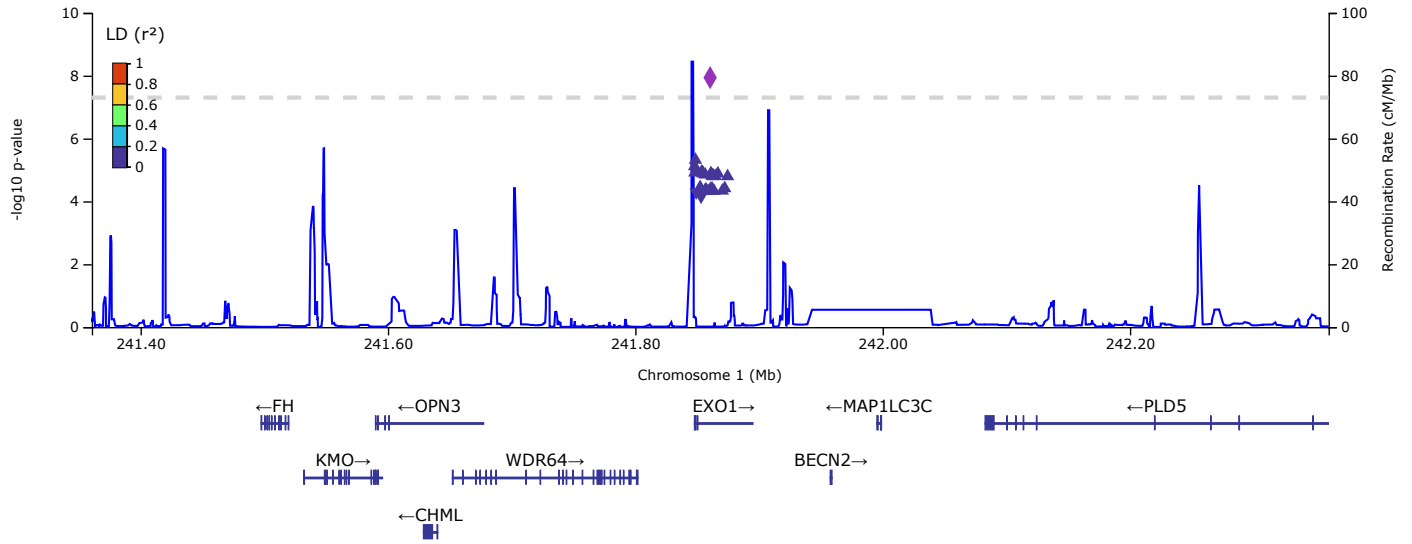
## Evidence of a causal effect of genetic tendency to gain muscle mass on uterine leiomyomata

Eeva Sliz, Jaakko Tyrmi, Nilufer Rahmioglu, Krina T. Zondervan, Christian M. Becker, FinnGen, Outi Uimari\*, Johannes Kettunen\*

### Content

|   |    |
|---|----|
| Figure S1. Regional plot of the novel UL association on chr1 near <i>EXO1</i> .....                     | 1  |
| Figure S2. Regional plot of the novel UL association on chr1 near <i>ZBTB18</i> .....                   | 2  |
| Figure S3. Regional plot of the novel UL association on chr2 near <i>MYOSLID</i> .....                  | 3  |
| Figure S4. Regional plot of the novel UL association on chr3 near <i>IGF2BP2</i> .....                  | 4  |
| Figure S5. Regional plot of the novel UL association on chr4 near <i>METAP1 (EIF4E, ADH5)</i> .....     | 5  |
| Figure S6. Regional plot of the novel UL association on chr5 near <i>HSPA4</i> .....                    | 6  |
| Figure S7. Regional plot of the novel UL association on chr6 near <i>SESN1</i> .....                    | 7  |
| Figure S8. Regional plot of the novel UL association on chr7 near <i>NT5C3A</i> .....                   | 8  |
| Figure S9. Regional plot of the novel UL association on chr7 near <i>CPED1 (WNT16)</i> .....            | 9  |
| Figure S10. Regional plot of the novel UL association on chr7 near <i>LINC-PINT</i> .....               | 10 |
| Figure S11. Regional plot of the novel UL association on chr10 near <i>SKIDA1 (DNAJC1)</i> .....        | 11 |
| Figure S12. Regional plot of the novel UL association on chr10 near <i>RNLS</i> .....                   | 12 |
| Figure S13. Regional plot of the novel UL association on chr11 near <i>ENSG00000285769</i> .....        | 13 |
| Figure S14. Regional plot of the novel UL association on chr20 near <i>CTCF/RBM38</i> .....             | 14 |
| Figure S15. Regional plot of the novel UL association on chr21 near <i>RUNX1</i> .....                  | 15 |
| Figure S16. Regional plot of the novel UL association on chr22 near <i>MYH9</i> .....                   | 16 |
| Figure S17. Regional plot of the novel UL association on chr10 near <i>KCNMA1 [META-2]</i> .....        | 17 |
| Figure S18. Regional plot of the novel UL association on chr12 near <i>NUP107 [META-2]</i> .....        | 17 |
| Figure S19. Regional plot of the association signal at 10q24.32 spanning to a 6MB region [META-2].....  | 18 |
| Figure S20. Quantile-quantile plots of the P-values.....  | 18 |
| Figure S21. Forest plot of the effect estimates of the association lead variants in the novel loci..... | 19 |
| Figure S22. <i>MYOCD</i> expression in tissues.....   | 20 |
| Figure S23. The association of rs13039273-C with <i>RBM38</i> expression.....                           | 21 |
| Figure S24. Results of MAGMA tissue expression analysis.....  | 22 |
| Figure S25. MR scatter plots: UL as outcome, other traits as exposure.....                              | 26 |
| Figure S26. MR scatter plots: UL as exposure, other traits as outcome.....                              | 30 |
| Figure S27. Funnel plots of MR causal estimates vs. their precision.....                                | 31 |
| Figure S28. Leave-one-out: exposure basal metabolic rate, outcome UL.....                               | 32 |
| Figure S29. Leave-one-out: exposure body mass index (BMI), outcome UL.....                              | 33 |
| Figure S30. Leave-one-out: exposure diastolic blood pressure, outcome UL.....                           | 34 |
| Figure S31: Leave-one-out: exposure HDL cholesterol, outcome UL.....                                    | 35 |
| Figure S32: Leave-one-out: exposure impedance of whole body, outcome UL.....                            | 36 |
| Figure S33: Leave-one-out: exposure waist circumference, outcome UL.....                                | 37 |
| Figure S34: Leave-one-out: exposure whole body fat-free mass, outcome UL.....                           | 38 |
| Figure S35: Leave-one-out: exposure whole body water mass, outcome UL.....                              | 39 |
| Table S1. Genome-wide significant ( $p < 5 \times 10^{-8}$ ) loci in META-1.....                        | 40 |
| Table S2. Genome-wide significant ( $p < 5 \times 10^{-8}$ ) loci in META-2.....                        | 41 |
| Table S3. Fine-mapping results of META-1.....   | 43 |
| Table S4. Fine-mapping results of META-2.....   | 44 |
| Table S5. Fine-mapping results of the secondary signals.....  | 45 |
| Table S6. RegulomeDB annotation of the association lead variants near <i>MYOCD</i> .....                | 46 |
| Table S7. RegulomeDB annotation of the association lead variants near <i>MYOSLID</i> .....              | 47 |
| Table S8. ChIP-seq data of rs10804157.....  | 48 |
| Table S9. RegulomeDB annotation of the association lead variants near <i>CDKN1A</i> .....               | 50 |
| Table S10. Results of MAGMA enrichment analysis.....  | 51 |
| Table S11. Genetic correlations of UL with 20 metabolic and anthropometric traits.....                  | 52 |
| Table S12. Results of the bi-directional two-sample Mendelian randomization.....                        | 53 |
| Table S13. Results of multivariable MR.....   | 57 |
| Table S14. Results of outlier-corrected MR-PRESSO.....  | 58 |
| Table S15. Results of MRMix.....  | 59 |
| References.....   | 60 |

### META-1



### META-2

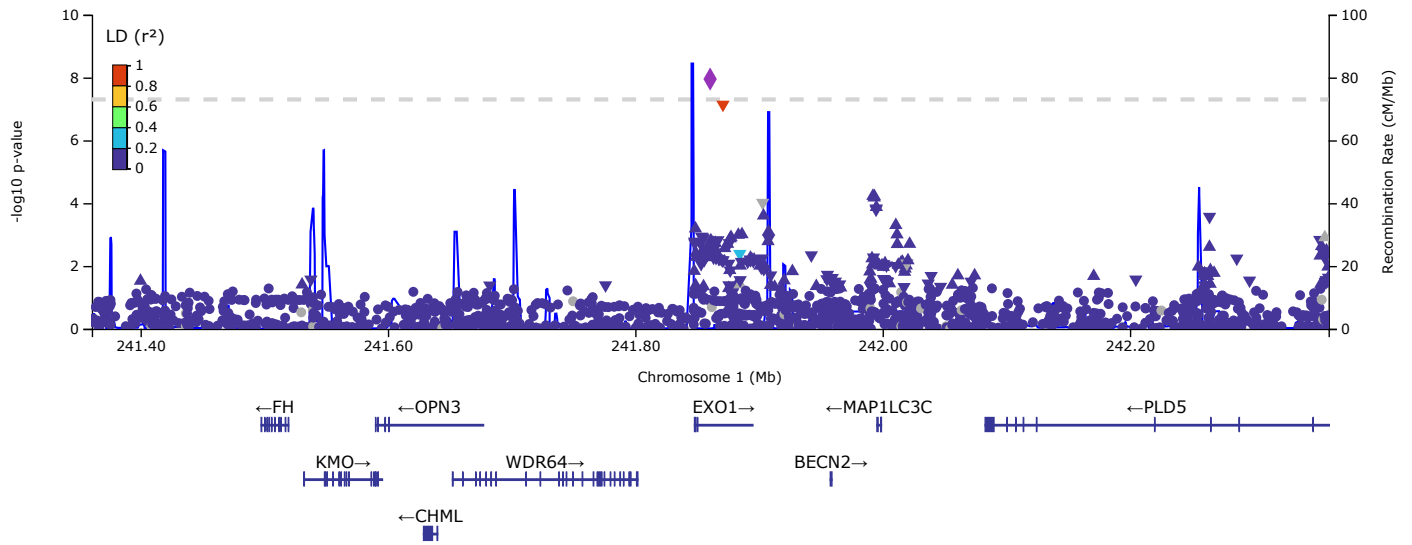
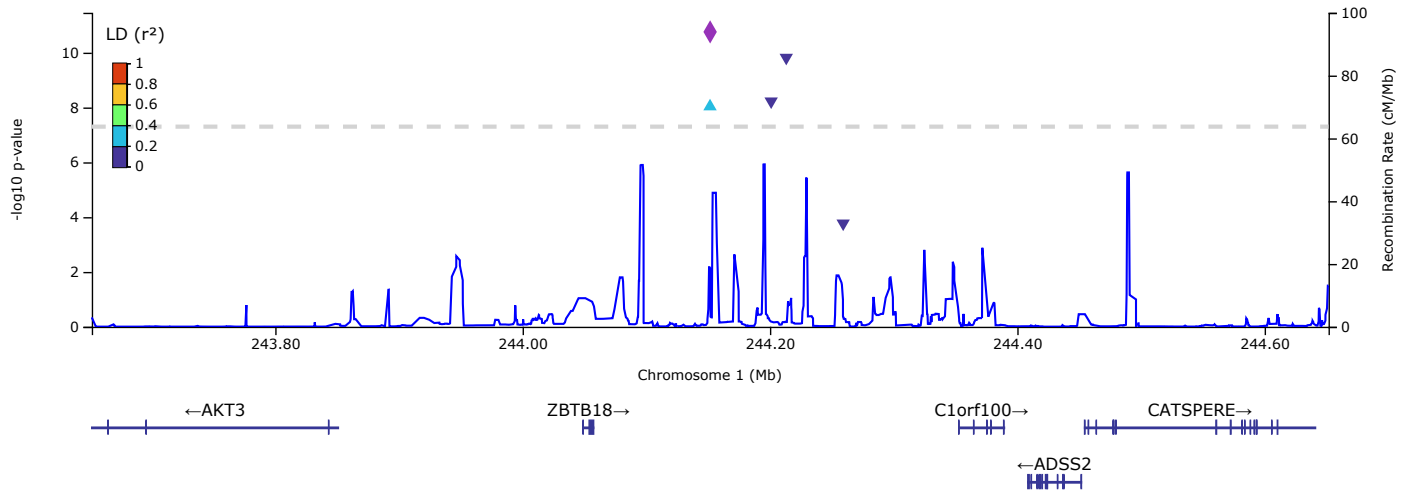


**Figure S1. Regional plot of the novel UL association on chr1 near *EXO1*.**

The plot on the top shows the result in META-1, and the plot on the bottom shows the result in META-2.

### META-1



### META-2

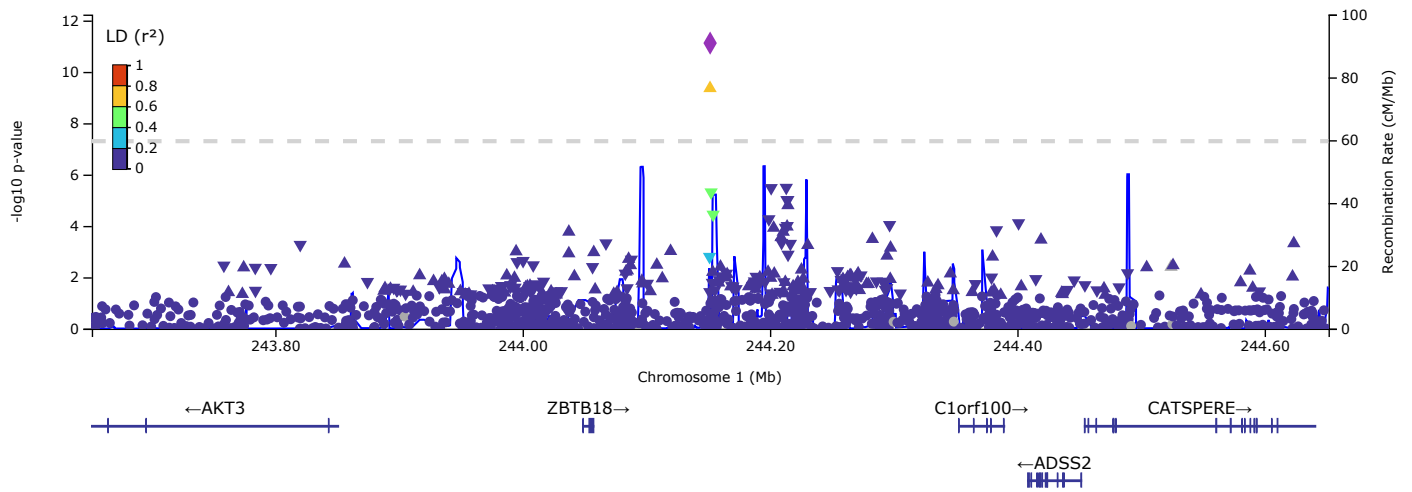
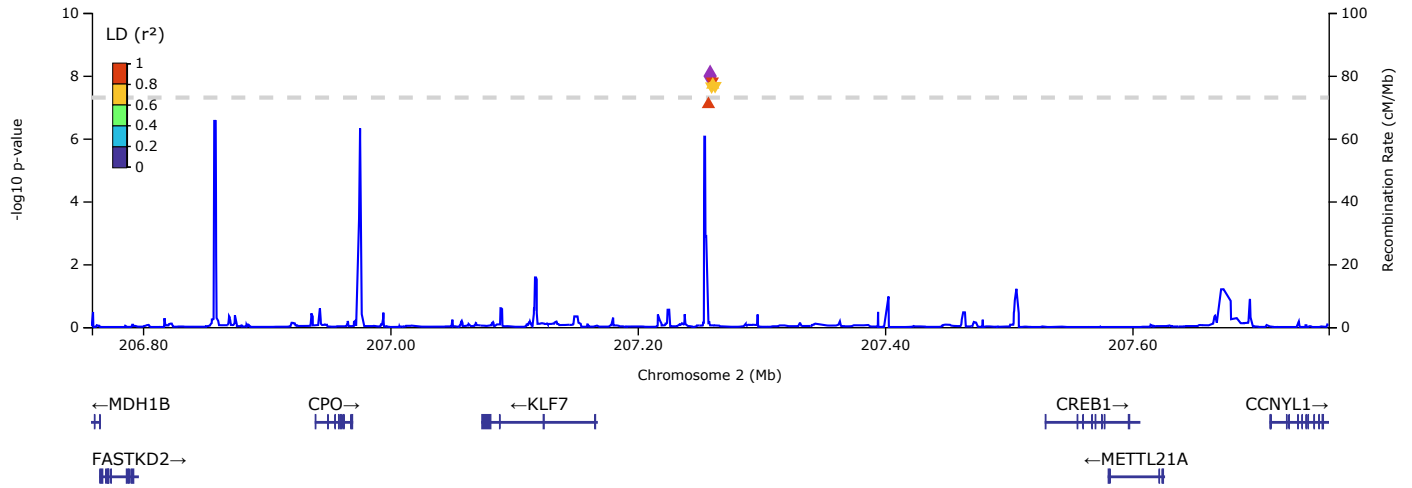


**Figure S2. Regional plot of the novel UL association on chr1 near *ZBTB18*.**

The plot on the top shows the result in META-1, and the plot on the bottom shows the result in META-2.

### META-1



### META-2

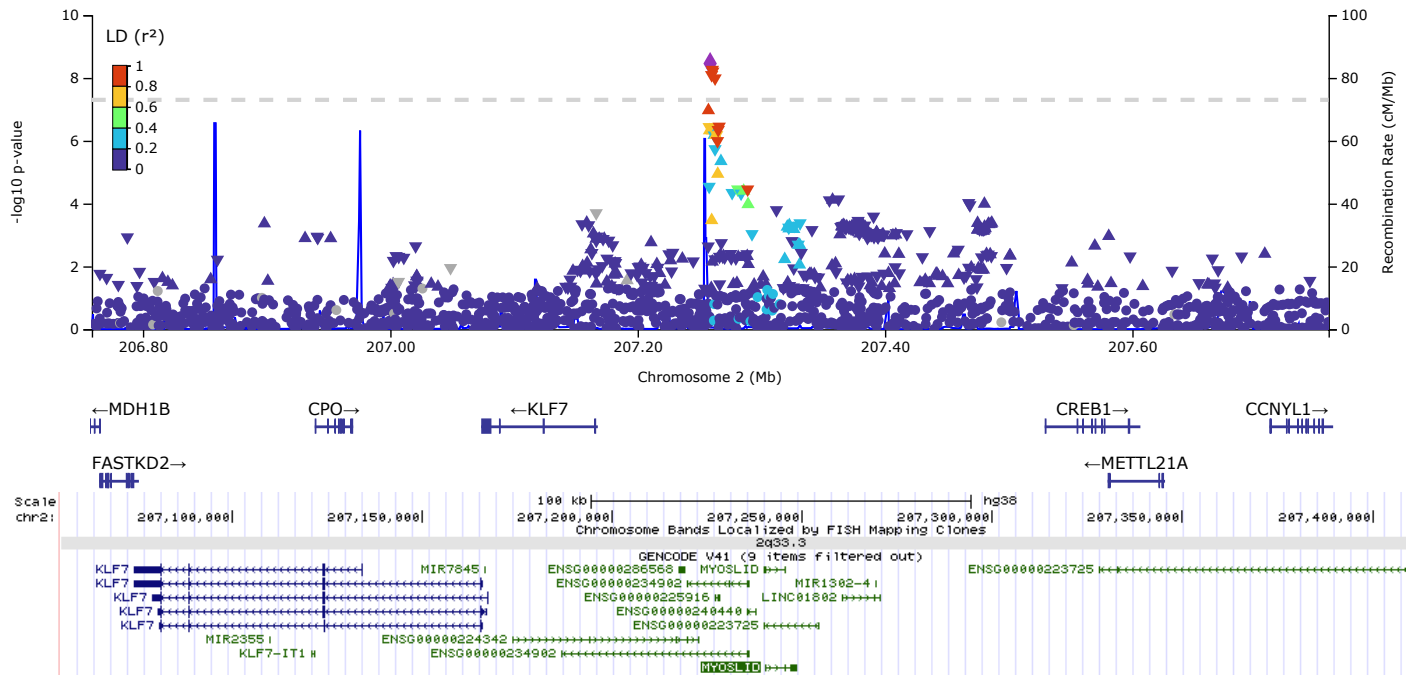
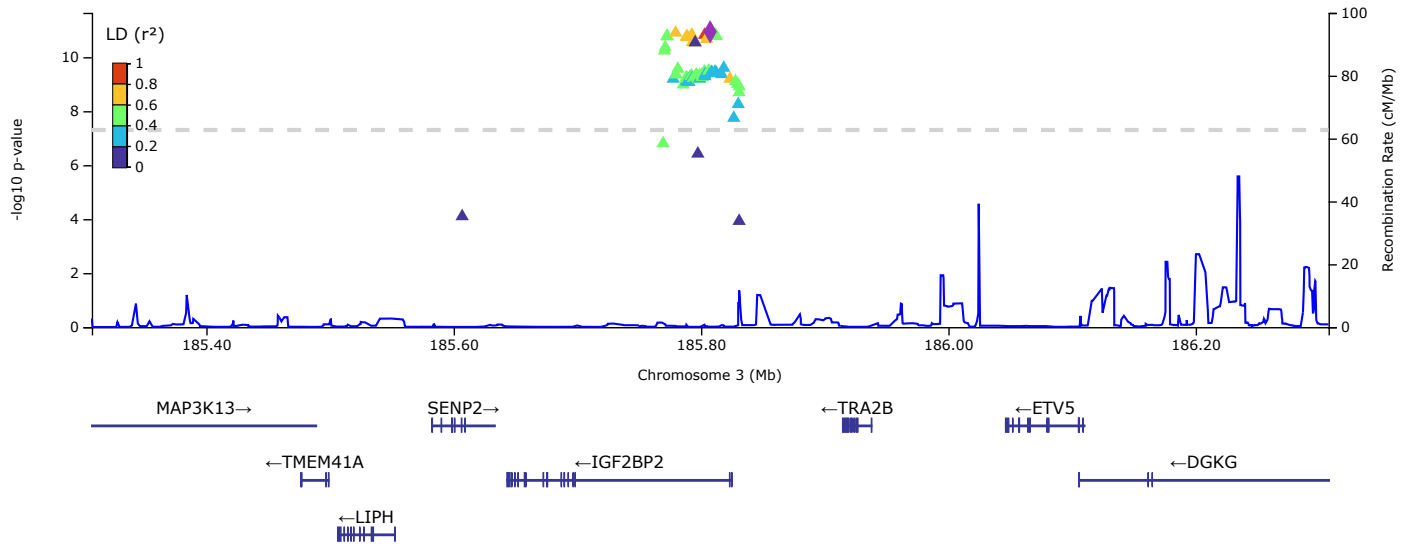


**Figure S3. Regional plot of the novel UL association on chr2 near *MYOSLID*.**

The plot on the top shows the result in META-1, and the plot in the middle shows the result in META-2. *MYOSLID* location was unavailable for LocusZoom: it locates on chr2: 207,239,811-207,245,887 which is ~78kb downstream from *KLF7*, as indicated in the image extracted from UCSC Genome Browser (bottom).

### META-1



### META-2

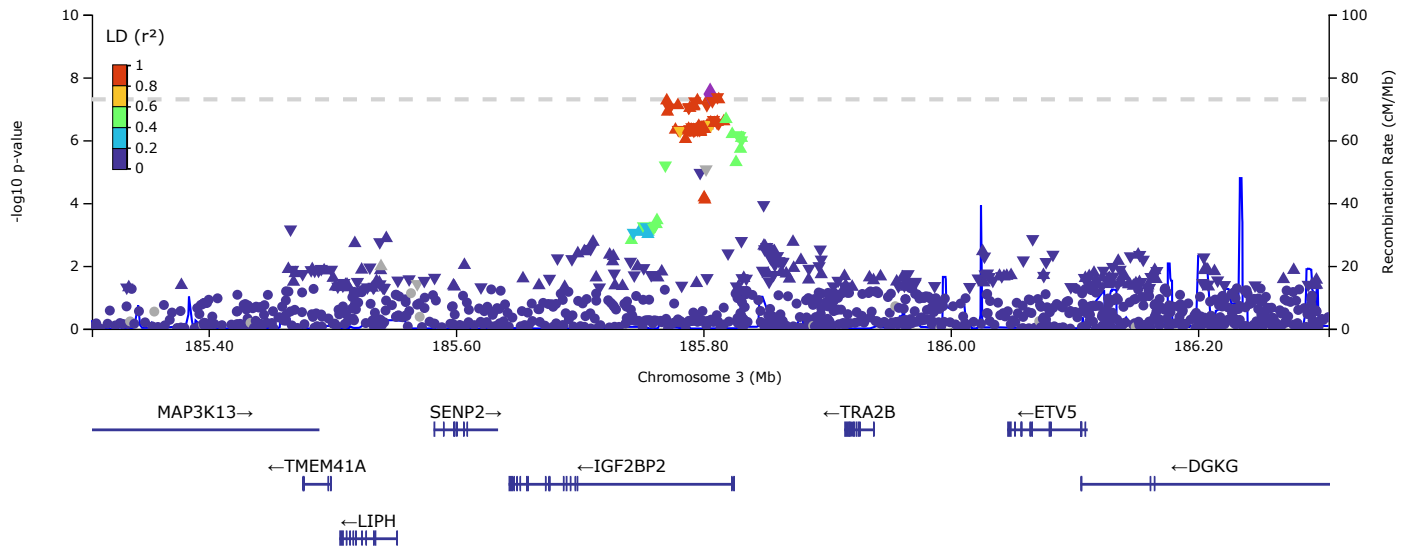
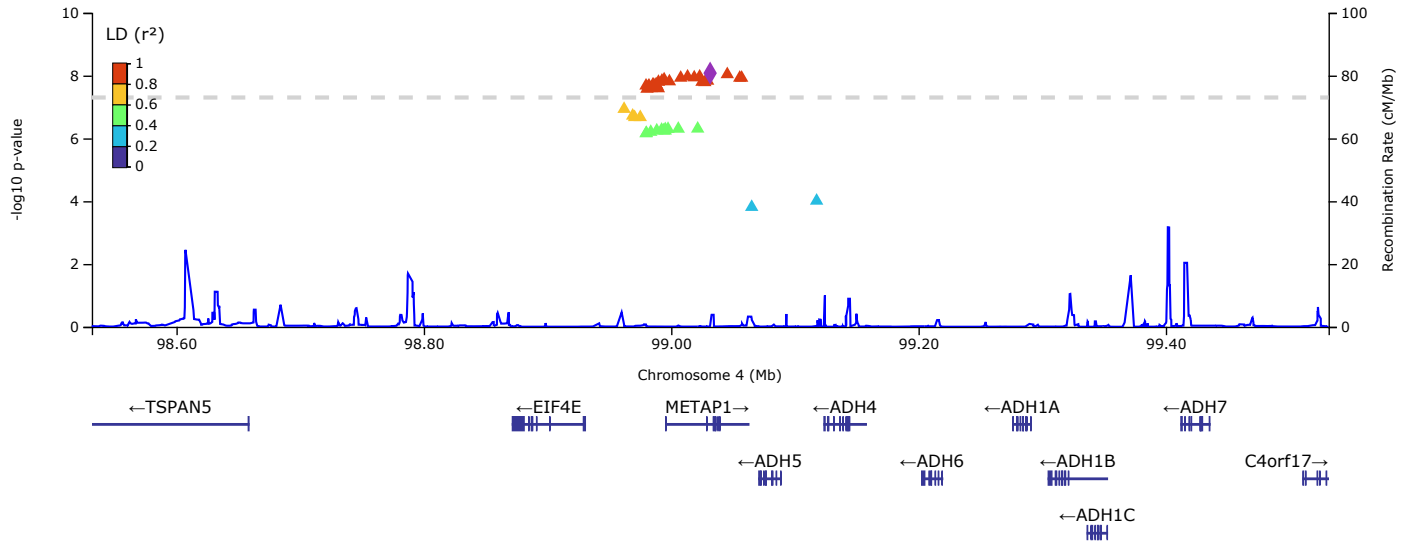


**Figure S4. Regional plot of the novel UL association on chr3 near *IGF2BP2*.**

The plot on the top shows the result in META-1, and the plot on the bottom shows the result in META-2.

### META-1



### META-2

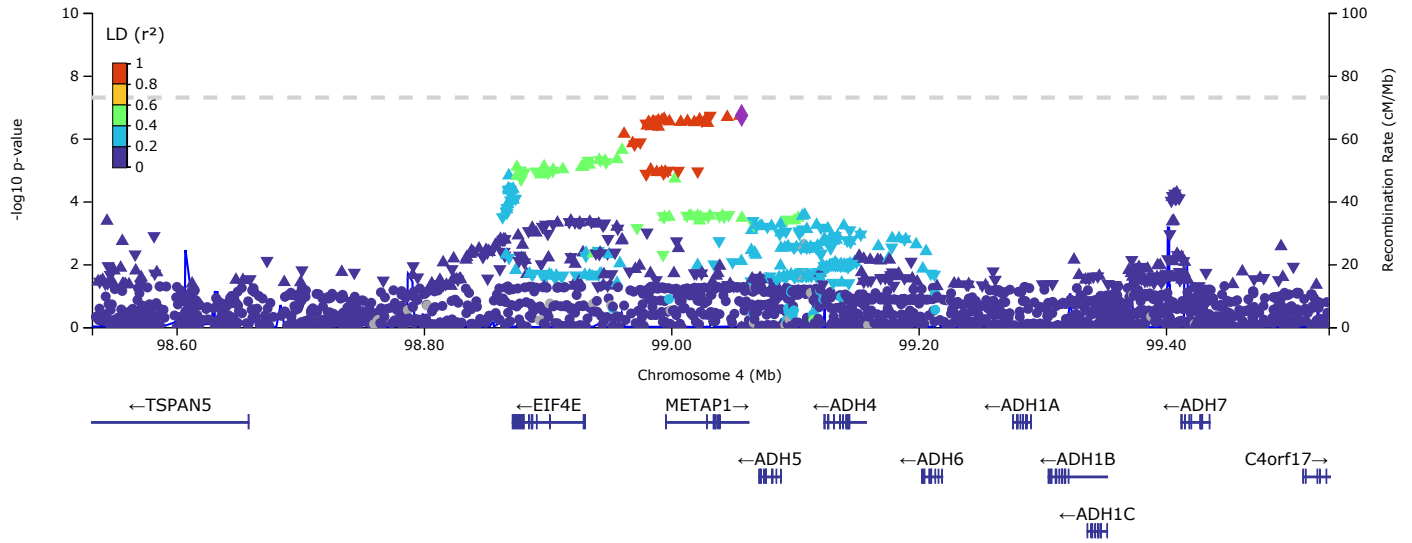
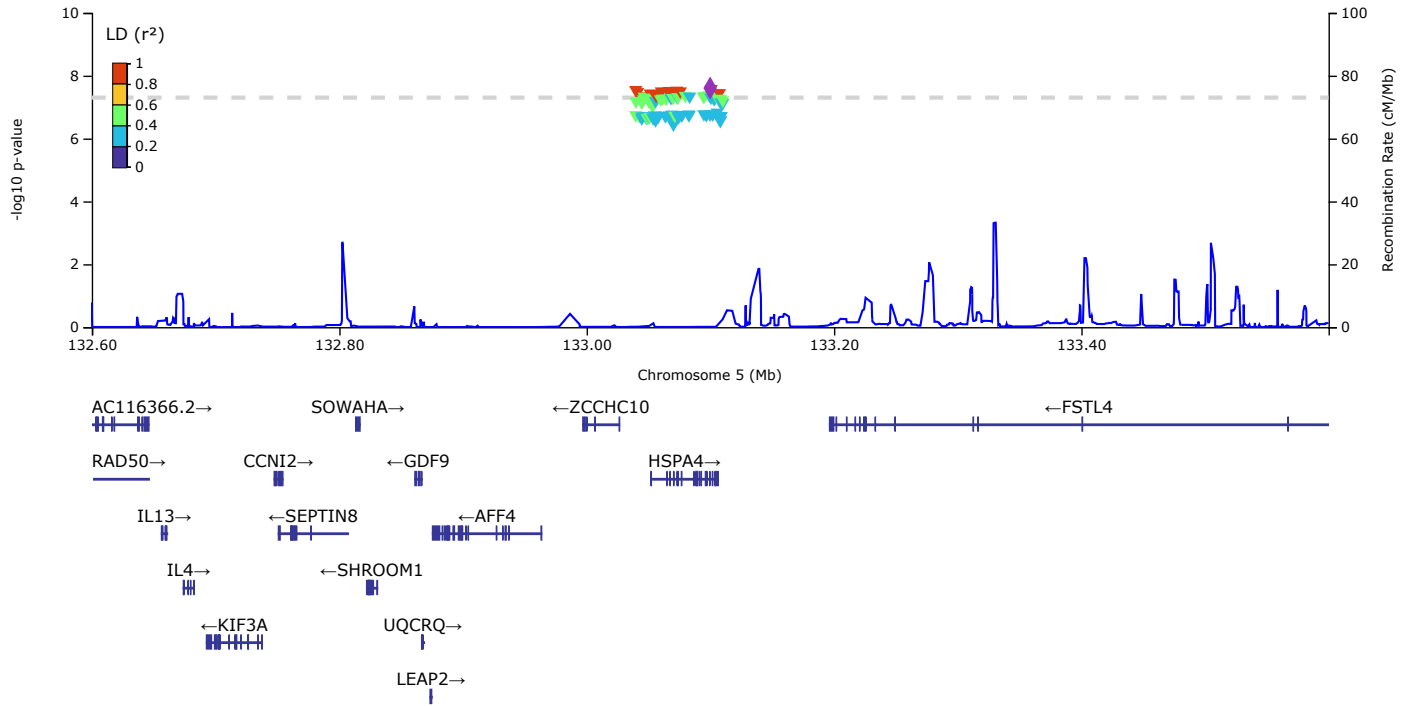


**Figure S5. Regional plot of the novel UL association on chr4 near *METAP1* (*EIF4E*, *ADH5*).** The plot on the top shows the result in META-1, and the plot on the bottom shows the result in META-2.

### META-1



### META-2

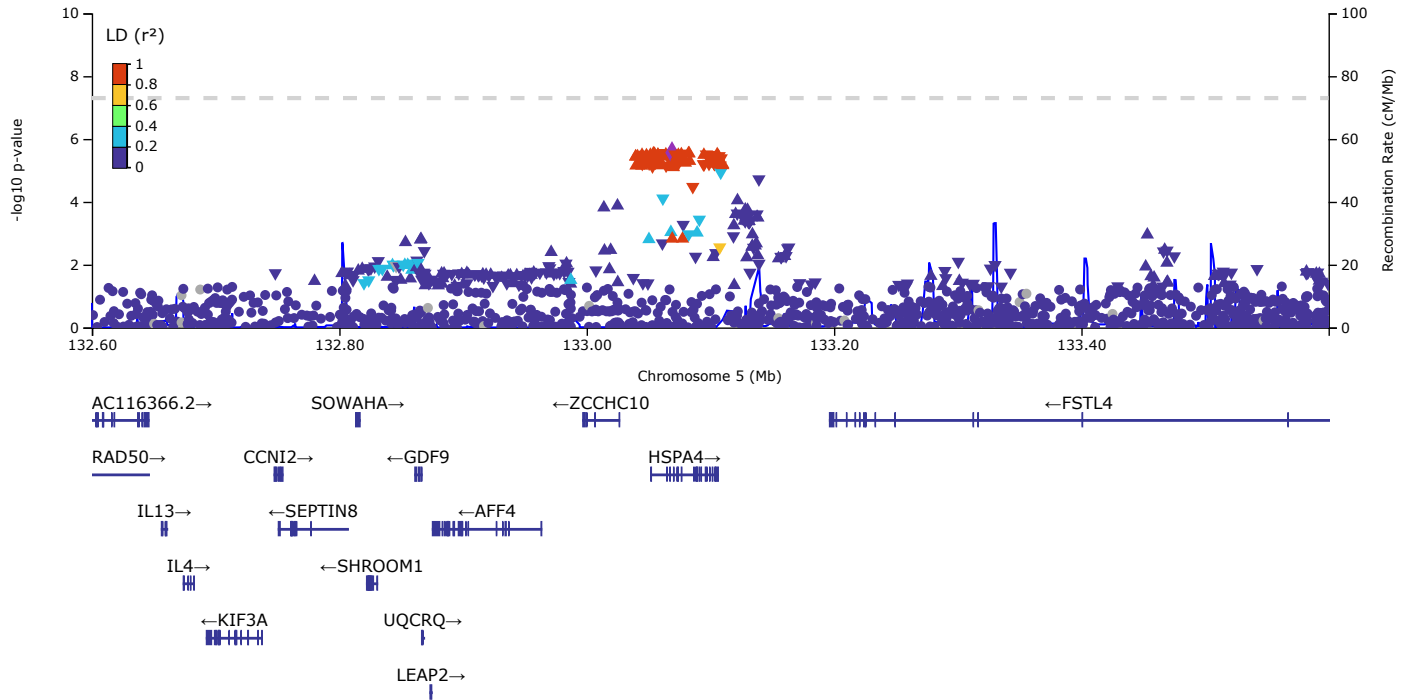
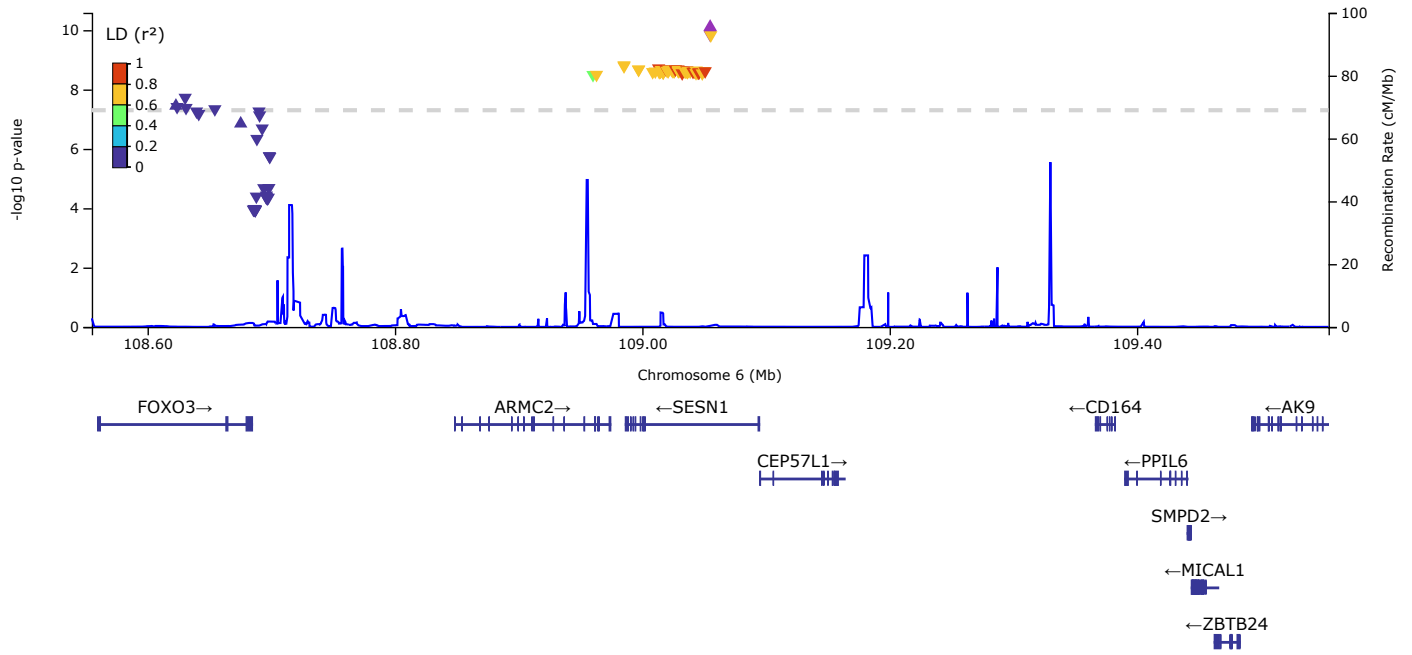


**Figure S6. Regional plot of the novel UL association on chr5 near *HSPA4*.**

The plot on the top shows the result in META-1, and the plot on the bottom shows the result in META-2.

### META-1



### META-2

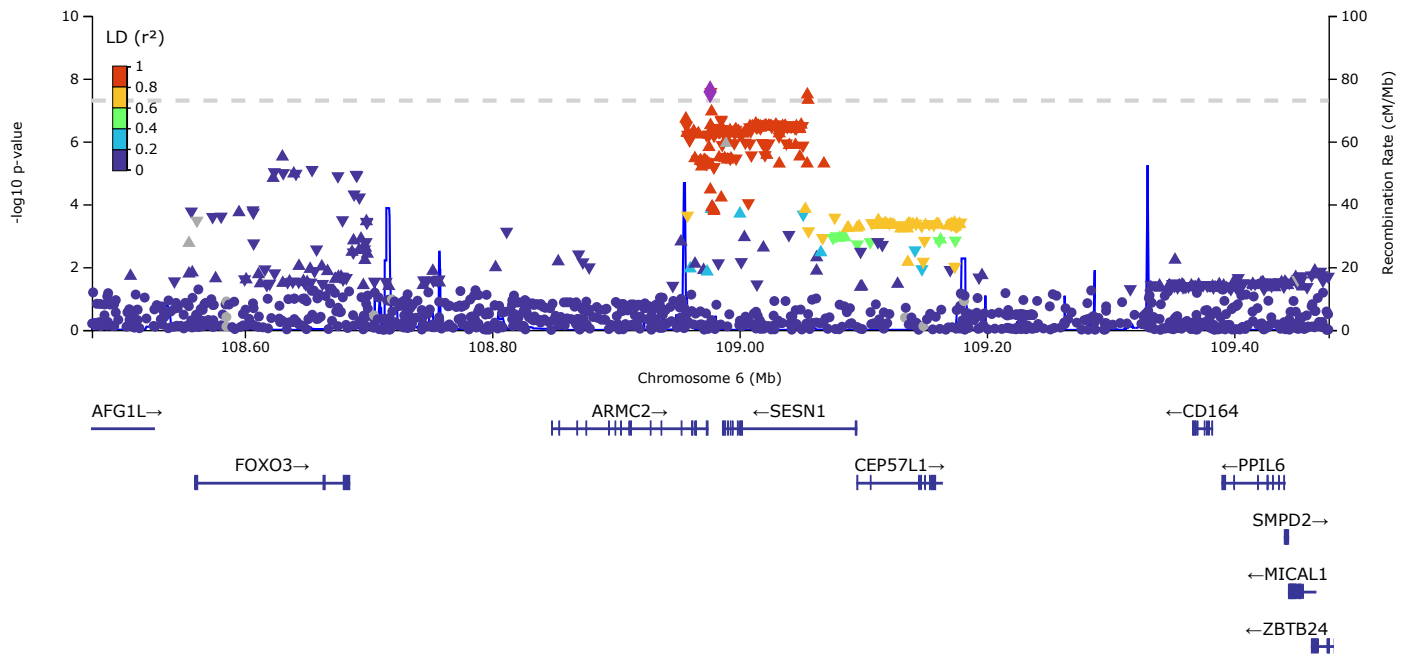
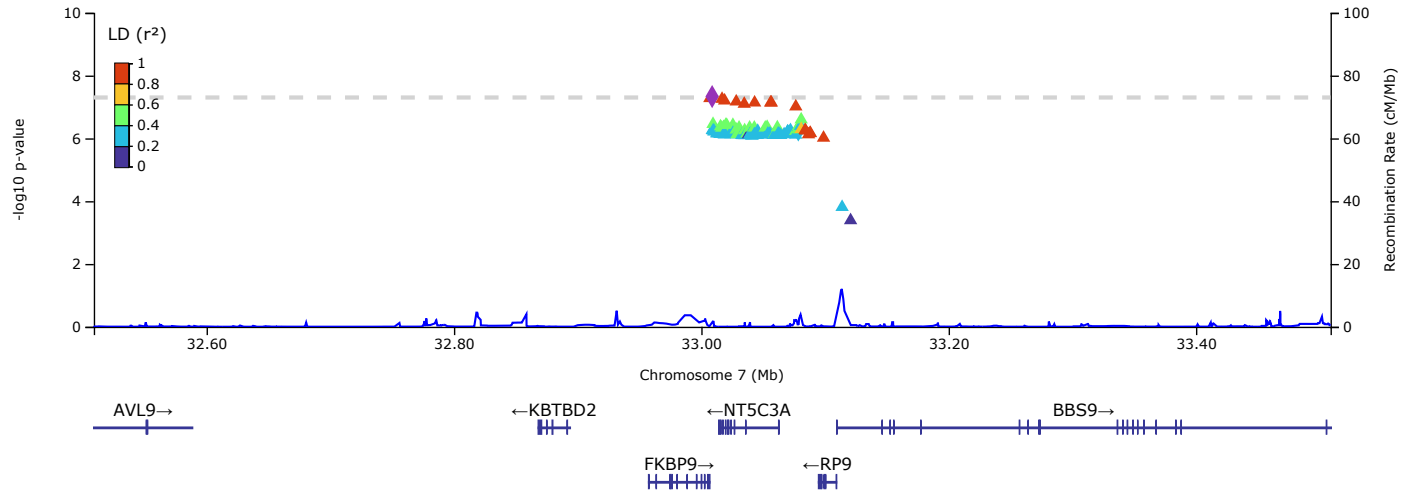


**Figure S7. Regional plot of the novel UL association on chr6 near *SESN1*.**

The plot on the top shows the result in META-1, and the plot on the bottom shows the result in META-2.



### META-1



### META-2

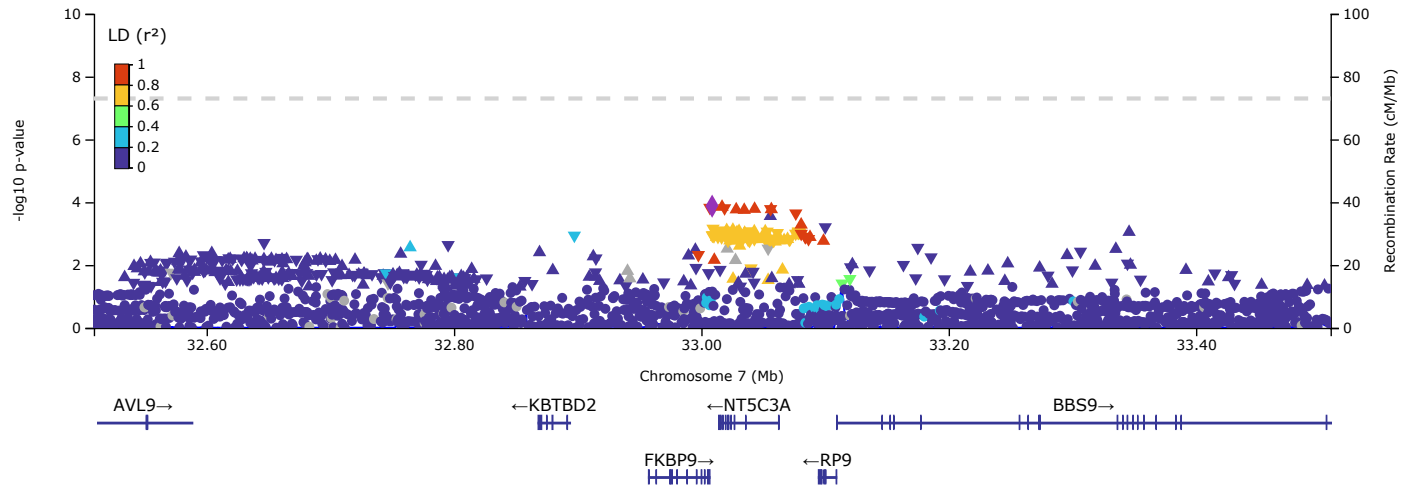
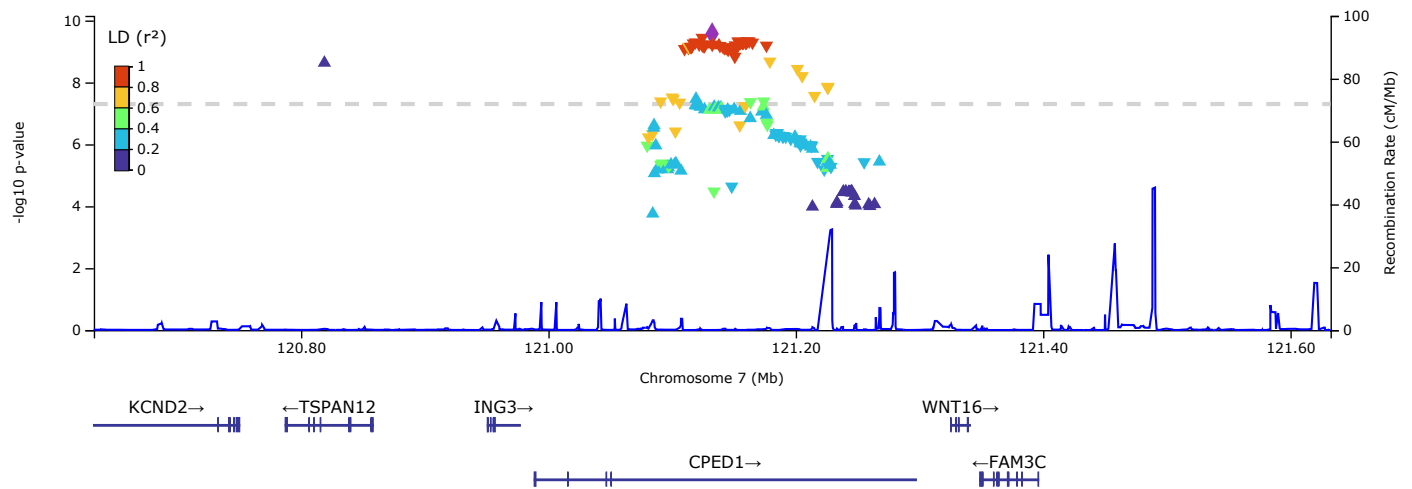


**Figure S8. Regional plot of the novel UL association on chr7 near *NT5C3A*.**

The plot on the top shows the result in META-1, and the plot on the bottom shows the result in META-2.

### META-1



### META-2

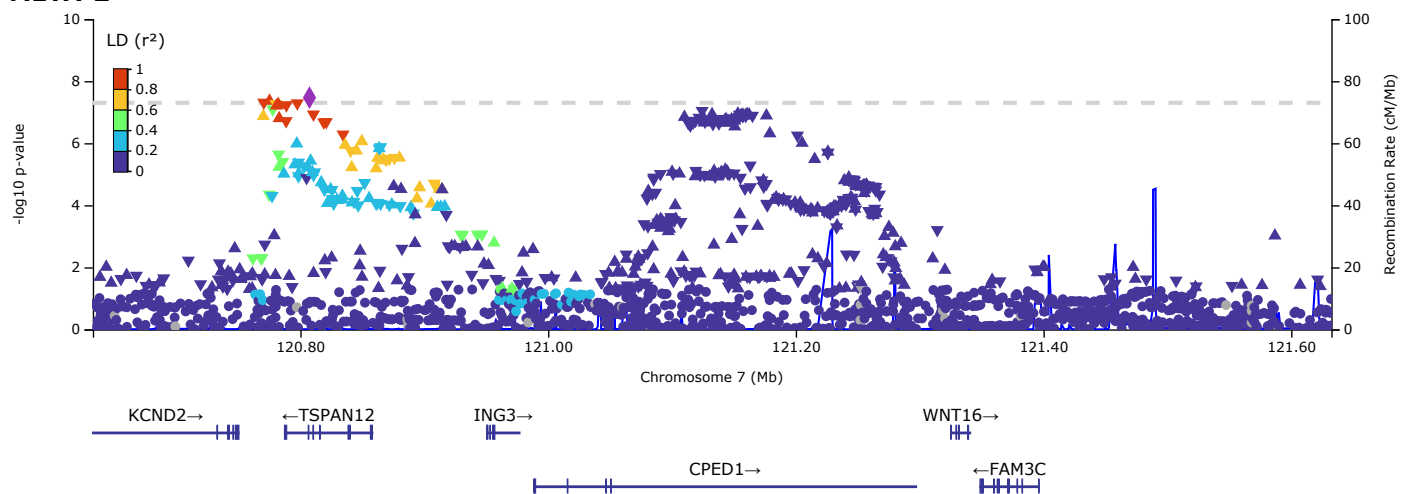
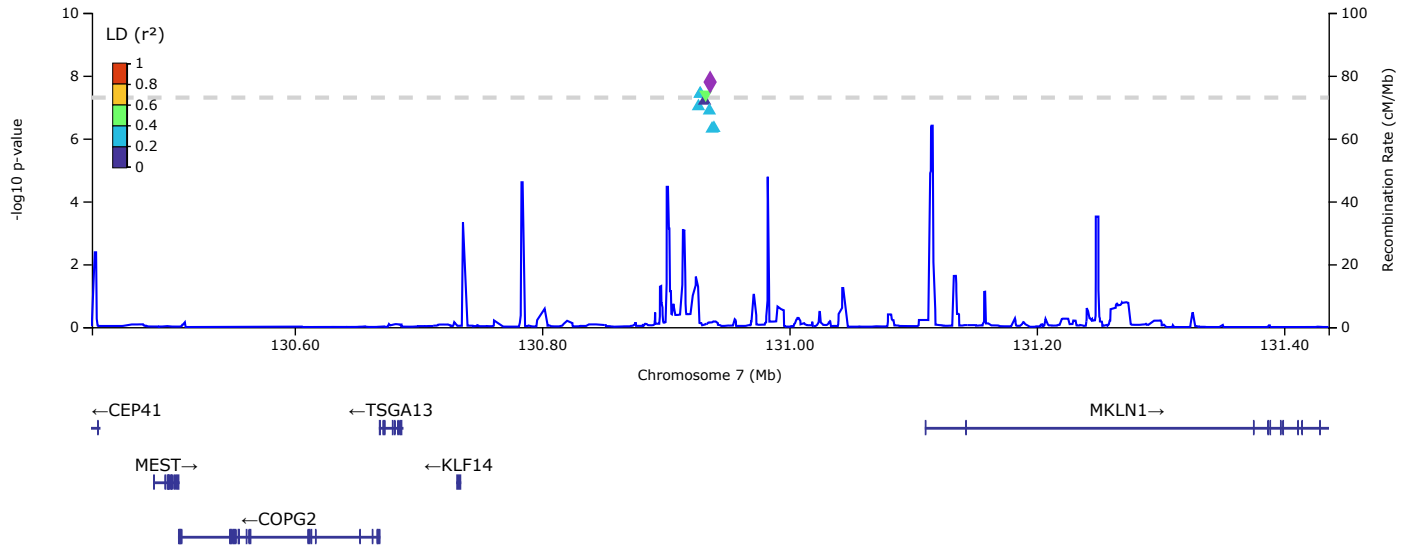


**Figure S9. Regional plot of the novel UL association on chr7 near *CPED1* (*WNT16*).**

The plot on the top shows the result in META-1, and the plot on the bottom shows the result in META-2.

### META-1



### META-2

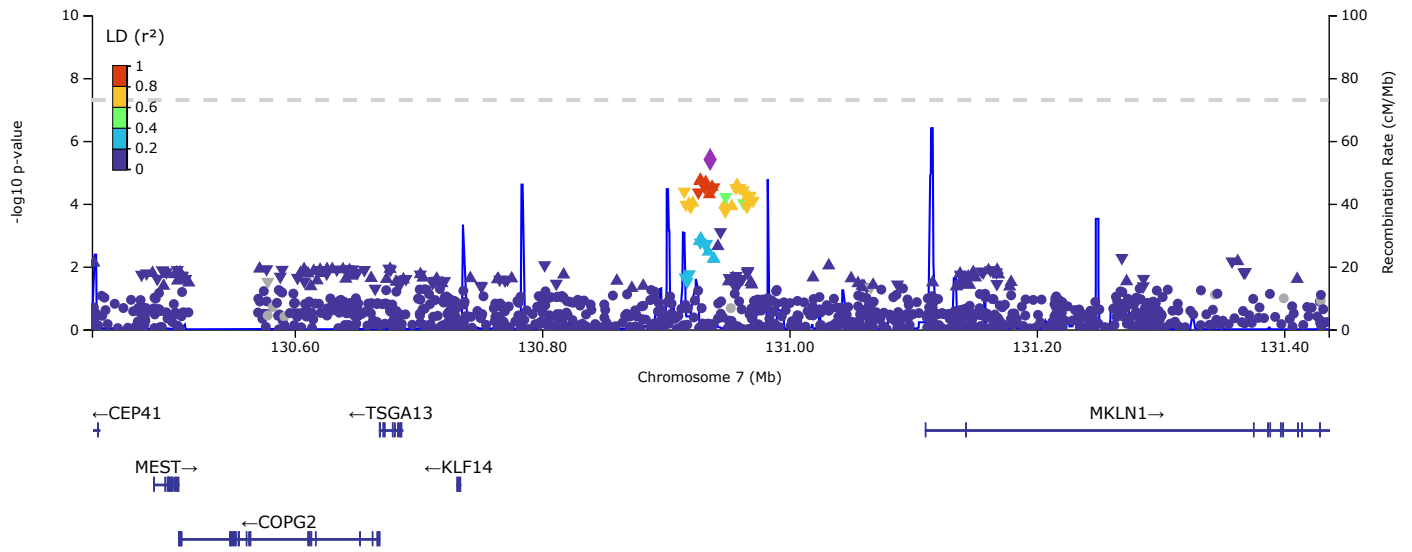
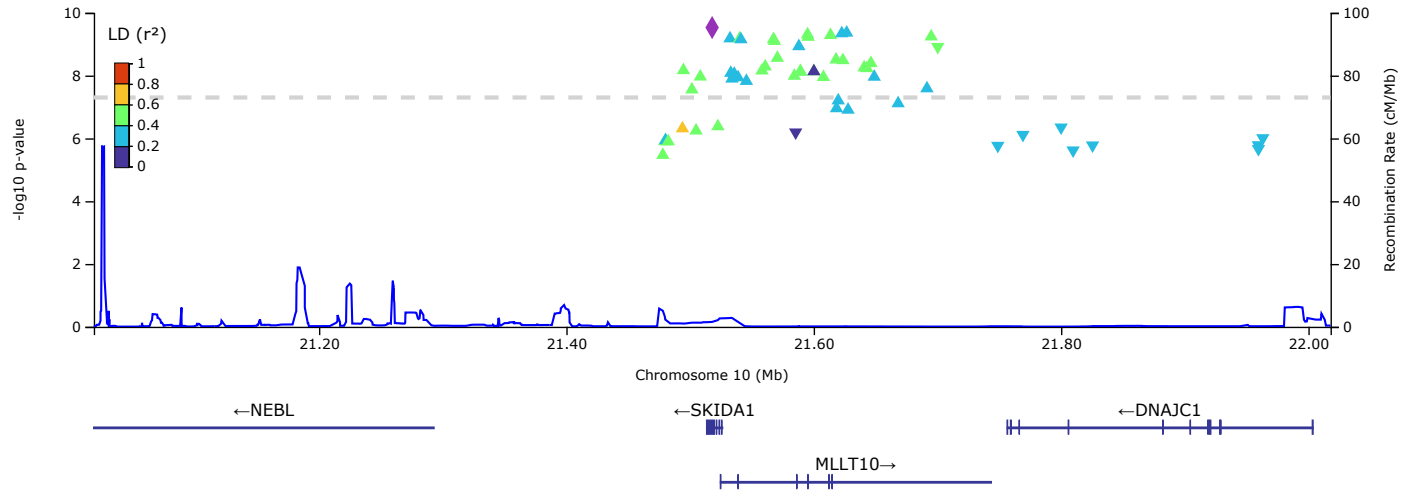


**Figure S10. Regional plot of the novel UL association on chr7 near *LINC-PINT*.**

The plot on the top shows the result in META-1, and the plot on the bottom shows the result in META-2.

### META-1



### META-2

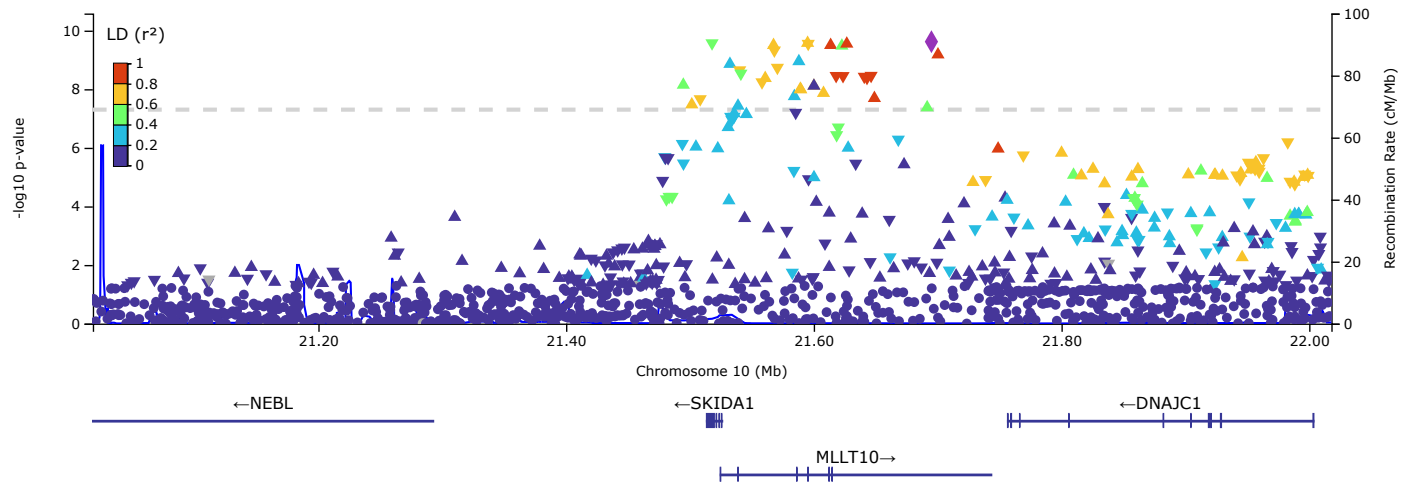
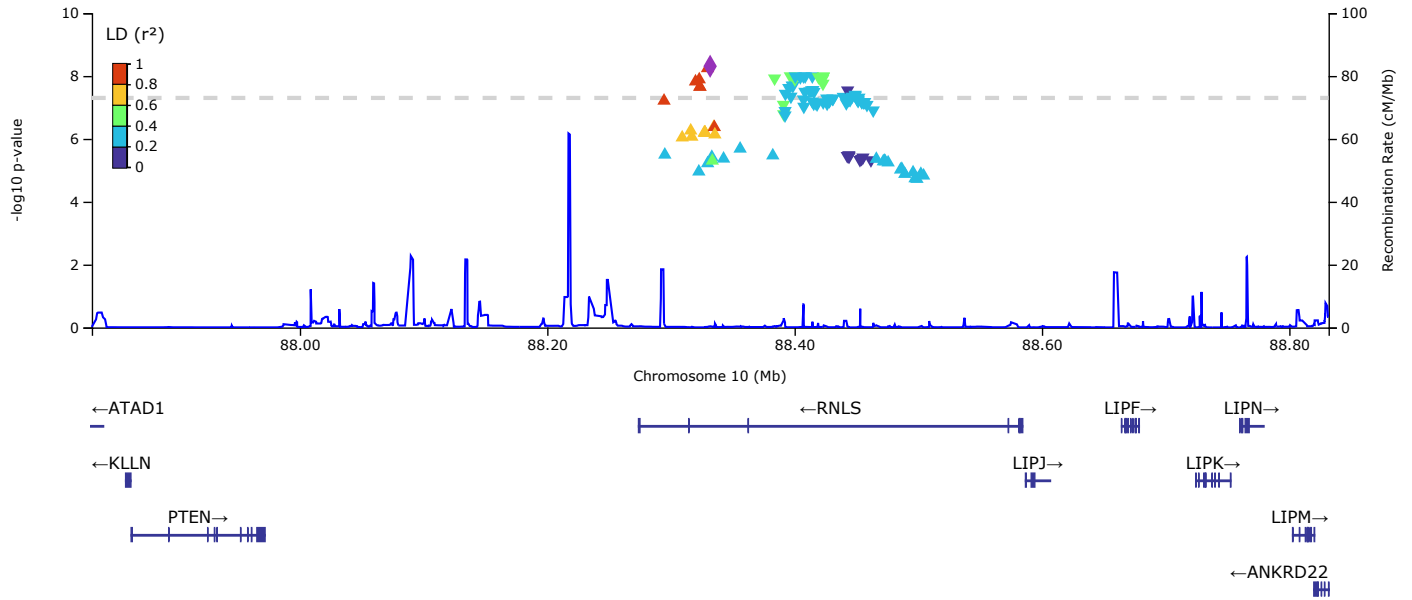


**Figure S11. Regional plot of the novel UL association on chr10 near *SKIDA1* (*DNAJC1*).**

The plot on the top shows the result in META-1, and the plot on the bottom shows the result in META-2.

### META-1



### META-2

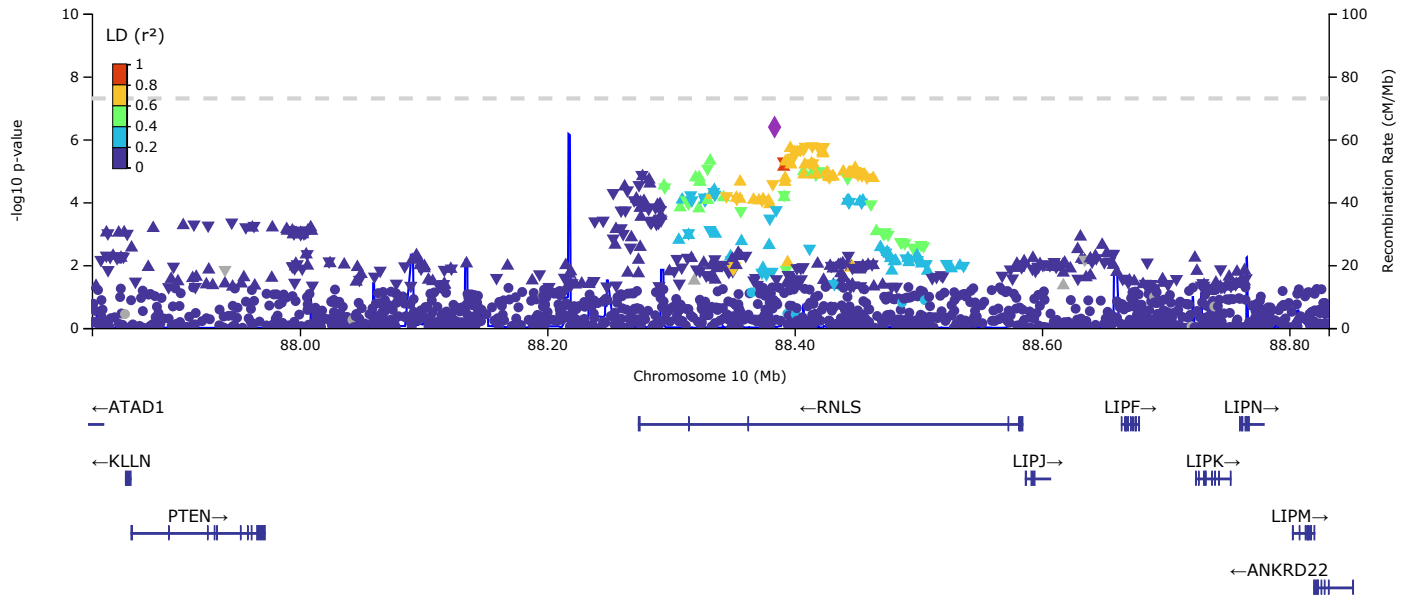
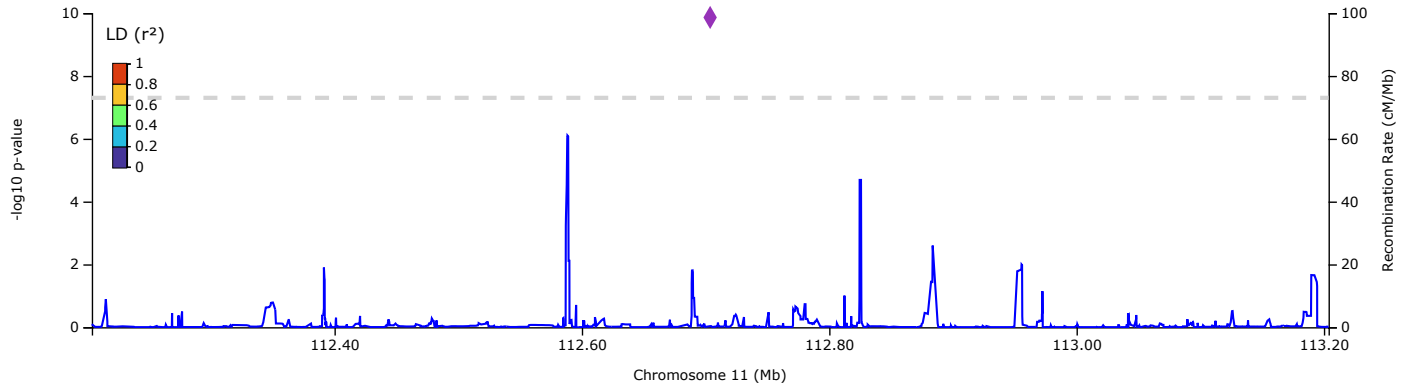


**Figure S12. Regional plot of the novel UL association on chr10 near *RNLS*.**

The plot on the top shows the result in META-1, and the plot on the bottom shows the result in META-2.

### META-1



### META-2

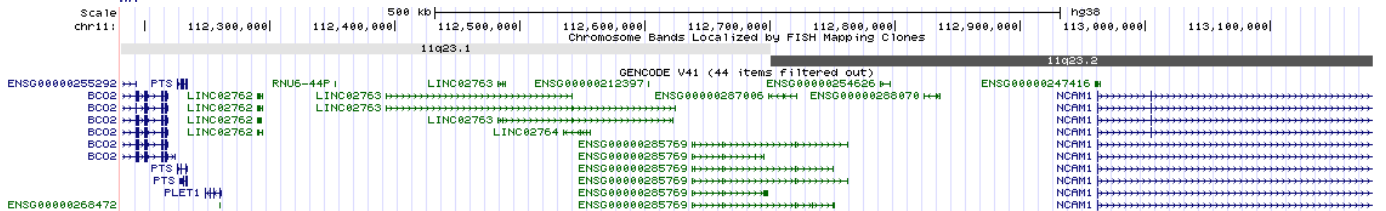
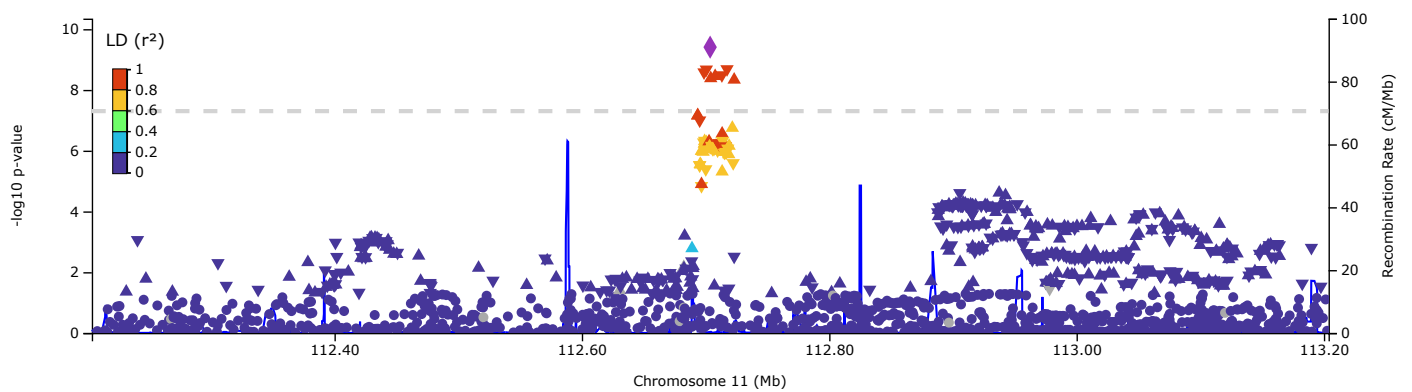
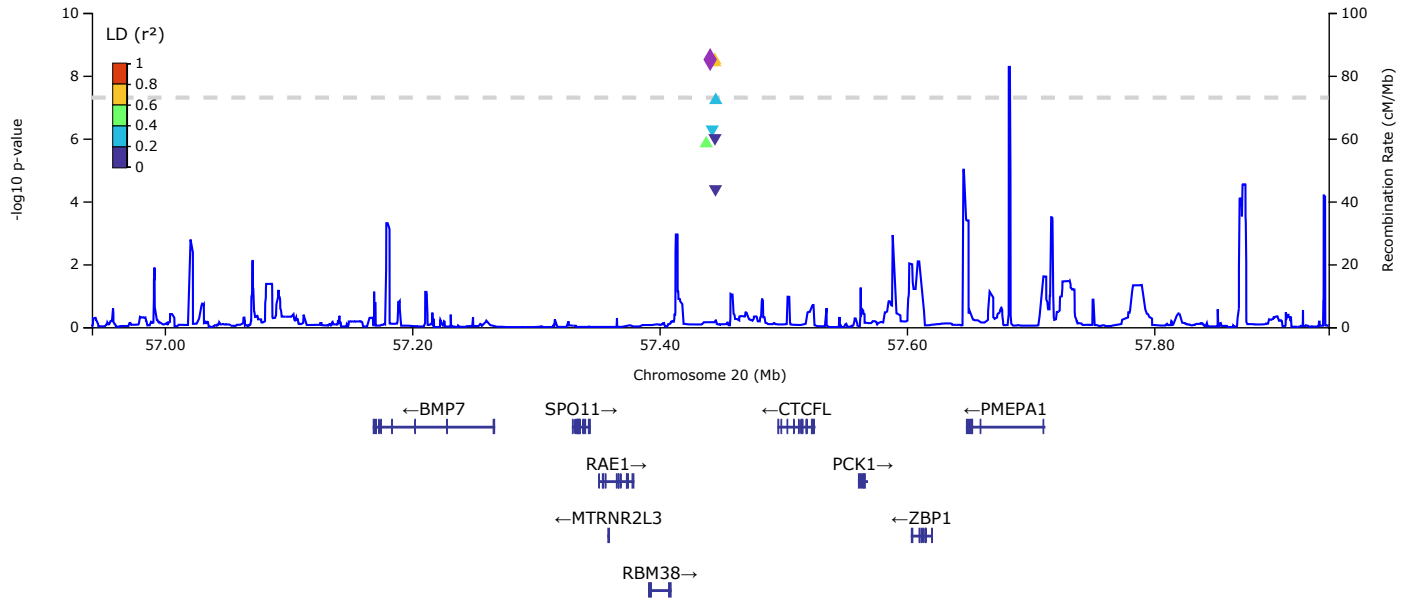


**Figure S13. Regional plot of the novel UL association on chr11 near *ENSG00000285769*.**

The plot on the top shows the result in META-1, and the plot in the middle shows the result in META-2. ENSG00000285769 location was unavailable for LocusZoom: it locates on chr11:112,637,324-112,761,375 which is ~200kb upstream from *NCAM1*, as indicated in the image extracted from UCSC Genome Browser (bottom).

### META-1



### META-2

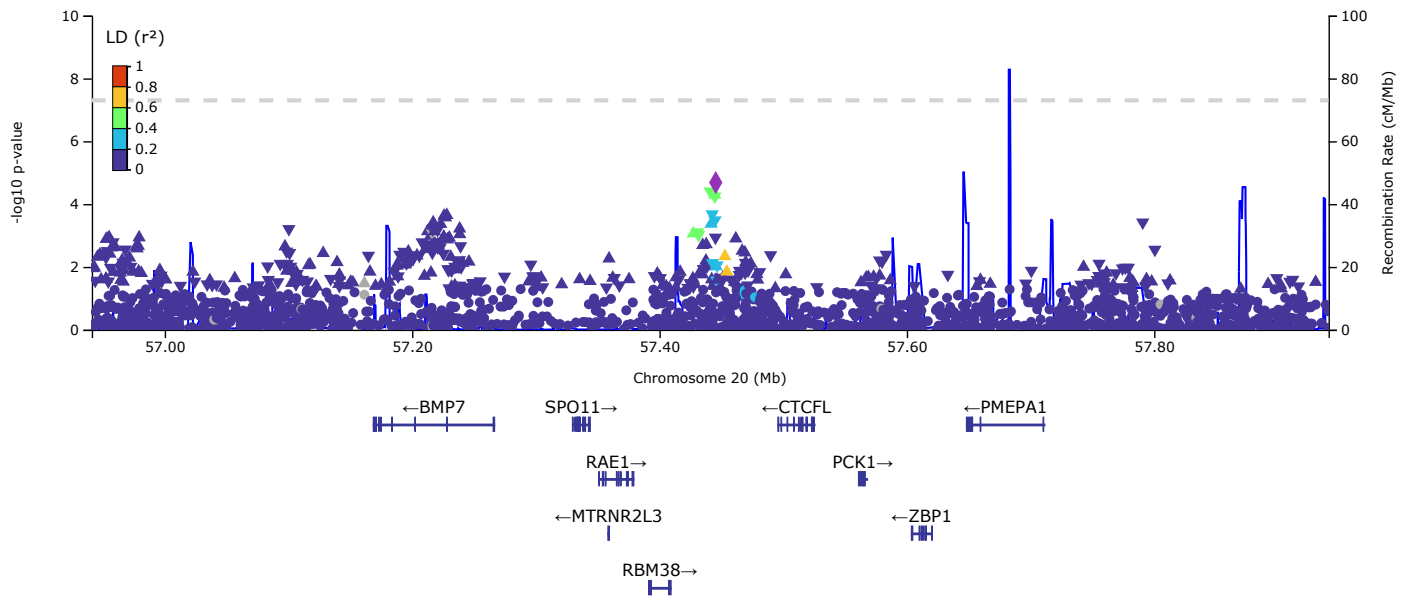
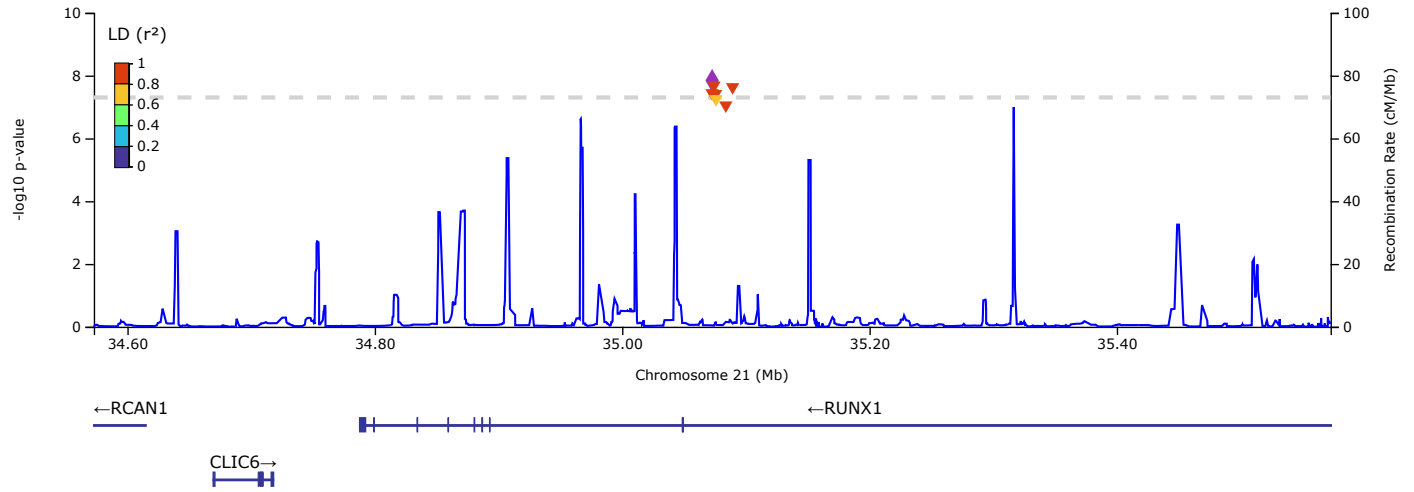


**Figure S14. Regional plot of the novel UL association on chr20 near *CTCFL/RBM38*.**

The plot on the top shows the result in META-1, and the plot on the bottom shows the result in META-2.

### META-1



### META-2

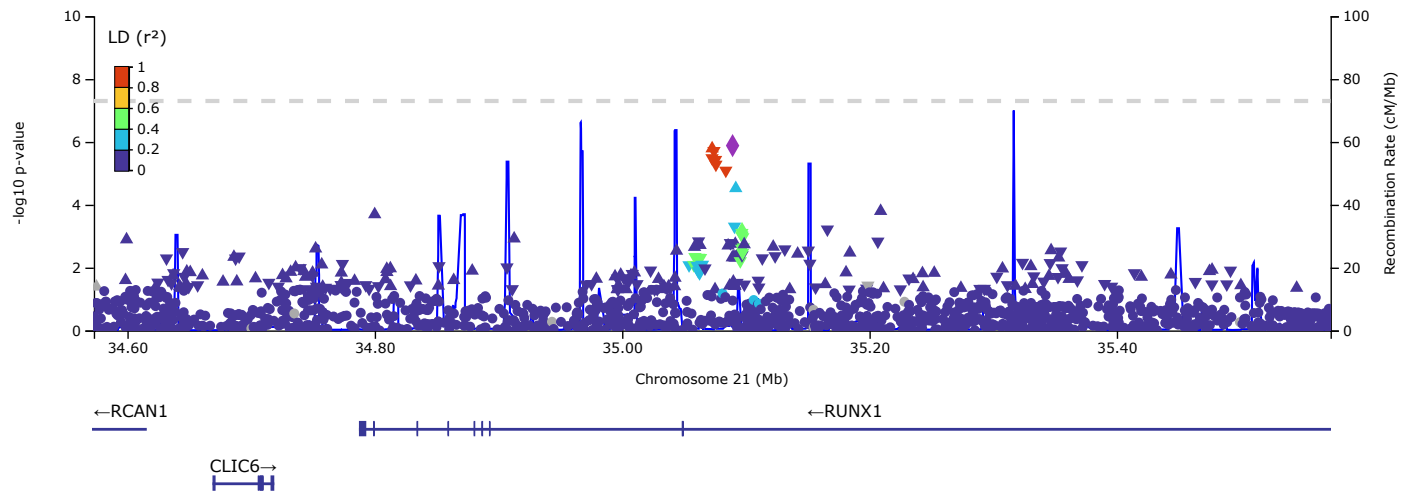
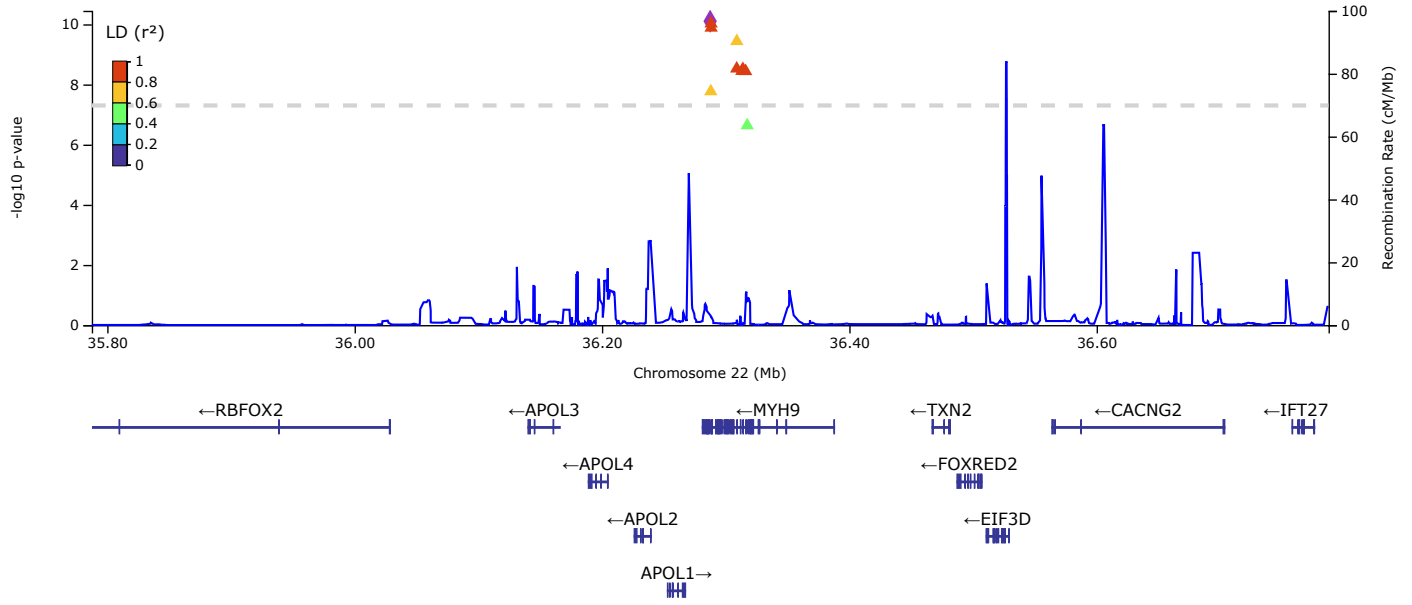


**Figure S15. Regional plot of the novel UL association on chr21 near *RUNX1*.**

The plot on the top shows the result in META-1, and the plot on the bottom shows the result in META-2.



### META-1



### META-2

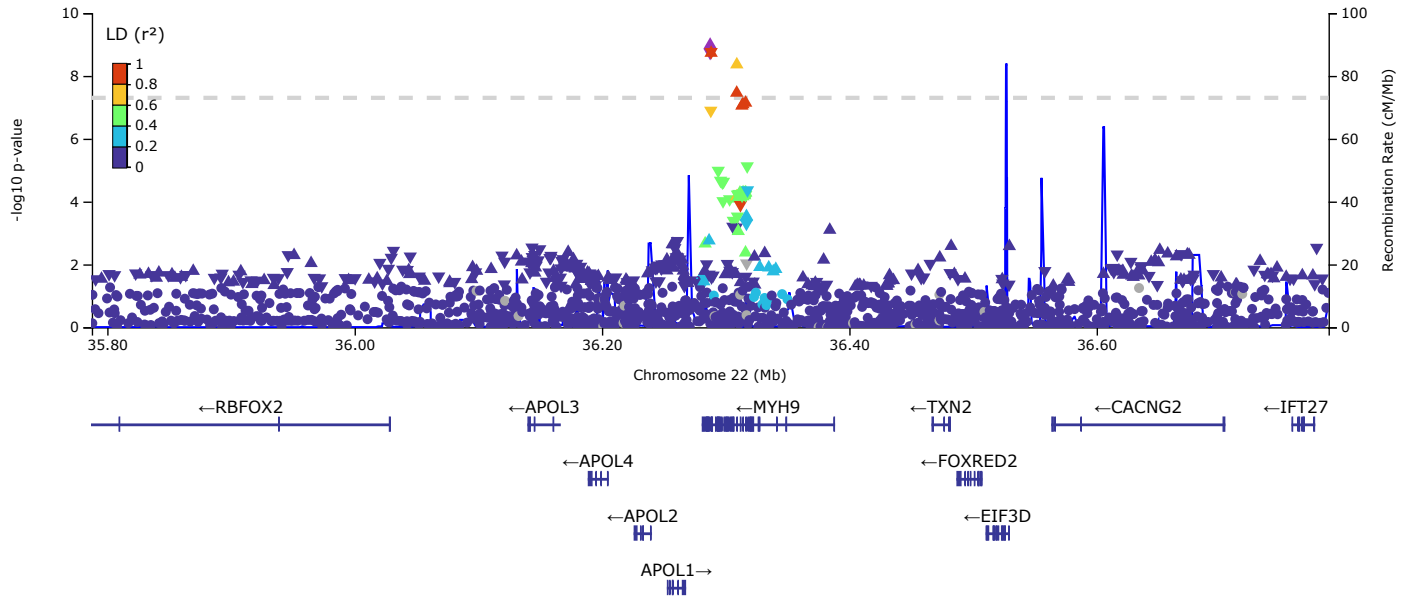


**Figure S16. Regional plot of the novel UL association on chr22 near *MYH9*.**

The plot on the top shows the result in META-1, and the plot on the bottom shows the result in META-2.

**META-2**

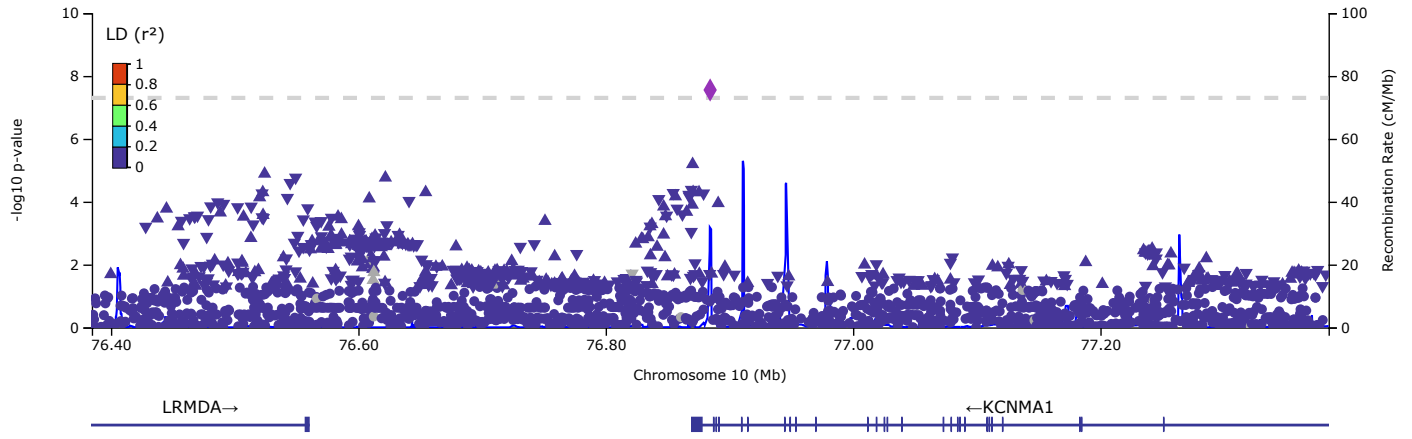


**Figure S17. Regional plot of the novel UL association on chr10 near *KCNMA1* [META-2].**

**META-2**

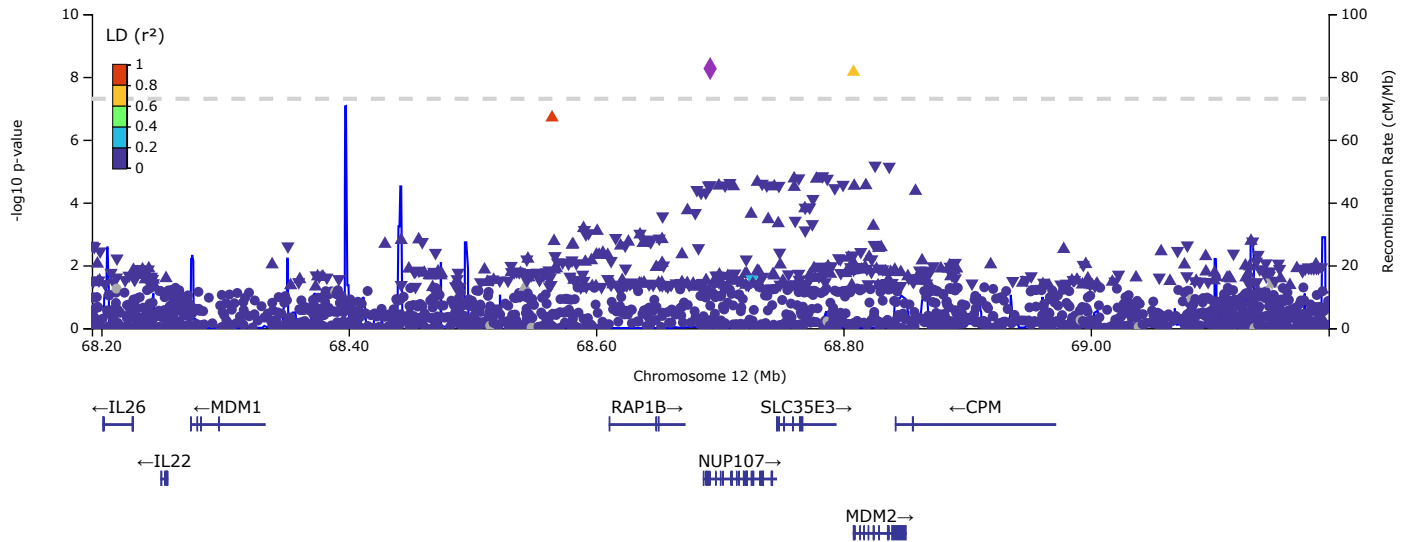


**Figure S18. Regional plot of the novel UL association on chr12 near *NUP107* [META-2].**

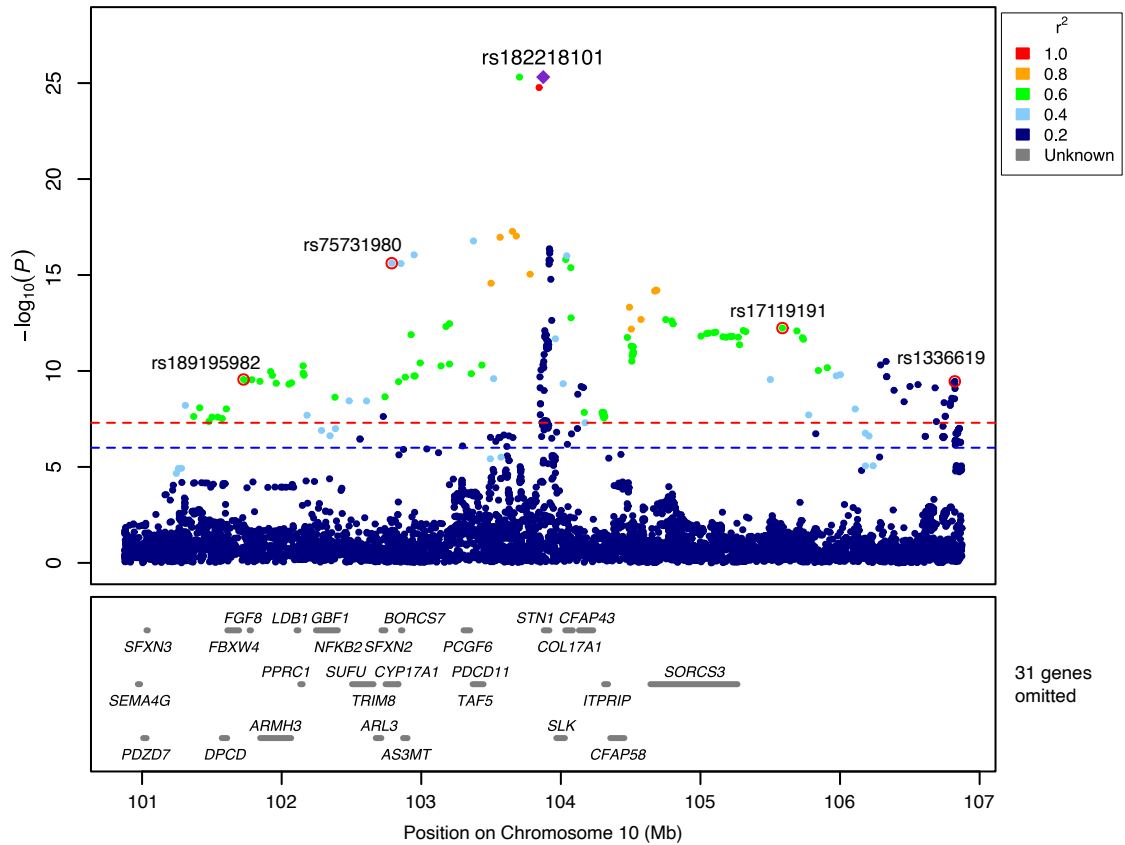


**Figure S19. Regional plot of the association signal at 10q24.32 spanning to a 6MB region [META-2].**

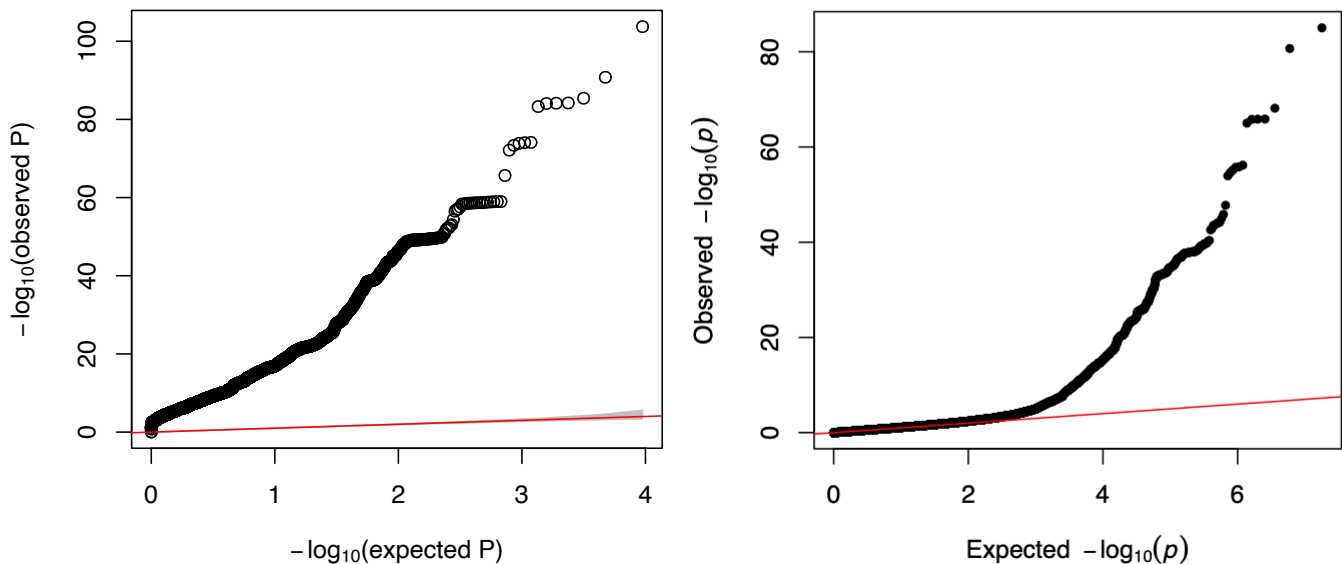


**Figure S20. Quantile-quantile plots of the P-values.**

We conducted two sets of meta-analyses with data from FinnGen and a previous UL GWAS<sup>1</sup>. META-1 was limited to the top 10,000 variants from the previous study resulting in an atypical distribution of p-values compared with standard genome-wide analyses (left). META-2 was conducted genome-widely (right). Genomic inflation factor obtained using LDSC software<sup>2</sup> and genome-wide results from META-2 was 1.105 suggesting minor inflation in the test statistics that was mostly accounted by a polygenic signal with the intercept being close to one (1.0066)<sup>2</sup>.

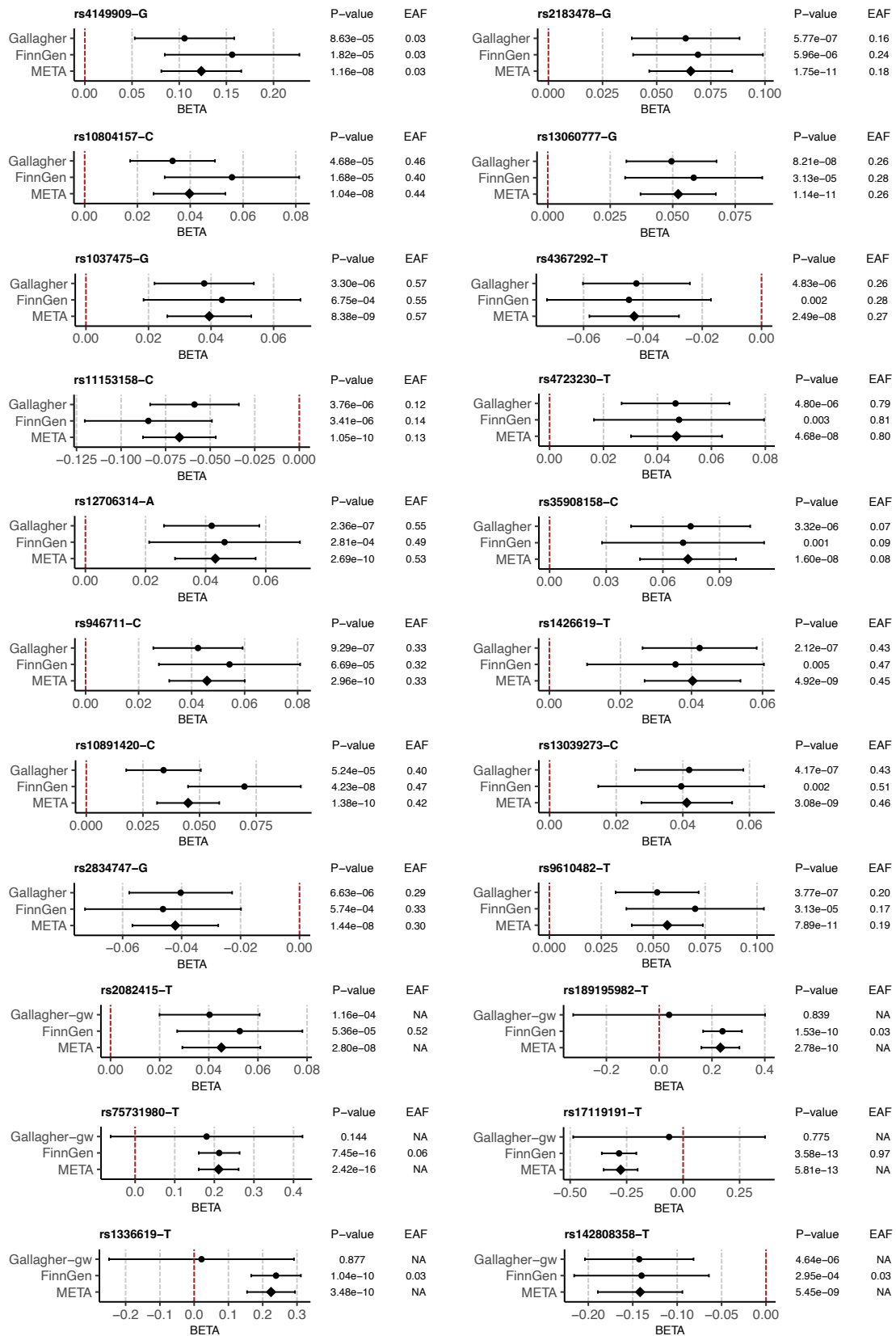


**Figure S21. Forest plot of the effect estimates of the association lead variants in the novel loci.**

The effect estimates and p-values are extracted from the original genetic association results (FinnGen, Gallagher top 10,000 [Gallagher], Gallagher genome-wide [Gallagher-gw]) and the corresponding meta-analyses. The horizontal lines represent the 95% confidence intervals of the effect estimates.

FinnGen, n=123,579; Gallagher, n=302,979; Gallagher genome-wide (gw), n=244,324; META (with Gallagher, i.e. META-1), n=426,558; META (with Gallagher-gw, i.e. META-2), n=367,903.

Gene expression for MYOCD (ENSG00000141052.17)

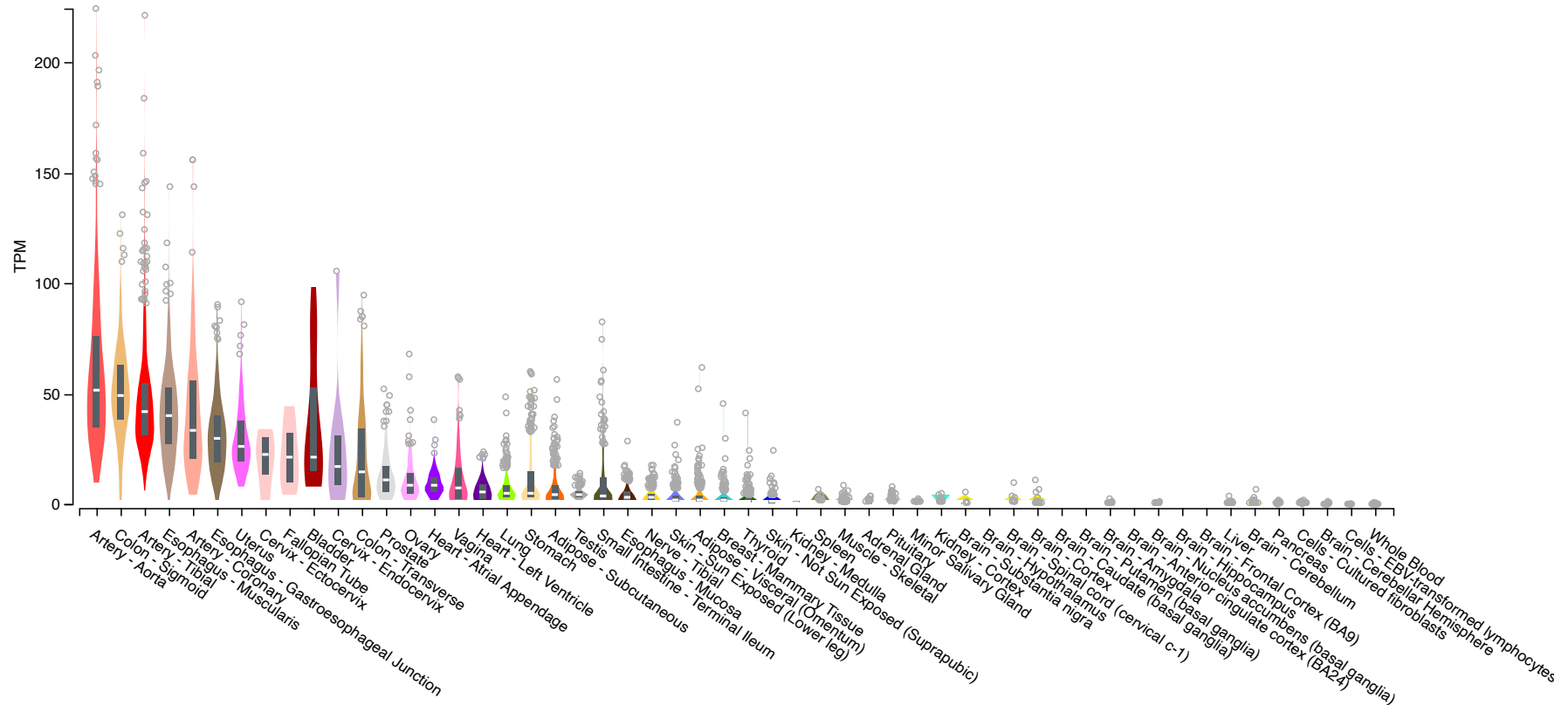


**Figure S22. MYOCD expression in tissues.**

The data was extracted from the GTEx Portal<sup>3</sup> on 02/10/2021. Expression values are shown in Transcripts Per Million (TPM); box plots are shown as median and 25<sup>th</sup> and 75<sup>th</sup> percentiles; points are displayed as outliers if they are above or below 1.5 times the interquartile range.

Artery – Aorta, n=432; Colon – Sigmoid, n=373; Artery – Tibial, n=663; Esophagus – Muscularis, n=515; Artery – Coronary, n=240; Esophagus – Gastroesophageal Junction, n=375; Uterus, n=142; Cervix – Ectocervix, n=9; Fallopian Tube, n=9; Bladder, n=21; Cervix – Endocervix, n=10; Colon – Transverse, n=406; Prostate, n=245; Ovary, n=180; Heart – Atrial Appendage, n=429; Vagina, n=156; Heart – Left Ventricle, n=423; Lung, n=578; Stomach, n=359; Adipose – Subcutaneous, n=663; Testis, n=361; Small Intestine – Terminal Ileum, n=187; Esophagus – Mucosa, n=555; Nerve – Tibial, n=619; Skin – Sun Exposed (lower leg), n=701; Adipose – Visceral (Omentum), n=541; Breast – Mammary Tissue, n=459; Thyroid, n=653; Skin – Not Sun Exposed (Suprapubic), n=604; Kidney – Medulla, n=4; Spleen, n=241; Muscle – Skeletal, n=803; Adrenal Gland, n=258; Pituitary, n=283; Minor Salivary Gland, n=162; Kidney – Cortex, n=85; Brain – Substantia nigra, n=139; Brain – Hypothalamus, n=202; Brain – Spinal cord (cervical c-1), n=159; Brain – Cortex, n=255; Brain – Caudate (basal ganglia), n=246; Brain – Putamen (basal ganglia), n=205; Brain – Amygdala, n=152; Brain – Anterior cingulate cortex (BA24), n=176; Brain – Nucleus accumbens (basal ganglia), n=246; Brain – Hippocampus, n=197; Brain – Frontal Cortex (BA9), n=209; Liver, n=226; Brain – Cerebellum, n=241; Pancreas, n=328; Cells – Cultured fibroblasts, n=504; Brain – Cerebellar Hemisphere, n=215; Cells – EBV-transformed lymphocytes, n=174; Whole Blood, n=755.

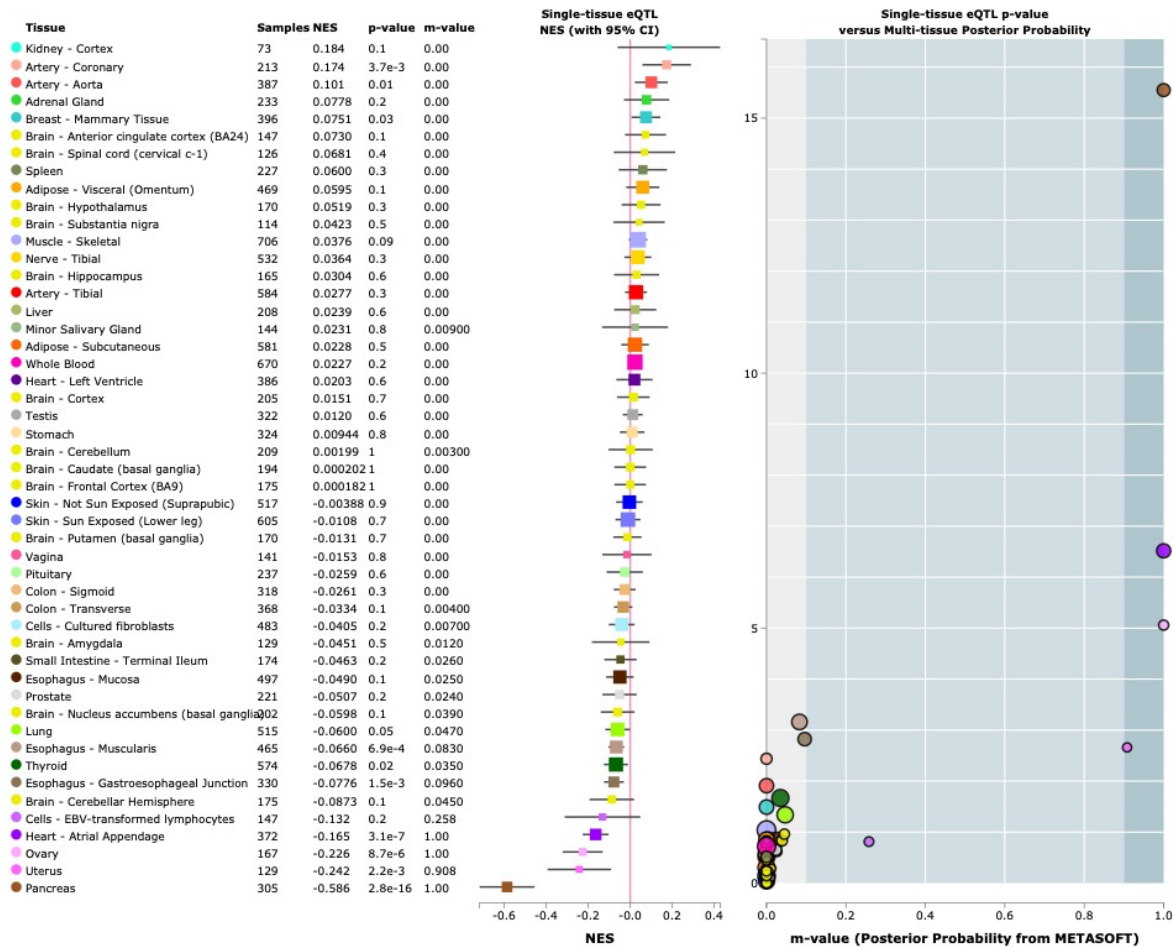


**Figure S23. The association of rs13039273-C with *RBM38* expression.**

‘Samples’ indicate the number of RNA-seq samples with genotype. Normalized effect size (NES) is the slope of the linear regression of the normalized data versus the three genotype categories using single-tissue expression quantitative trait (eQTL) analysis, representing eQTL effect size; the error bars represent the corresponding 95% confidence intervals. ‘P-value’ originates from a t-test that compares observed NES from single-tissue eQTL analysis to a null NES of 0 ( $p=1.38 \times 10^{-19}$  for the meta-analyzed effects). ‘M-value’ indicates the posterior probability that an eQTL effect exists in each tissue tested in the cross-tissue meta-analysis. NES are given for the C allele that was the effect allele in the present study. The eQTL screening was considered exploratory and no multiple testing correction was applied.

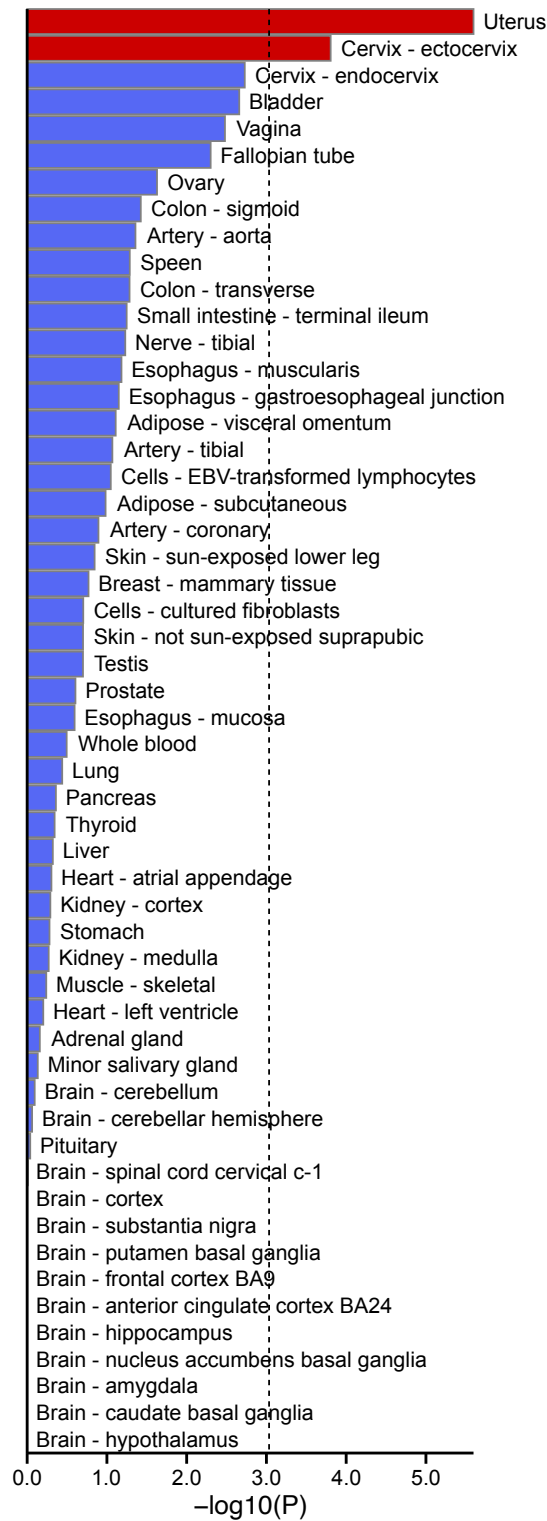


**Figure S24. Results of MAGMA tissue expression analysis.**

MAGMA<sup>4</sup> tissue expression analysis tests for a positive relationship between tissue-specific gene expression profiles and disease-gene associations. Tissue-specific gene expression data were from GTEx v8<sup>3</sup>. The analysis was conducted using FUMA<sup>5</sup>.

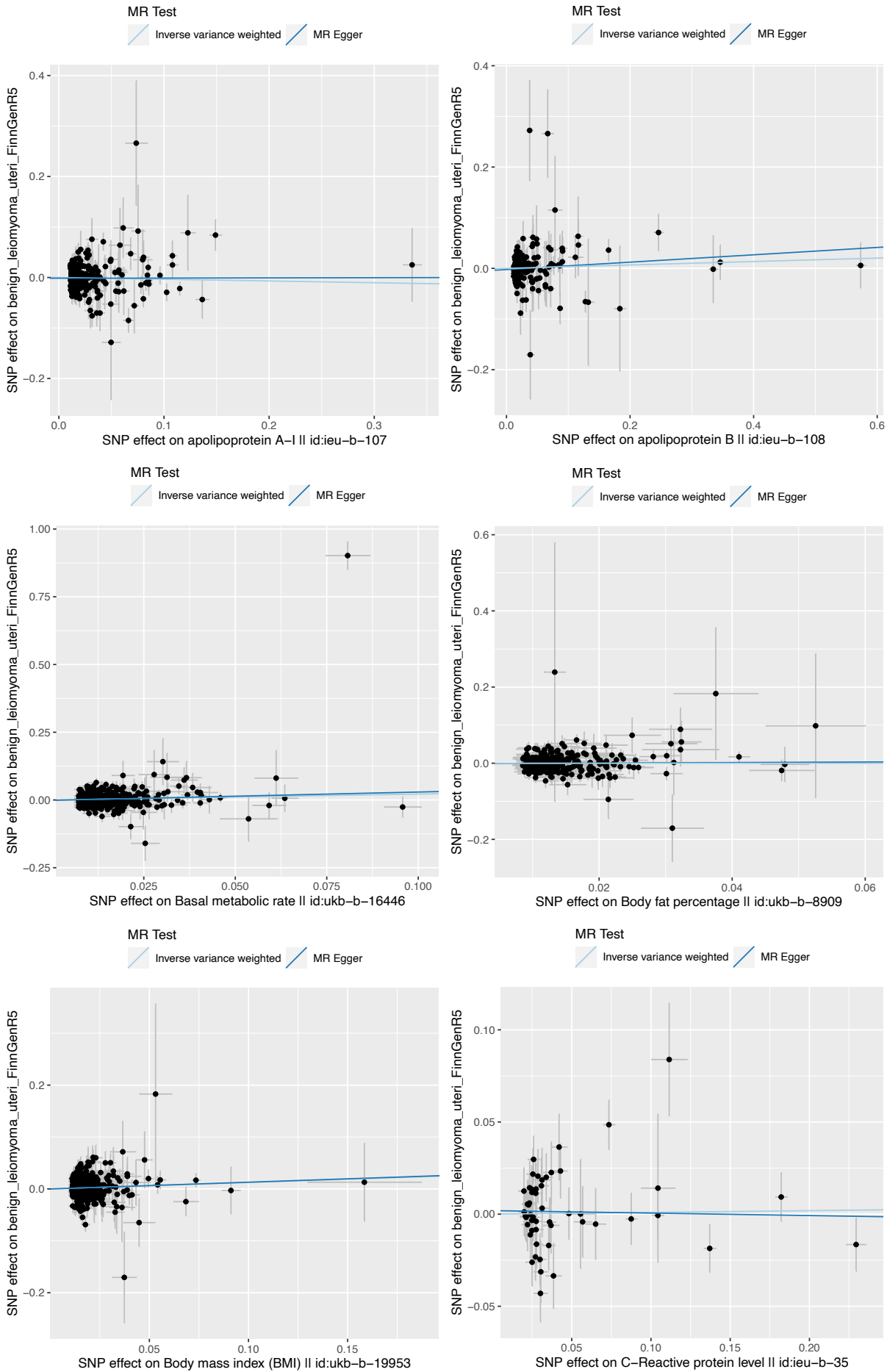


(Figure S25. Figure legend on page 26.)



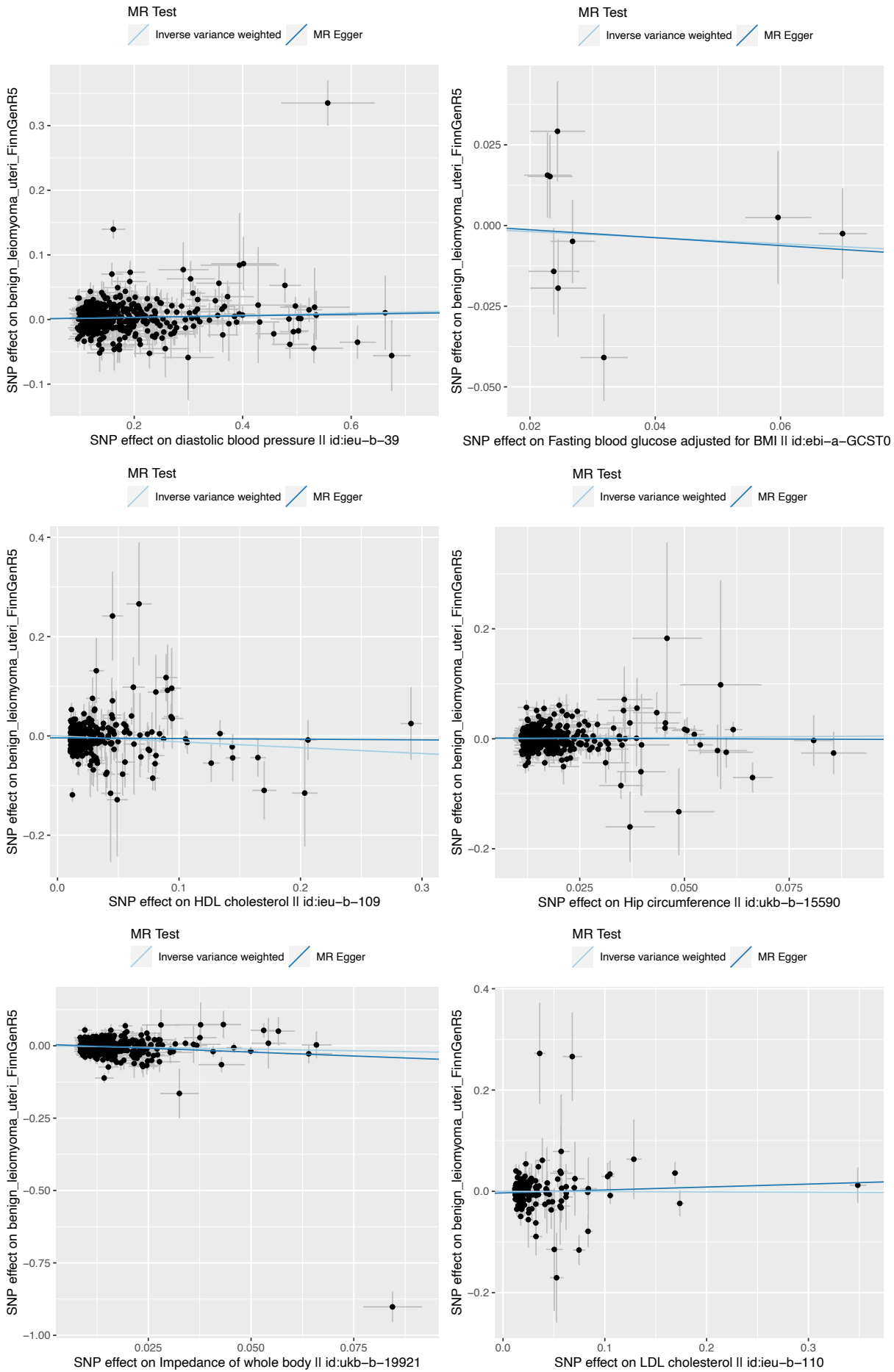


(Figure S25. Figure legend on page 26.)

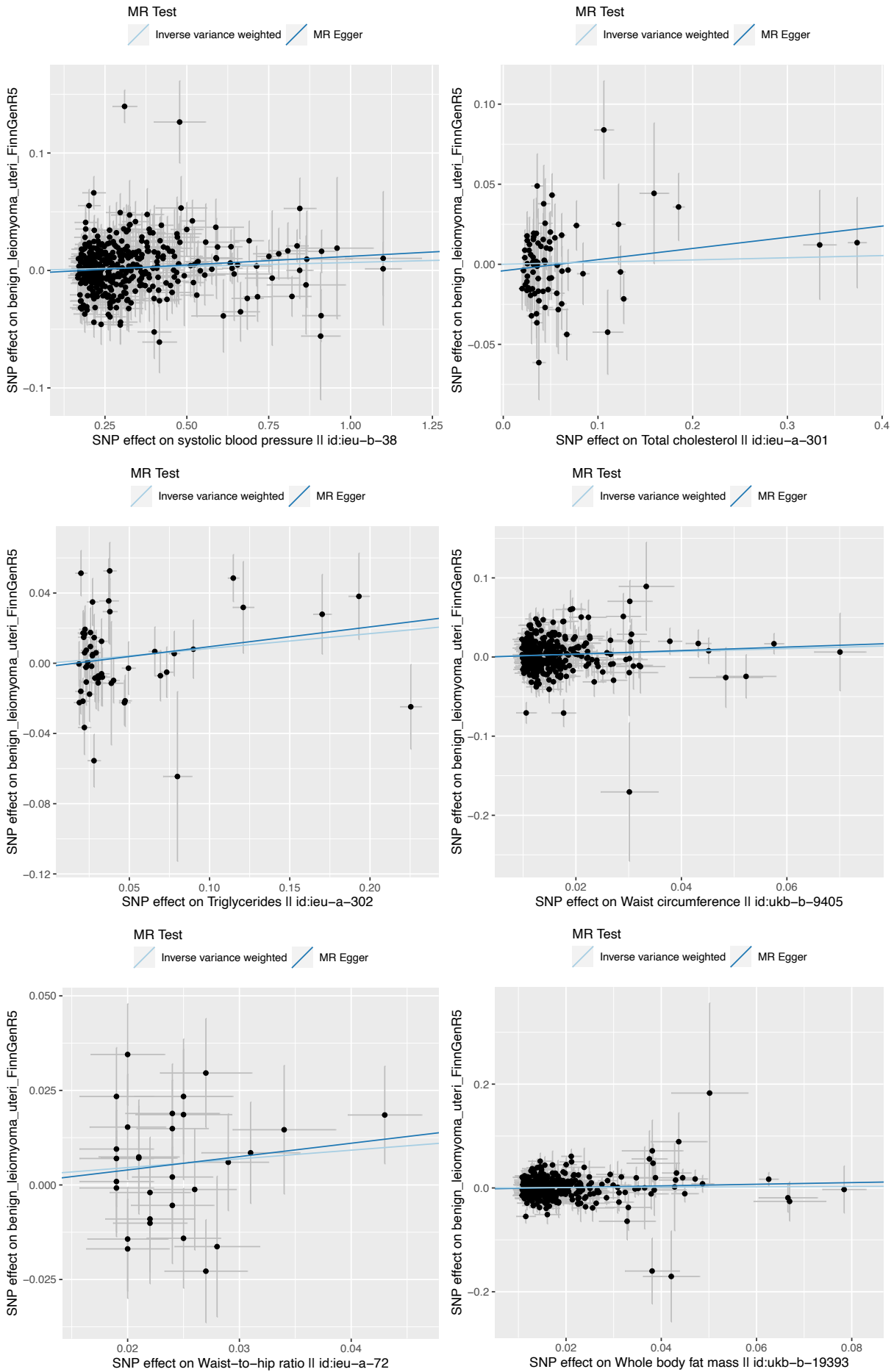


(Figure S25. Figure legend on page 26.)

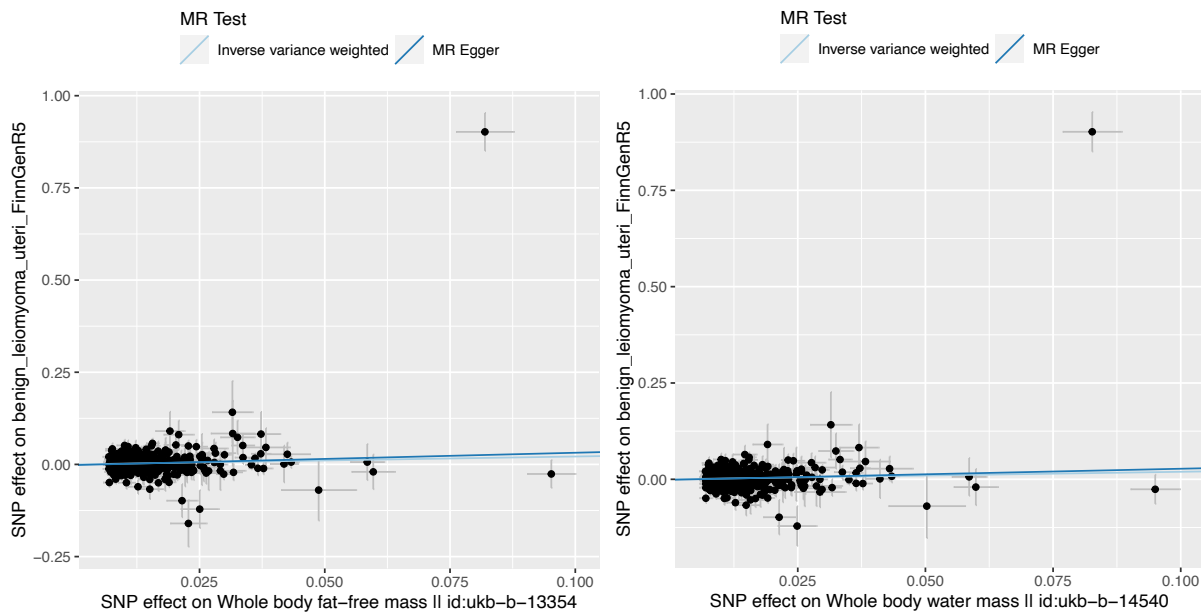


**Figure S25. MR scatter plots: UL as outcome, other traits as exposure.**

Genetic instruments for UL were extracted from the GWAS results obtained from FinnGen ( $n=123,579$ ), and for other traits from the GWAS database provided by the MRC IEU as integrated in the TwoSampleMR R library (sample sizes are given below). LD pruning was completed using European population reference, threshold of  $r^2=0.001$ , and clumping window of 10 kb. The error bars represent the 95% confidence intervals of the SNP effects.

Apolipoprotein A-I (ieu-b-107),  $n=393,193$ ; Apolipoprotein B (ieu-b-108),  $n=439,214$ ; Basal metabolic rate (ukb-b-16446),  $n=454,874$ ; Body fat percentage (ukb-b-8909),  $n=454,633$ ; Body mass index (BMI) (ukb-b-19953),  $n=461,460$ ; C-reactive protein (bbj-a-14),  $n=75,391$ ; Diastolic blood pressure (ieu-b-39),  $n=757,601$ ; Fasting blood glucose adjusted for BMI (ebi-a-GCST007858),  $n=33,231$ ; HDL cholesterol (ieu-b-1099),  $n=403,943$ ; Hip circumference (ukb-b-15590),  $n=462,117$ ; Impedance of whole body (ukb-b-19921),  $n=454,840$ ; LDL cholesterol (ieu-b-110),  $n=440,546$ ; Systolic blood pressure (ieu-b-38),  $n=757,601$ ; Total cholesterol (ieu-a-301),  $n=187,365$ ; Triglycerides (ieu-b-111),  $n=441,016$ ; Waist circumference (ukb-b-9405),  $n=462,166$ ; Waist-to-hip ratio (ieu-a-72),  $n=224,459$ ; Whole body fat mass (ukb-b-19393),  $n=454,137$ ; Whole body fat-free mass (ukb-b-13354),  $n=454,850$ ; Whole body water mass (ukb-b-14540),  $n=454,888$ .

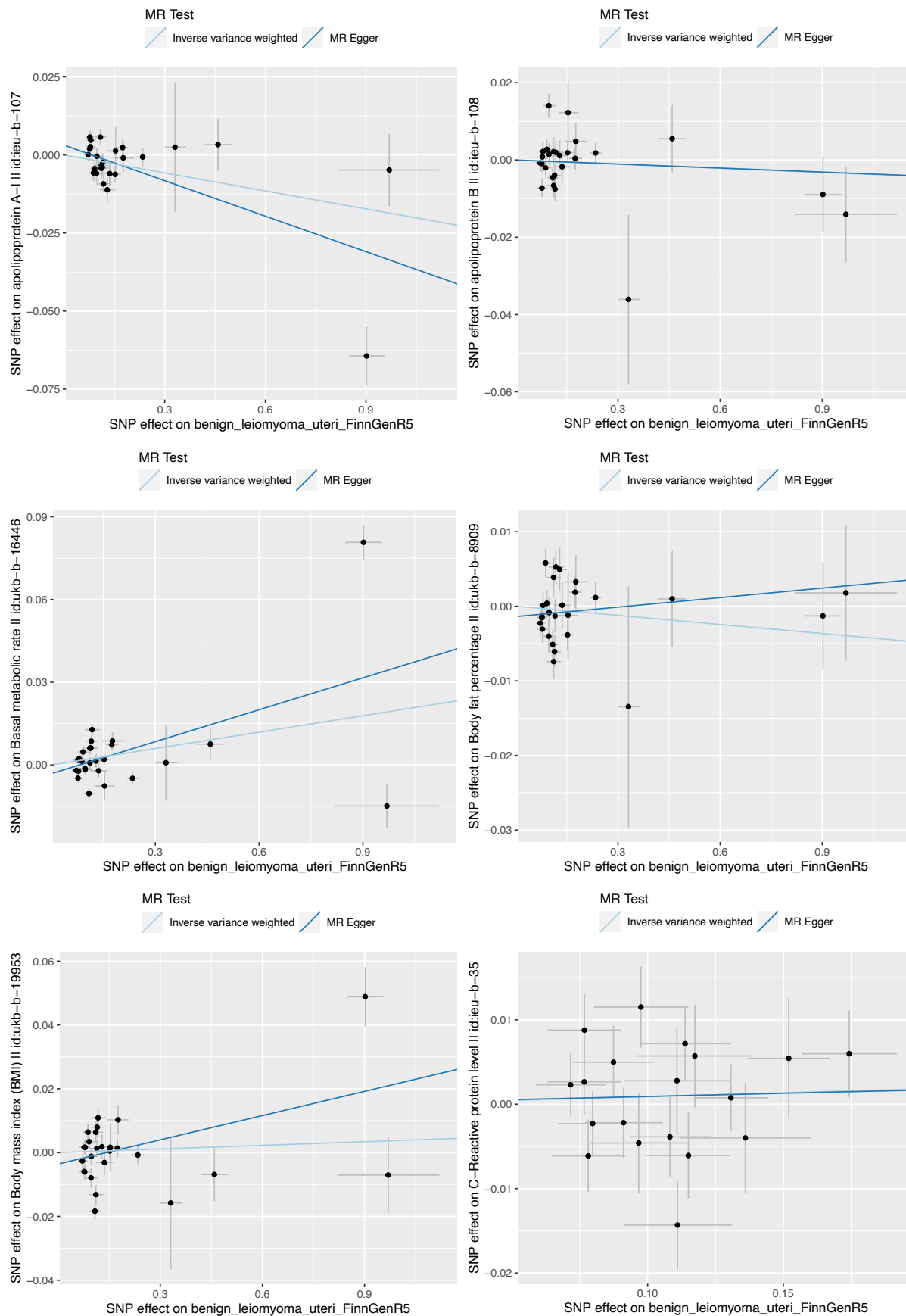


(Figure S26. Figure legend on page 30.)

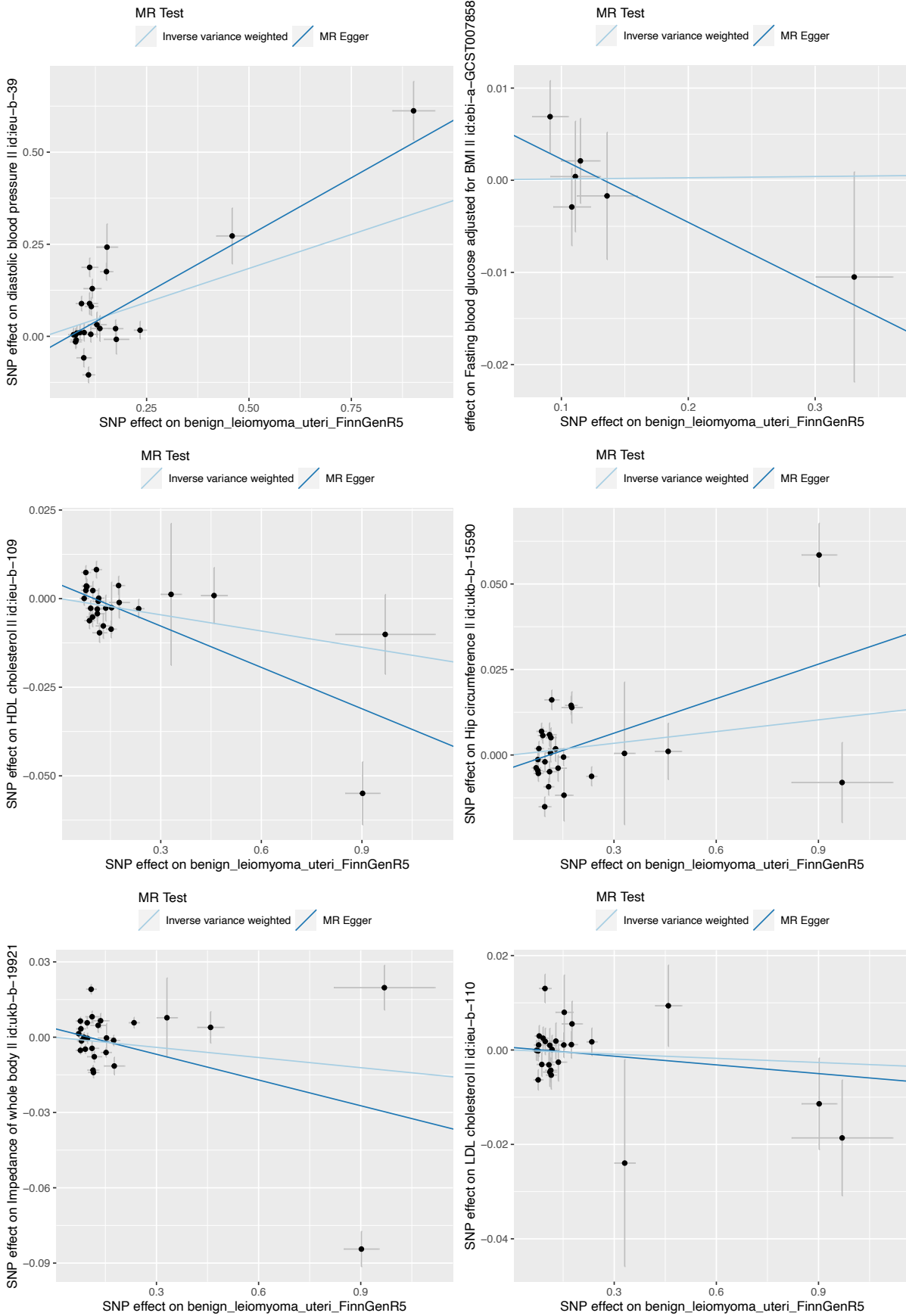


(Figure S26. Figure legend on page 30.)

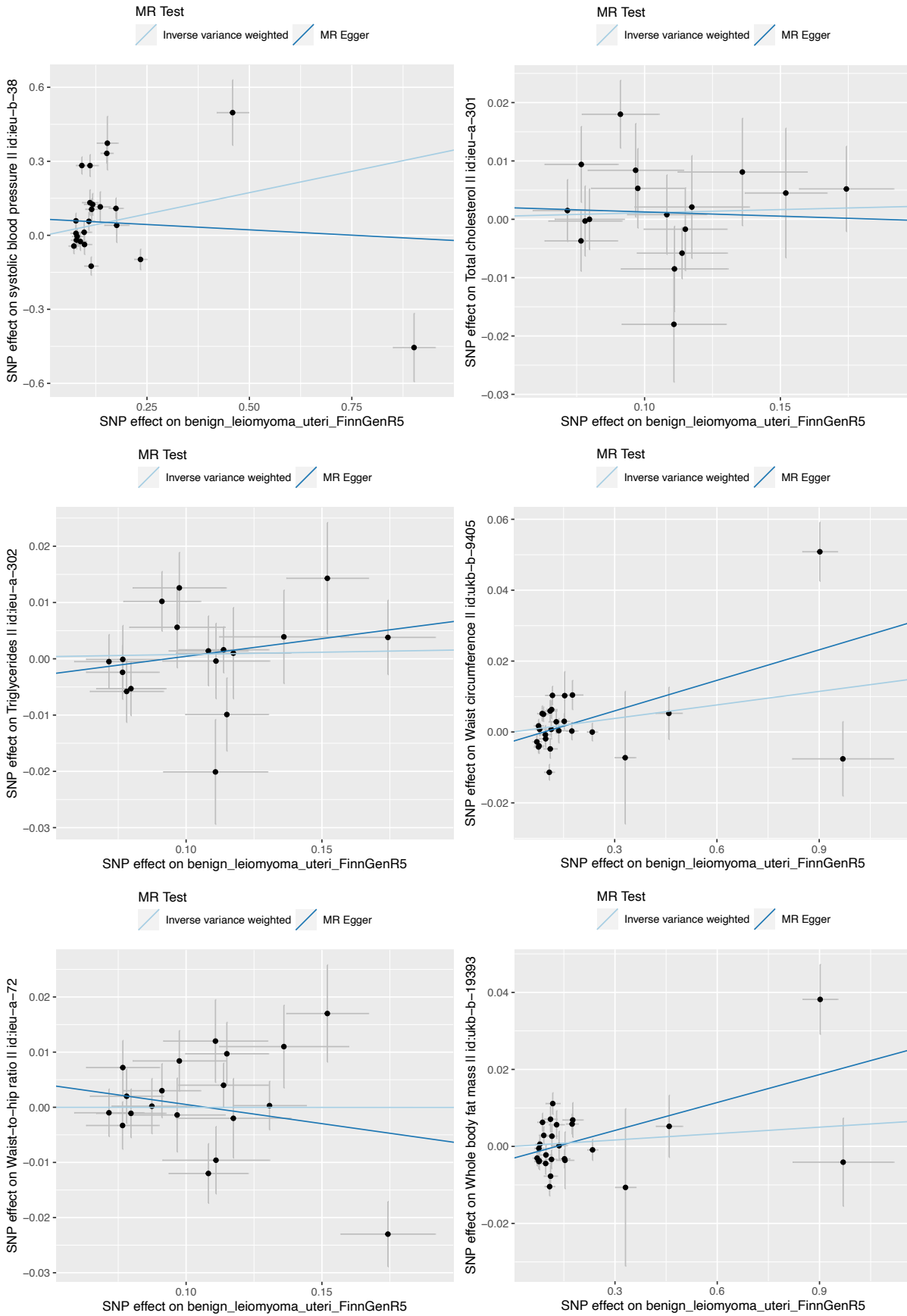


(Figure S26. Figure legend on page 30.)

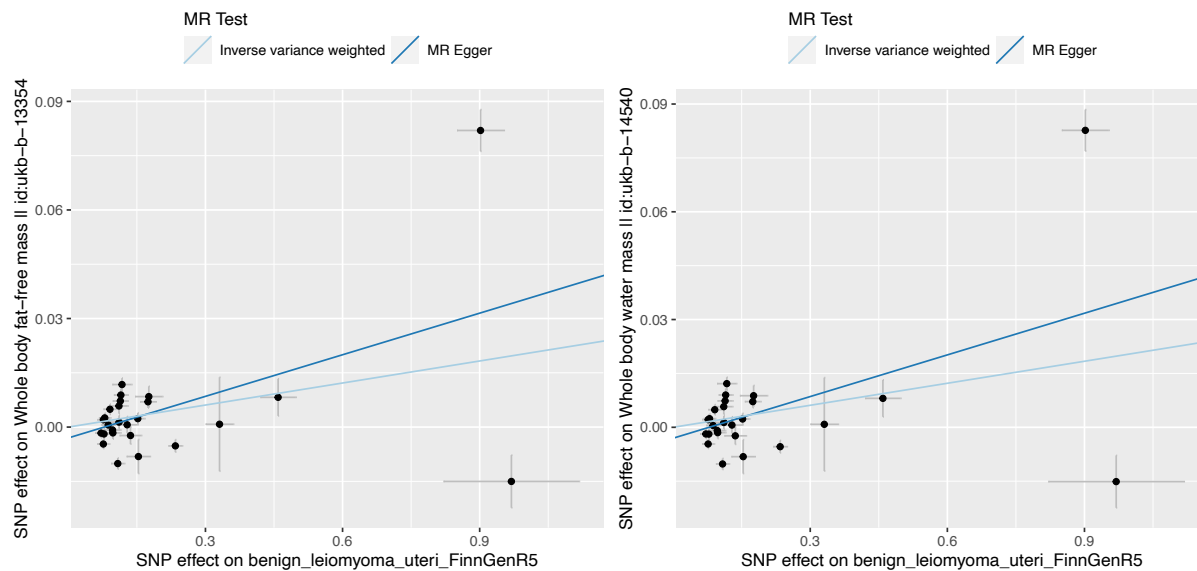


**Figure S26. MR scatter plots: UL as exposure, other traits as outcome.**

Genetic instruments for UL were extracted from the GWAS results obtained from FinnGen ( $n=123,579$ ), and for other traits from the GWAS database provided by the MRC IEU as integrated in the TwoSampleMR R library (sample sizes are given below). LD pruning was completed using European population reference, threshold of  $r^2=0.001$ , and clumping window of 10 kb. The error bars represent the 95% confidence intervals of the SNP effects.

Apolipoprotein A-I (ieu-b-107),  $n=393,193$ ; Apolipoprotein B (ieu-b-108),  $n=439,214$ ; Basal metabolic rate (ukb-b-16446),  $n=454,874$ ; Body fat percentage (ukb-b-8909),  $n=454,633$ ; Body mass index (BMI) (ukb-b-19953),  $n=461,460$ ; C-reactive protein (bbj-a-14),  $n=75,391$ ; Diastolic blood pressure (ieu-b-39),  $n=757,601$ ; Fasting blood glucose adjusted for BMI (ebi-a-GCST007858),  $n=33,231$ ; HDL cholesterol (ieu-b-1099),  $n=403,943$ ; Hip circumference (ukb-b-15590),  $n=462,117$ ; Impedance of whole body (ukb-b-19921),  $n=454,840$ ; LDL cholesterol (ieu-b-110),  $n=440,546$ ; Systolic blood pressure (ieu-b-38),  $n=757,601$ ; Total cholesterol (ieu-a-301),  $n=187,365$ ; Triglycerides (ieu-b-111),  $n=441,016$ ; Waist circumference (ukb-b-9405),  $n=462,166$ ; Waist-to-hip ratio (ieu-a-72),  $n=224,459$ ; Whole body fat mass (ukb-b-19393),  $n=454,137$ ; Whole body fat-free mass (ukb-b-13354),  $n=454,850$ ; Whole body water mass (ukb-b-14540),  $n=454,888$ .

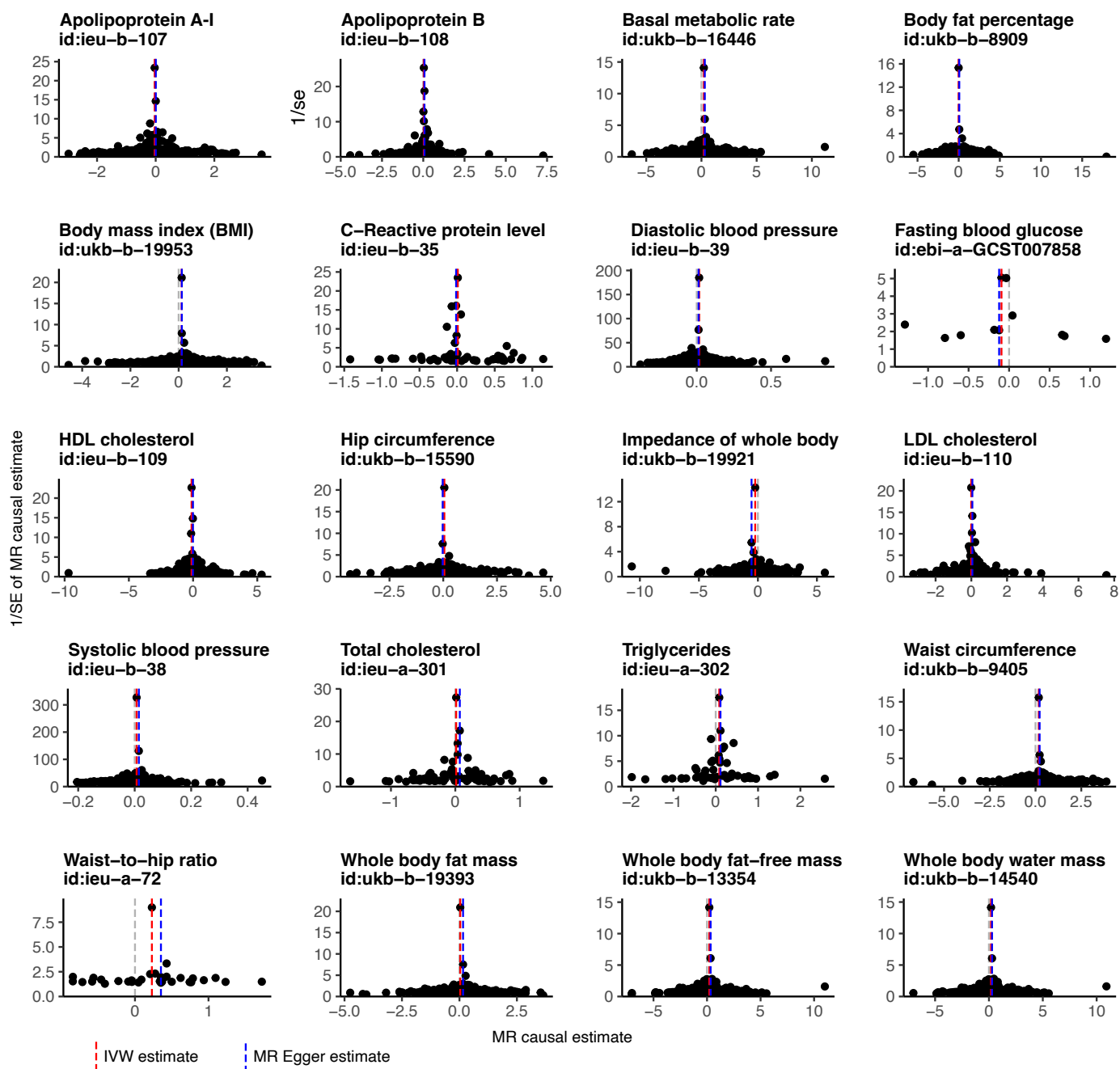


**Figure S27. Funnel plots of MR causal estimates vs. their precision.**

Each data point corresponds to an individual genetic variant. The x-axis corresponds to the coefficient of the variant's UL association divided by the coefficient of the variant's exposure association, *i.e.*, Wald ratio. Genetic instruments for UL were extracted from the GWAS results obtained from FinnGen, and for other traits from the GWAS database provided by the MRC IEU as integrated in the TwoSampleMR R library. LD pruning was completed using European population reference, threshold of  $r^2=0.001$ , and clumping window of 10 kb.



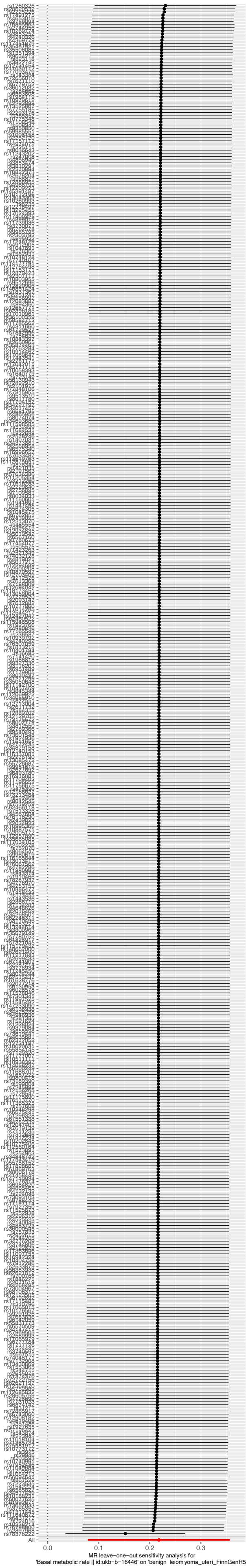


Figure S28. Leave-one-out: exposure basal metabolic rate, outcome UL.

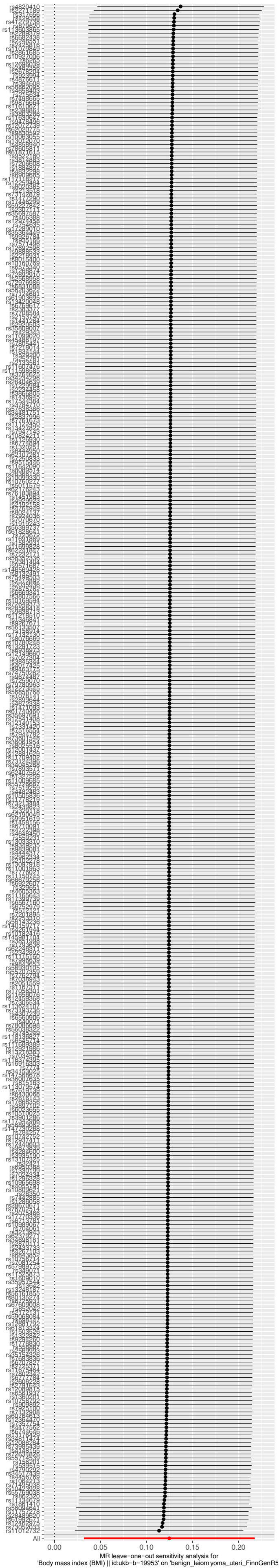


Figure S29. Leave-one-out: exposure body mass index (BMI), outcome UL.

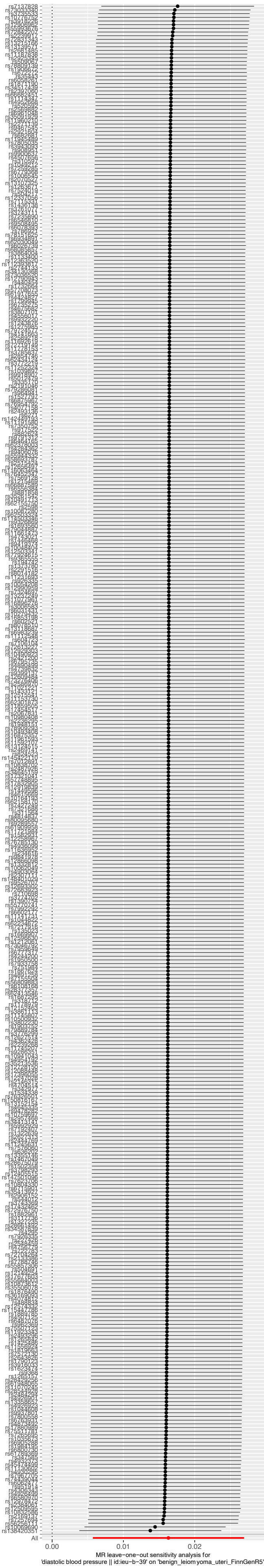
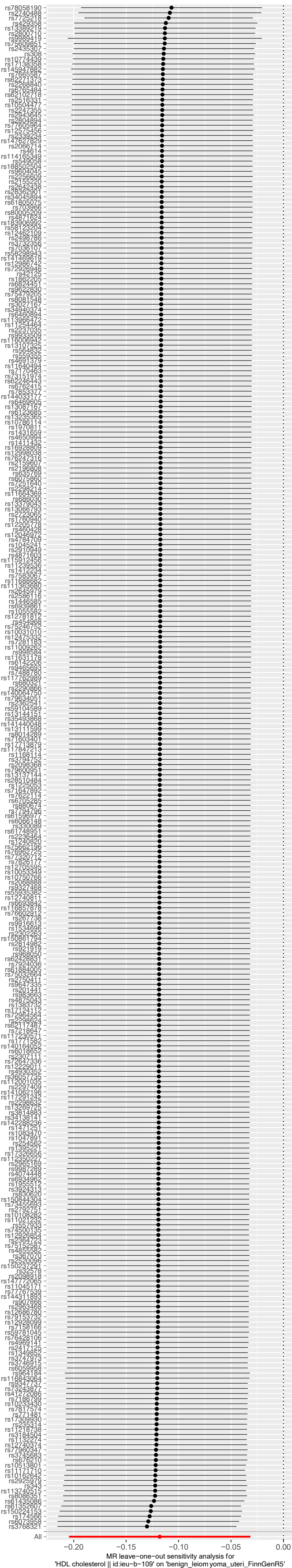


Figure S30. Leave-one-out: exposure diastolic blood pressure, outcome UL.



**Figure S31: Leave-one-out: exposure HDL cholesterol, outcome UL.**

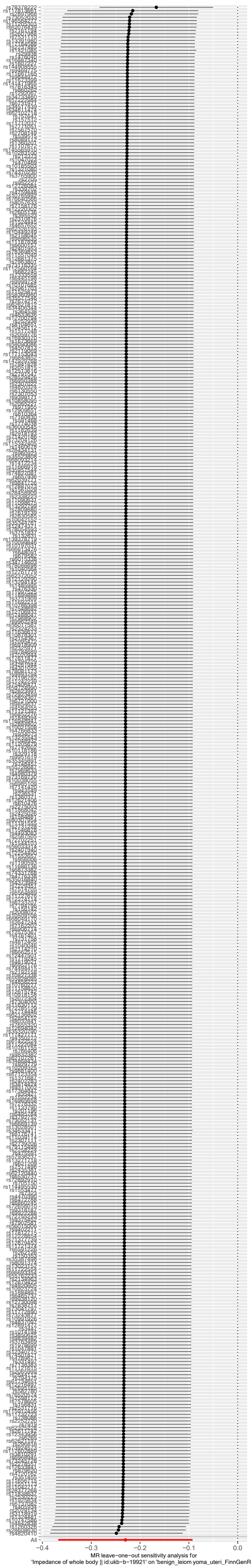
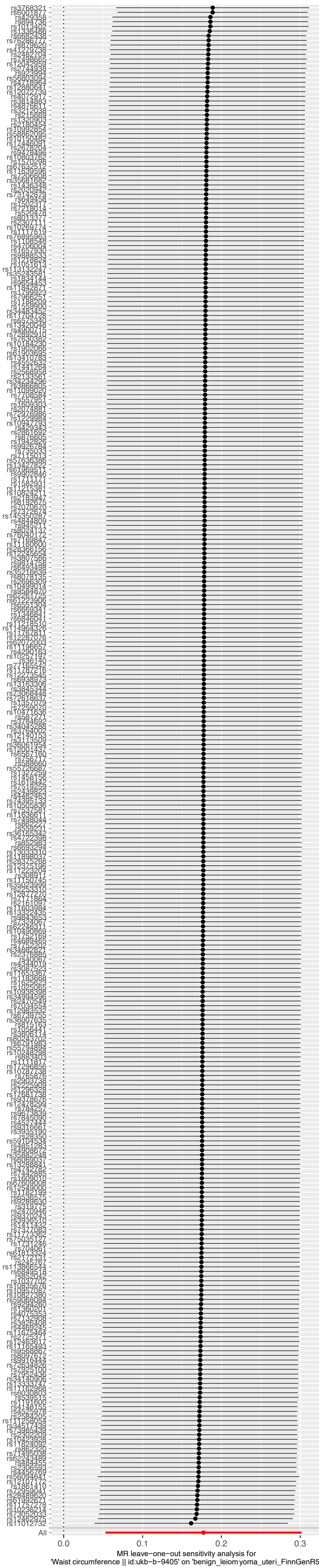


Figure S32: Leave-one-out: exposure impedance of whole body, outcome UL.



**Figure S33: Leave-one-out: exposure waist circumference, outcome UL.**

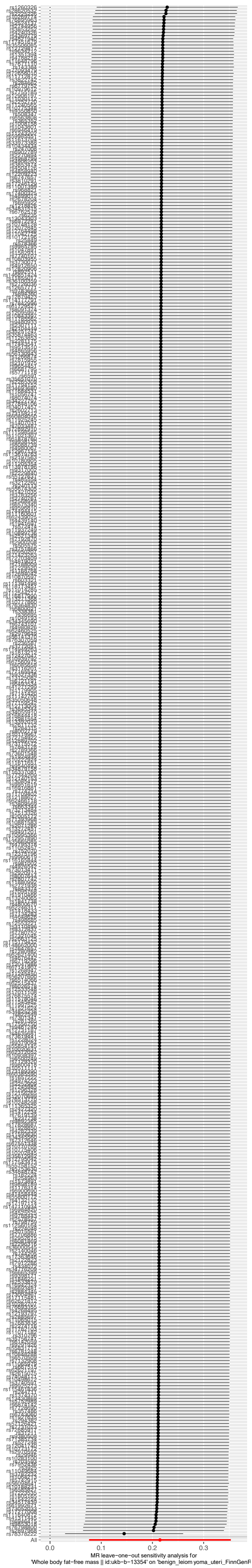
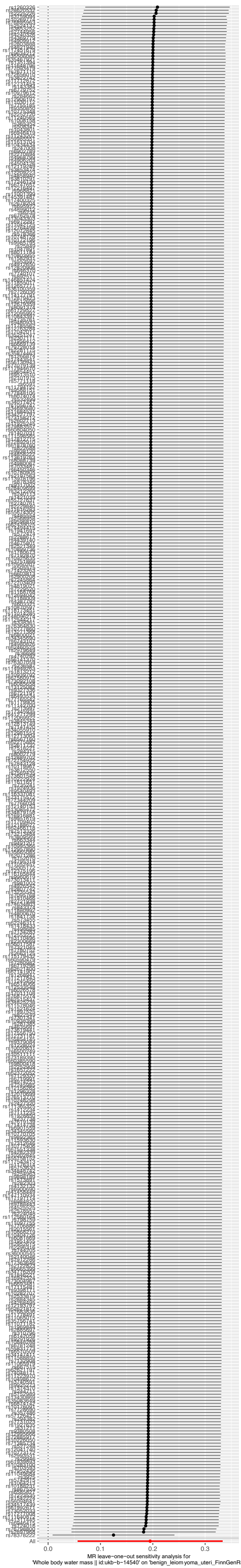


Figure S34: Leave-one-out: exposure whole body fat-free mass, outcome UL.



**Figure S35: Leave-one-out: exposure whole body water mass, outcome UL.**



**Table S1. Genome-wide significant ( $p < 5 \times 10^{-8}$ ) loci in META-1.**

The table reports distinct loci (more than 1Mb apart) containing at least one variant associated with uterine leiomyomata (UL) at  $p < 5 \times 10^{-8}$ , *i.e.*, the standard threshold for genome-wide significance. META-1 was conducted in 53,534 UL cases and 373,024 female controls from FinnGen and a previous UL meta-analysis<sup>1</sup> using fixed-effect inverse variance-weighted method implemented in METAL. Due to data usage policies, META-1 was limited to the top 10,000 variants from the previous study.

| Chr:Pos (hg38) | Nearest gene            | Candidate gene      | rsID        | EA | NEA | EAF   | OR (95% CI)      | P-value   | HetPVal  |
|----------------|-------------------------|---------------------|-------------|----|-----|-------|------------------|-----------|----------|
| 1:22141722     | <i>WNT4</i>             | <i>WNT4</i>         | rs3820282   | T  | C   | 0.154 | 1.15 (1.13-1.17) | 2.60E-49  | 0.016    |
| 1:172162145    | <i>DNM3</i>             | <i>DNM3</i>         | rs61807787  | T  | C   | 0.290 | 1.04 (1.03-1.06) | 3.89E-08  | 0.729    |
| 1:241860596    | <i>EXO1</i>             | <i>EXO1, FH</i>     | rs4149909   | G  | A   | 0.033 | 1.13 (1.08-1.18) | 1.16E-08  | 0.265    |
| 1:244151650    | <i>ZBTB18, C1orf100</i> | <i>ZBTB18</i>       | rs2183478   | G  | A   | 0.182 | 1.07 (1.05-1.09) | 1.75E-11  | 0.774    |
| 1:248897507    | <i>PGBD2</i>            | <i>ZNF692</i>       | rs4335411   | A  | G   | 0.760 | 1.06 (1.04-1.08) | 4.12E-10  | 0.376    |
| 2:11540277     | <i>GREB1</i>            | <i>GREB1</i>        | rs35417544  | T  | C   | 0.735 | 1.08 (1.07-1.10) | 3.94E-24  | 0.716    |
| 2:28106534     | <i>BABAM2</i>           | <i>BABAM2</i>       | rs74576866  | G  | A   | 0.080 | 1.09 (1.06-1.11) | 7.74E-11  | 0.780    |
| 2:66863235     | <i>MEIS1</i>            | <i>MEIS1</i>        | rs17631680  | C  | T   | 0.100 | 0.93 (0.91-0.95) | 1.93E-10  | 0.127    |
| 2:99454113     | <i>REV1</i>             | <i>REV1</i>         | rs13392042  | G  | A   | 0.577 | 1.05 (1.03-1.06) | 4.21E-11  | 0.217    |
| 2:207258660    | <i>MYOSLID, KLF7</i>    | <i>MYOSLID</i>      | rs10804157  | C  | T   | 0.443 | 1.04 (1.03-1.05) | 1.04E-08  | 0.143    |
| 2:241720139    | <i>ING5</i>             | <i>ING5</i>         | rs34766121  | T  | C   | 0.237 | 1.06 (1.04-1.08) | 5.02E-10  | 0.278    |
| 3:4674530      | <i>ITPR1</i>            | <i>ITPR1</i>        | rs3804984   | C  | T   | 0.384 | 0.95 (0.93-0.96) | 8.06E-15  | 0.021    |
| 3:24213259     | <i>THR1</i>             | <i>THR1</i>         | rs1010961   | A  | T   | 0.447 | 1.04 (1.03-1.06) | 1.64E-10  | 0.109    |
| 3:27488262     | <i>SLC4A7</i>           | <i>NEK10</i>        | rs35701251  | A  | T   | 0.243 | 1.05 (1.03-1.06) | 1.59E-08  | 0.909    |
| 3:169768720    | <i>ACTR3, TERC</i>      | <i>TERC</i>         | rs35446936  | A  | G   | 0.252 | 0.94 (0.92-0.95) | 1.01E-16  | 0.033    |
| 3:185807411    | <i>IGF2BP2</i>          | <i>IGF2BP2</i>      | rs13060777  | G  | A   | 0.264 | 1.05 (1.04-1.07) | 1.14E-11  | 0.595    |
| 4:53684007     | <i>LNX1</i>             | <i>LNX1</i>         | rs62323682  | C  | T   | 0.064 | 1.16 (1.13-1.19) | 5.67E-25  | 0.498    |
| 4:69735020     | <i>SULT1B1</i>          | <i>SULT1E1</i>      | rs12640488  | G  | A   | 0.475 | 1.07 (1.05-1.08) | 6.21E-21  | 0.511    |
| 4:94572095     | <i>PDLIM5</i>           | <i>BMPR1B</i>       | rs2452597   | G  | A   | 0.306 | 1.05 (1.03-1.06) | 9.42E-11  | 0.781    |
| 4:99031559     | <i>METAP1, ADH5</i>     | <i>ADH5</i>         | rs1037475   | G  | A   | 0.566 | 1.04 (1.03-1.05) | 8.38E-09  | 0.707    |
| 5:1279913      | <i>TERT</i>             | <i>TERT</i>         | rs2242652   | A  | G   | 0.205 | 1.12 (1.11-1.14) | 5.86E-41  | 0.005    |
| 5:133099880    | <i>HSPA4</i>            | <i>HSPA4</i>        | rs4367292   | T  | C   | 0.266 | 0.96 (0.94-0.97) | 2.49E-08  | 0.882    |
| 5:177023836    | <i>ZNF346</i>           | <i>UIMC1, FGFR4</i> | rs2456181   | G  | C   | 0.494 | 1.05 (1.04-1.07) | 4.20E-12  | 0.059    |
| 6:34240996     | <i>HMGAI</i>            | <i>HMGAI</i>        | rs41269026  | A  | C   | 0.041 | 1.11 (1.07-1.15) | 4.02E-09  | 0.998    |
| 6:36653670     | <i>CDKN1A</i>           | <i>CDKN1A</i>       | rs10456443  | A  | G   | 0.203 | 0.95 (0.93-0.96) | 2.67E-10  | 0.039    |
| 6:109054915    | <i>SESN1</i>            | <i>SESN1</i>        | rs11153158  | C  | T   | 0.126 | 0.93 (0.92-0.95) | 1.05E-10  | 0.243    |
| 6:152241136    | <i>SYNE1</i>            | <i>ESR1</i>         | rs58415480  | G  | C   | 0.178 | 1.22 (1.19-1.24) | 1.86E-104 | 0.002    |
| 7:33008785     | <i>FKBP9, NT5C3A</i>    | <i>BBS9</i>         | rs4723230   | T  | C   | 0.797 | 1.05 (1.03-1.07) | 4.68E-08  | 0.946    |
| 7:117273513    | <i>WNT2</i>             | <i>WNT2</i>         | rs2270206   | A  | C   | 0.153 | 1.06 (1.04-1.08) | 1.24E-09  | 0.525    |
| 7:121132432    | <i>CPED1, WNT16</i>     | <i>WNT16</i>        | rs12706314  | A  | G   | 0.531 | 1.04 (1.03-1.06) | 2.69E-10  | 0.777    |
| 7:130935964    | <i>LINC-PINT</i>        | <i>LINC-PINT</i>    | rs35908158  | C  | T   | 0.077 | 1.08 (1.05-1.10) | 1.60E-08  | 0.883    |
| 8:30452819     | <i>RBPMS</i>            | <i>RBPMS</i>        | rs13275869  | C  | T   | 0.486 | 0.96 (0.95-0.97) | 8.64E-09  | 0.520    |
| 8:128506035    | <i>LINC00824</i>        | <i>LINC00824</i>    | rs1516980   | C  | A   | 0.248 | 0.96 (0.94-0.97) | 2.72E-08  | 0.987    |
| 9:680714       | <i>KANK1, ANKRD15</i>   | <i>KANK1</i>        | rs10815466  | A  | G   | 0.168 | 1.10 (1.08-1.12) | 9.51E-24  | 0.060    |
| 9:89639982     | <i>GADD45G, SEMA4D</i>  | <i>GADD45G</i>      | rs28508285  | G  | A   | 0.091 | 1.07 (1.04-1.09) | 1.49E-08  | 0.362    |
| 10:21517903    | <i>SKIDA1</i>           | <i>DNAJC1</i>       | rs946711    | C  | A   | 0.331 | 1.05 (1.03-1.06) | 2.96E-10  | 0.460    |
| 10:31678920    | <i>ZEB1, ARHGAP12</i>   | <i>ZEB1</i>         | rs72784785  | C  | T   | 0.225 | 0.93 (0.92-0.95) | 2.35E-16  | 0.598    |
| 10:88331783    | <i>RNLS</i>             | <i>RNLS</i>         | rs1426619   | T  | C   | 0.445 | 1.04 (1.03-1.06) | 4.92E-09  | 0.653    |
| 10:103918139   | <i>STN1</i>             | <i>SH3PXD2A</i>     | rs4387287   | C  | A   | 0.842 | 0.91 (0.89-0.92) | 5.61E-25  | 0.235    |
| 11:197557      | <i>ODF3, BET1L</i>      | <i>PKP3</i>         | rs7103852   | G  | A   | 0.923 | 1.13 (1.10-1.16) | 5.10E-21  | 0.575    |
| 11:30204981    | <i>FSHB</i>             | <i>FSHB</i>         | rs11031006  | A  | G   | 0.150 | 0.91 (0.89-0.93) | 1.62E-22  | 0.708    |
| 11:32342641    | <i>WT1</i>              | <i>WT1</i>          | rs2057178   | A  | G   | 0.131 | 1.14 (1.12-1.17) | 7.32E-41  | 3.23E-05 |
| 11:35062086    | <i>PDHX</i>             | <i>CD44</i>         | rs2553773   | G  | C   | 0.561 | 1.07 (1.06-1.09) | 1.19E-23  | 0.074    |
| 11:108444879   | <i>C11orf65</i>         | <i>ATM</i>          | rs149934734 | T  | C   | 0.021 | 1.36 (1.29-1.42) | 4.74E-36  | 0.018    |
| 11:112703765   | <i>LOC105369496</i>     | <i>LOC105369496</i> | rs10891420  | C  | T   | 0.421 | 1.05 (1.03-1.06) | 1.38E-10  | 0.019    |
| 12:46402739    | <i>SLC38A2</i>          | <i>SLC38A2</i>      | rs2131371   | C  | A   | 0.685 | 1.08 (1.06-1.09) | 1.03E-23  | 0.462    |
| 12:70756878    | <i>PTPRR</i>            | <i>PTPRR</i>        | rs11178393  | C  | T   | 0.102 | 0.92 (0.90-0.95) | 7.46E-12  | 0.402    |
| 12:123379073   | <i>KMT5A, PITPNM2</i>   | <i>KMT5A</i>        | rs28583837  | A  | G   | 0.207 | 0.95 (0.93-0.96) | 9.67E-10  | 0.379    |
| 13:40149807    | <i>FOXO1</i>            | <i>FOXO1</i>        | rs117245733 | A  | G   | 0.021 | 1.42 (1.35-1.49) | 1.78E-41  | 0.000    |
| 15:67922458    | <i>SKOR1, PIAS1</i>     | <i>PIAS1</i>        | rs12148374  | C  | T   | 0.442 | 0.96 (0.95-0.97) | 1.37E-09  | 0.832    |
| 16:50059327    | <i>HEATR3</i>           | <i>BRD7</i>         | rs12599260  | A  | G   | 0.728 | 1.05 (1.04-1.07) | 1.09E-11  | 0.002    |
| 16:51447685    | <i>AC007344.1</i>       | <i>AC007344.1</i>   | rs66998222  | A  | G   | 0.193 | 0.94 (0.93-0.96) | 7.53E-12  | 0.345    |
| 17:7668434     | <i>TP53</i>             | <i>TP53</i>         | rs78378222  | G  | T   | 0.014 | 1.81 (1.71-1.92) | 3.88E-86  | 1.50E-13 |
| 17:12652500    | <i>MYOCD</i>            | <i>MYOCD</i>        | rs12601765  | T  | G   | 0.299 | 1.04 (1.03-1.06) | 3.08E-08  | 0.400    |
| 19:22032639    | <i>ZNF257</i>           | <i>ZNF257</i>       | rs8105767   | G  | A   | 0.298 | 1.05 (1.03-1.06) | 2.63E-09  | 0.143    |
| 20:5967581     | <i>MCM8</i>             | <i>MCM8</i>         | rs16991615  | A  | G   | 0.052 | 1.12 (1.09-1.15) | 5.15E-13  | 0.081    |
| 20:57441016    | <i>CTCF</i>             | <i>RBM38</i>        | rs13039273  | C  | T   | 0.456 | 1.04 (1.03-1.06) | 3.08E-09  | 0.874    |
| 20:63638397    | <i>STMN3</i>            | <i>SLC2A4RG</i>     | rs75691080  | T  | C   | 0.095 | 0.92 (0.90-0.95) | 7.79E-11  | 0.044    |
| 21:35072824    | <i>RUNX1</i>            | <i>RUNX1</i>        | rs2834747   | G  | T   | 0.302 | 0.96 (0.94-0.97) | 1.44E-08  | 0.711    |
| 22:36287509    | <i>MYH9, APOL1</i>      | <i>MYH9</i>         | rs9610482   | T  | C   | 0.189 | 1.06 (1.04-1.08) | 7.89E-11  | 0.354    |
| 22:40269221    | <i>TNRC6B</i>           | <i>MKL1</i>         | rs112251865 | T  | C   | 0.223 | 1.09 (1.07-1.11) | 1.21E-26  | 0.157    |
| X:70928740     | <i>SLC7A3, MED12</i>    | <i>FOXO4</i>        | rs5936604   | C  | T   | 0.683 | 0.93 (0.91-0.94) | 1.00E-17  | 0.008    |
| X:132178061    | <i>FRMD7, RAP2C</i>     | <i>RAP2C</i>        | rs5930554   | C  | T   | 0.312 | 1.16 (1.14-1.18) | 1.04E-59  | 0.0007   |

**Table S2. Genome-wide significant ( $p < 5 \times 10^{-8}$ ) loci in META-2.**

The table reports distinct loci (more than 1Mb apart) containing at least one variant associated with uterine leiomyomata (UL) at  $p < 5 \times 10^{-8}$ , *i.e.*, the standard threshold for genome-wide significance. META-2 was conducted genome-widely in 38,466 uterine leiomyomata (UL) cases and 329,437 female controls from FinnGen and a previous UL meta-analysis<sup>1</sup> using fixed-effect inverse variance-weighted method implemented in METAL. Indented rows indicate the lead variants of the independent association signals that were observed after conditioning the association tests on the locus-specific lead variant on the preceding row. The loci spanning over the  $\pm 1$ Mb locus definition are marked with asterisk (\*).

| Chr:Pos (hg38) | Nearest gene            | Candidate gene      | rsID        | EA | OA | EA <sub>FinnGen</sub> | OR (95% CI)      | P.value  | HetPVal |
|----------------|-------------------------|---------------------|-------------|----|----|-----------------------|------------------|----------|---------|
| 1:22141722     | <i>WNT4</i>             | <i>WNT4</i>         | rs3820282   | t  | c  | 0.157                 | 1.16 (1.13-1.18) | 4.11E-41 | 0.02952 |
| 1:172162145    | <i>DNM3</i>             | <i>DNM3</i>         | rs61807787  | t  | c  | 0.258                 | 1.05 (1.03-1.07) | 8.45E-09 | 0.2702  |
| 1:241860596    | <i>EXO1</i>             | <i>EXO1, FH</i>     | rs4149909   | a  | g  | 0.968                 | 0.87 (0.83-0.91) | 1.12E-08 | 0.4515  |
| 1:244151650    | <i>ZBTB18, C1orf100</i> | <i>ZBTB18</i>       | rs2183478   | a  | g  | 0.764                 | 0.93 (0.91-0.95) | 7.58E-12 | 0.4729  |
| 1:248897507    | <i>PGBD2</i>            | <i>ZNF692</i>       | rs4335411   | a  | g  | 0.752                 | 1.07 (1.04-1.09) | 3.56E-09 | 0.1961  |
| 2:11562535     | <i>GREB1</i>            | <i>GREB1</i>        | rs10929757  | a  | c  | 0.338                 | 0.93 (0.92-0.95) | 5.53E-17 | 0.4803  |
| 2:11515558     | <i>GREB1</i>            | <i>GREB1</i>        | rs13407702  | t  | g  | 0.115                 | 1.07 (1.04-1.09) | 2.19E-08 | n.a.    |
| 2:28213441     | <i>BABAM2</i>           | <i>BABAM2</i>       | rs4637064   | a  | g  | 0.707                 | 0.95 (0.93-0.97) | 2.78E-09 | 0.1366  |
| 2:66863235     | <i>MEIS1</i>            | <i>MEIS1</i>        | rs17631680  | t  | c  | 0.893                 | 1.09 (1.06-1.12) | 1.46E-10 | 0.3255  |
| 2:99447821     | <i>REV1</i>             | <i>REV1</i>         | rs1451246   | a  | c  | 0.445                 | 1.05 (1.03-1.07) | 5.32E-10 | 0.2963  |
| 2:207258660    | <i>MYOSLID, KLF7</i>    | <i>MYOSLID</i>      | rs10804157  | t  | c  | 0.595                 | 0.95 (0.94-0.97) | 3.50E-09 | 0.3833  |
| 2:207848303    | <i>PLEKHM3</i>          | <i>MYOSLID</i>      | rs7584910   | a  | g  | 0.443                 | 0.96 (0.94-0.97) | 4.75E-08 | n.a.    |
| 2:241710378    | <i>ING5</i>             | <i>ING5</i>         | rs6437284   | c  | g  | 0.727                 | 0.94 (0.92-0.96) | 2.07E-09 | 0.2493  |
| 3:4674530      | <i>ITPR1</i>            | <i>ITPR1</i>        | rs3804984   | t  | c  | 0.532                 | 1.06 (1.04-1.08) | 5.01E-13 | 0.0314  |
| 3:24213261     | <i>THRB</i>             | <i>THRB</i>         | rs2017200   | a  | t  | 0.444                 | 1.05 (1.03-1.07) | 5.50E-10 | 0.2165  |
| 3:27488262     | <i>SLC4A7</i>           | <i>NEK10</i>        | rs35701251  | a  | t  | 0.202                 | 1.05 (1.04-1.07) | 8.45E-09 | 0.6348  |
| 3:169768720    | <i>ACTRT3, TERC</i>     | <i>TERC</i>         | rs35446936  | a  | g  | 0.272                 | 0.93 (0.91-0.94) | 1.33E-16 | 0.1353  |
| 3:185805582    | <i>IGF2BP2</i>          | <i>IFG2BP2</i>      | rs66513933  | t  | c  | 0.709                 | 0.95 (0.94-0.97) | 3.40E-08 | 0.3404  |
| 4:53634371     | <i>LNX1</i>             | <i>LNX1</i>         | rs4864806   | a  | g  | 0.051                 | 1.17 (1.13-1.20) | 5.00E-21 | 0.6683  |
| 4:52992781     | <i>SCFD2</i>            | <i>LNX1</i>         | rs11735529  | c  | g  | 0.608                 | 0.95 (0.94-0.97) | 6.61E-09 | n.a.    |
| 4:53301527     | <i>SCFD2</i>            | <i>LNX1</i>         | rs188378292 | a  | g  | 0.002                 | 1.97 (1.55-2.51) | 2.98E-08 | n.a.    |
| 4:69658940     | <i>UGT2A1</i>           | <i>SULT1E1</i>      | rs4694227   | a  | t  | 0.687                 | 1.07 (1.06-1.09) | 3.99E-17 | 0.1984  |
| 4:69750098     | <i>SULT1B1</i>          | <i>SULT1E1</i>      | rs41292311  | t  | c  | 0.016                 | 0.80 (0.75-0.85) | 6.82E-12 | n.a.    |
| 4:94572095     | <i>PDLIM5</i>           | <i>BMPR1B</i>       | rs2452597   | a  | g  | 0.717                 | 0.95 (0.94-0.97) | 5.05E-09 | 0.8824  |
| 5:1279675      | <i>TERT</i>             | <i>TERT</i>         | rs10069690  | t  | c  | 0.296                 | 1.12 (1.10-1.14) | 1.60E-34 | 0.0054  |
| 5:177023836    | <i>ZNF346</i>           | <i>UIMC1, FGFR4</i> | rs2456181   | c  | g  | 0.499                 | 0.95 (0.94-0.97) | 2.38E-09 | 0.0382  |
| 6:108976313    | <i>ARMC2</i>            | <i>SESNI</i>        | rs12196819  | a  | g  | 0.150                 | 0.94 (0.91-0.96) | 2.62E-08 | 0.1554  |
| 6:152241136    | <i>SYNE1</i>            | <i>SYNE1, ESRI</i>  | rs58415480  | c  | g  | 0.769                 | 0.82 (0.81-0.84) | 2.08E-81 | 0.0004  |
| 6:152551137    | <i>SYNE1</i>            | <i>SYNE1, ESRI</i>  | rs9397523   | a  | g  | 0.542                 | 0.94 (0.93-0.96) | 1.33E-12 | n.a.    |
| 6:152245912    | <i>SYNE1</i>            | <i>SYNE1, ESRI</i>  | rs6901631   | t  | c  | 0.909                 | 1.07 (1.04-1.10) | 4.02E-08 | n.a.    |
| 7:120807406    | <i>TSPAN12</i>          | <i>WNT16</i>        | rs4730982   | t  | g  | 0.674                 | 0.95 (0.94-0.97) | 3.41E-08 | 0.0842  |
| 8:30444949     | <i>RBPMS</i>            | <i>RBPMS</i>        | rs4545054   | t  | c  | 0.536                 | 1.05 (1.03-1.06) | 6.29E-09 | 0.9012  |
| 8:129467485    | <i>GSDMC</i>            | <i>LINC00824</i>    | rs11786929  | t  | c  | 0.743                 | 0.95 (0.94-0.97) | 5.12E-09 | 0.0224  |
| 9:680714       | <i>KANK1, ANKRD15</i>   | <i>DMRT1, KANK1</i> | rs10815466  | a  | g  | 0.211                 | 1.11 (1.09-1.14) | 3.76E-25 | 0.4772  |
| 9:806912       | <i>DMRT1</i>            | <i>DMRT1, KANK1</i> | rs35469085  | c  | g  | 0.523                 | 0.93 (0.91-0.94) | 3.31E-20 | n.a.    |
| 9:854375       | <i>DMRT1</i>            | <i>DMRT1, KANK1</i> | rs7856727   | t  | g  | 0.581                 | 0.95 (0.94-0.97) | 4.75E-08 | n.a.    |
| 10:21695031    | <i>MLLT10</i>           | <i>DNAJC1</i>       | rs1243192   | a  | c  | 0.302                 | 1.06 (1.04-1.07) | 2.39E-10 | 0.4954  |
| 10:31666087    | <i>ZEB1, ARHGAP12</i>   | <i>ZEB1</i>         | rs7090544   | a  | g  | 0.728                 | 1.07 (1.05-1.09) | 3.64E-13 | 0.5477  |
| 10:76884502    | <i>KCNMA1</i>           | <i>KCNMA1</i>       | rs2082415   | t  | g  | 0.520                 | 1.05 (1.03-1.06) | 2.80E-08 | 0.4600  |
| *10:101726828  | <i>FGF8</i>             | <i>SLK</i>          | rs189195982 | t  | c  | 0.030                 | 1.26 (1.17-1.36) | 2.78E-10 | 0.2851  |
| *10:102788270  | <i>WBP1L</i>            | <i>SLK</i>          | rs75731980  | t  | c  | 0.064                 | 1.23 (1.17-1.30) | 2.42E-16 | 0.8007  |
| *10:103873824  | <i>OBFC1</i>            | <i>SLK</i>          | rs182218101 | t  | c  | 0.972                 | 0.66 (0.61-0.72) | 4.86E-26 | 0.3644  |
| 10:103918139   | <i>OBFC1</i>            | <i>SLK</i>          | rs4387287   | a  | c  | 0.137                 | 1.10 (1.08-1.12) | 2.44E-18 | n.a.    |
| 10:103895645   | <i>OBFC1</i>            | <i>SLK</i>          | rs188848367 | t  | c  | 0.019                 | 1.31 (1.20-1.43) | 3.92E-09 | n.a.    |
| *10:105587387  | <i>SORCS3</i>           | <i>SLK</i>          | rs17119191  | t  | g  | 0.972                 | 0.76 (0.70-0.82) | 5.81E-13 | 0.3142  |
| *10:106822067  | <i>SORCS1</i>           | <i>SLK</i>          | rs1336619   | t  | c  | 0.030                 | 1.25 (1.17-1.34) | 3.48E-10 | 0.1272  |
| 11:197557      | <i>ODF3, BETIL</i>      | <i>PKP3</i>         | rs7103852   | a  | g  | 0.078                 | 0.87 (0.85-0.90) | 2.02E-19 | 0.9974  |
| 11:224063      | <i>SIRT3</i>            | <i>PKP3</i>         | rs12222188  | a  | g  | 0.023                 | 0.86 (0.83-0.90) | 1.99E-12 | n.a.    |
| 11:30204981    | <i>FSHB</i>             | <i>FSHB</i>         | rs11031006  | a  | g  | 0.165                 | 0.92 (0.90-0.94) | 1.32E-15 | 0.3740  |
| 11:32343884    | <i>WT1</i>              | <i>WT1</i>          | rs11031731  | a  | g  | 0.074                 | 1.16 (1.14-1.19) | 1.24E-37 | 0.0005  |
| 11:32347198    | <i>WT1</i>              | <i>WT1</i>          | rs2207548   | a  | c  | 0.336                 | 1.07 (1.05-1.08) | 3.46E-15 | n.a.    |
| 11:32325691    | <i>WT1</i>              | <i>WT1</i>          | rs2038318   | t  | g  | 0.707                 | 1.06 (1.04-1.08) | 2.15E-11 | n.a.    |
| 11:35063906    | <i>PDHX</i>             | <i>CD44</i>         | rs2553772   | t  | g  | 0.472                 | 0.94 (0.92-0.95) | 9.85E-18 | 0.0799  |
| 11:108444879   | <i>C11orf65</i>         | <i>ATM</i>          | rs149934734 | t  | c  | 0.009                 | 1.38 (1.30-1.46) | 1.74E-27 | 0.0308  |
| 11:108177255   | <i>NPAT</i>             | <i>ATM</i>          | rs1519074   | a  | g  | 0.775                 | 1.11 (1.09-1.13) | 3.75E-23 | n.a.    |

| Chr:Pos (hg38) | Nearest gene        | Candidate gene      | rsID        | EA | OA   | EAF <sub>FinnGen</sub> | OR (95% CI)      | P.value  | HetPVal  |
|----------------|---------------------|---------------------|-------------|----|------|------------------------|------------------|----------|----------|
| 11:112703765   | <i>LOC105369496</i> | <i>LOC105369496</i> | rs10891420  | t  | c    | 0.531                  | 0.95 (0.94-0.97) | 3.93E-10 | 0.0477   |
| 12:46410392    | <i>SLC38A2</i>      | <i>SLC38A2</i>      | rs1472178   | t  | c    | 0.340                  | 0.94 (0.92-0.95) | 7.03E-15 | 0.9303   |
| 12:68692314    | <i>NUP107</i>       | <i>MDM2</i>         | rs142808358 | t  | c    | 0.028                  | 0.87 (0.83-0.91) | 5.45E-09 | 0.9583   |
| 12:70756878    | <i>PTPRR</i>        | <i>PTPRR</i>        | rs11178393  | t  | c    | 0.916                  | 1.08 (1.05-1.11) | 2.82E-09 | 0.3833   |
| 12:123405729   | <i>KMT5A</i>        | <i>KMT5A</i>        | rs28576953  | t  | c    | 0.211                  | 0.94 (0.92-0.96) | 9.46E-10 | 0.1098   |
| *13:38939164   | <i>STOML3</i>       | <i>FOXO1</i>        | rs149775438 | a  | c    | 0.980                  | 0.76 (0.70-0.83) | 1.10E-09 | 0.8152   |
| 13:39726408    | <i>COG6</i>         | <i>FOXO1</i>        | rs9548898   | a  | g    | 0.537                  | 1.05 (1.04-1.07) | 1.05E-11 | n.a.     |
| *13:40149807   | <i>FOXO1</i>        | <i>FOXO1</i>        | rs117245733 | a  | g    | 0.030                  | 1.46 (1.38-1.54) | 9.16E-39 | 0.0013   |
| 13:40605661    | <i>FOXO1</i>        | <i>FOXO1</i>        | rs7986407   | a  | g    | 0.642                  | 0.93 (0.91-0.95) | 1.79E-18 | n.a.     |
| 13:39726408    | <i>COG6</i>         | <i>FOXO1</i>        | rs9548898   | a  | g    | 0.537                  | 1.05 (1.04-1.07) | 1.45E-11 | n.a.     |
| 13:40162152    | <i>FOXO1</i>        | <i>FOXO1</i>        | rs6563799   | t  | c    | 0.245                  | 1.06 (1.04-1.08) | 1.04E-09 | n.a.     |
| 13:39898446    | <i>COG6</i>         | <i>FOXO1</i>        | rs9576914   | t  | c    | 0.554                  | 0.95 (0.94-0.97) | 2.84E-09 | n.a.     |
| 15:68335825    | <i>ITGA11</i>       | <i>PIAS1</i>        | rs2306022   | t  | c    | 0.088                  | 1.09 (1.06-1.12) | 1.68E-09 | 0.4266   |
| 16:50056732    | <i>HEATR3</i>       | <i>HEATR3, BRD7</i> | rs62033024  | c  | g    | 0.181                  | 0.93 (0.92-0.95) | 1.81E-12 | 0.0009   |
| 16:50048520    | <i>CNEP1R1</i>      | <i>HEATR3, BRD7</i> | rs2058814   | t  | g    | 0.198                  | 0.94 (0.92-0.96) | 2.05E-10 | n.a.     |
| 16:51447685    | <i>AC007344.1</i>   | <i>AC007344.1</i>   | rs66998222  | a  | g    | 0.153                  | 0.93 (0.91-0.95) | 2.12E-12 | 0.824    |
| *17:7668434    | <i>TP53</i>         | <i>TP53</i>         | rs78378222  | t  | g    | 0.983                  | 0.51 (0.47-0.54) | 9.36E-86 | 4.19E-09 |
| *17:8767403    | <i>SPDYE4</i>       | <i>TP53</i>         | rs74876186  | a  | g    | 0.013                  | 1.40 (1.26-1.56) | 1.10E-09 | 0.5213   |
| 17:7796745     | <i>DNAH2</i>        | <i>TP53</i>         | rs138420351 | t  | c    | 0.039                  | 1.38 (1.31-1.46) | 1.15E-30 | n.a.     |
| 17:12656880    | <i>MYOCD</i>        | <i>MYOCD</i>        | rs12449987  | t  | c    | 0.560                  | 0.96 (0.94-0.97) | 2.05E-08 | 0.1577   |
| 19:22032639    | <i>ZNF257</i>       | <i>ZNF257</i>       | rs8105767   | a  | g    | 0.682                  | 0.95 (0.94-0.97) | 9.89E-09 | 0.2546   |
| 20:5967581     | <i>MCM8</i>         | <i>MCM8</i>         | rs16991615  | a  | g    | 0.021                  | 1.14 (1.09-1.18) | 9.96E-12 | 0.1533   |
| 20:63638397    | <i>STMN3</i>        | <i>SLC2A4RG</i>     | rs75691080  | t  | c    | 0.114                  | 0.93 (0.90-0.95) | 2.38E-08 | 0.0181   |
| 22:28779069    | <i>CCDC117</i>      | ?? <i>Sakaue</i>    | rs71758825  | t  | tctc | 0.096                  | 1.13 (1.08-1.18) | 1.07E-08 | 0.5253   |
| 22:36287509    | <i>MYH9, APOL1</i>  | <i>MYH9</i>         | rs9610482   | t  | c    | 0.172                  | 1.06 (1.04-1.08) | 1.37E-09 | 0.5066   |
| 22:40269221    | <i>TNRC6B</i>       | <i>MKL1</i>         | rs112251865 | t  | c    | 0.252                  | 1.10 (1.08-1.12) | 1.20E-23 | 0.3355   |
| X:70762863     | <i>TEX11</i>        | <i>FOXO4</i>        | rs5936980   | a  | g    | 0.424                  | 1.09 (1.07-1.11) | 1.52E-15 | 0.0201   |
| X:132178061    | <i>FRMD7, RAP2C</i> | <i>RAPC2</i>        | rs5930554   | t  | c    | 0.684                  | 0.87 (0.85-0.89) | 8.36E-39 | 7.58E-06 |

n.a. = not available

**Table S3. Fine-mapping results of META-1.**

We applied the FinnGen finemapping pipeline (available at <https://github.com/FINNGEN/finemapping-pipeline>, accessed on 2/2/2022) with default parameters. In brief, the pipeline calculates linkage disequilibrium within the regions of interest with LDstore2<sup>6</sup> using FinnGen samples, generates 99 % credible sets using the SUM of Single Effects (SuSiE)<sup>7</sup> and provides a summary for the results.

| rsid        | position     | nearest gene        | credible set size | interval (bp) | start (bp) | end (bp)  |
|-------------|--------------|---------------------|-------------------|---------------|------------|-----------|
| rs3820282   | 1:22141722   | <i>WNT4</i>         | 6                 | 45495         | 22096228   | 22141722  |
| rs61807787  | 1:172162145  | <i>DNM3</i>         | 106               | 248185        | 171970150  | 172218334 |
| rs4149909   | 1:241860596  | <i>EXO1</i>         | 13                | 18808         | 241848042  | 241866849 |
| rs2183478   | 1:244151650  | <i>ZBTB18</i>       | 2                 | 61549         | 244151650  | 244213198 |
| rs4335411   | 1:248897507  | <i>PGBD2</i>        | 4                 | 35798         | 248861710  | 248897507 |
| rs35417544  | 2:11540277   | <i>GREB1</i>        | 24                | 23381         | 11522052   | 11545432  |
| rs74576866  | 2:28106534   | <i>BABAM2</i>       | 20                | 142094        | 28077447   | 28219540  |
| rs17631680  | 2:66863235   | <i>MEIS1</i>        | 1                 | 1             | 66863235   | 66863235  |
| rs13392042  | 2:99454113   | <i>REVI</i>         | 138               | 204163        | 99314447   | 99518609  |
| rs10804157  | 2:207258660  | <i>MYOSLID</i>      | 7                 | 608387        | 207257277  | 207865663 |
| rs34766121  | 2:241720139  | <i>ING5</i>         | 2                 | 6294          | 241720139  | 241726432 |
| rs3804984   | 3:4674530    | <i>ITPR1</i>        | 1                 | 1             | 4674530    | 4674530   |
| rs1010961   | 3:24213259   | <i>THRB</i>         | 7                 | 9101          | 24209772   | 24218872  |
| rs35701251  | 3:27488262   | <i>SLC4A7</i>       | 107               | 133939        | 27377371   | 27511309  |
| rs35446936  | 3:169768720  | <i>ACTRT3</i>       | 27                | 51018         | 169759718  | 169810735 |
| rs13060777  | 3:185807411  | <i>IGF2BP2</i>      | 58                | 52911         | 185770515  | 185823425 |
| rs62323682  | 4:53684007   | <i>LNX1</i>         | 14                | 49637         | 53634371   | 53684007  |
| rs12640488  | 4:69735020   | <i>SULT1B1</i>      | 32                | 123121        | 69658940   | 69782060  |
| rs2452597   | 4:94572095   | <i>PDLIM5</i>       | 41                | 136859        | 94537299   | 94674157  |
| rs1037475   | 4:99031559   | <i>METAP1</i>       | 32                | 95051         | 98961982   | 99057032  |
| rs2242652   | 5:1279913    | <i>TERT</i>         | 2                 | 239           | 1279675    | 1279913   |
| rs4367292   | 5:133099880  | <i>HSPA4</i>        | 83                | 70426         | 133039643  | 133110068 |
| rs2456181   | 5:177023836  | <i>ZNF346</i>       | 55                | 170805        | 176896297  | 177067101 |
| rs41269026  | 6:34240996   | <i>HMGAI</i>        | 57                | 196791        | 34197574   | 34394364  |
| rs10456443  | 6:36653670   | <i>CDKN1A</i>       | 16                | 9344          | 36650363   | 36659706  |
| rs11153158  | 6:109054915  | <i>SESNI</i>        | 57                | 95237         | 108960208  | 109055444 |
| rs58415480  | 6:152241136  | <i>SYNE1</i>        | 1                 | 1             | 152241136  | 152241136 |
| rs4723230   | 7:33008785   | <i>FKBP9</i>        | 103               | 81254         | 33006946   | 33088199  |
| rs2270206   | 7:117273513  | <i>WNT2</i>         | 3                 | 5825          | 117267689  | 117273513 |
| rs12706314  | 7:121132432  | <i>CPEDI</i>        | 60                | 407085        | 120818924  | 121226008 |
| rs35908158  | 7:130935964  | <i>LINC-PINT</i>    | 9                 | 12539         | 130926493  | 130939031 |
| rs13275869  | 8:30452819   | <i>RBPMS</i>        | 25                | 353697        | 30196778   | 30550474  |
| rs1516980   | 8:128506035  | <i>LINC00824</i>    | 134               | 220942        | 128298931  | 128519872 |
| rs10815466  | 9:680714     | <i>KANK1</i>        | 13                | 138136        | 667680     | 805815    |
| rs28508285  | 9:89639982   | <i>GADD45G</i>      | 3                 | 138334        | 89501649   | 89639982  |
| rs946711    | 10:21517903  | <i>SKIDA1</i>       | 35                | 205612        | 21494705   | 21700316  |
| rs72784785  | 10:31678920  | <i>ZEB1</i>         | 34                | 56512         | 31624962   | 31681473  |
| rs1426619   | 10:88331783  | <i>RNLS</i>         | 71                | 169136        | 88294511   | 88463646  |
| rs4387287   | 10:103918139 | <i>TN1</i>          | 7                 | 7443          | 103915096  | 103922538 |
| rs7103852   | 11:197557    | <i>ODF3,BETIL</i>   | 16                | 67925         | 197557     | 265481    |
| rs11031006  | 11:30204981  | <i>FSHB</i>         | 18                | 118370        | 30204809   | 30323178  |
| rs2057178   | 11:32342641  | <i>WT1</i>          | 9                 | 23547         | 32325288   | 32348834  |
| rs2553773   | 11:35062086  | <i>PDHX</i>         | 27                | 14634         | 35062086   | 35076719  |
| rs149934734 | 11:108444879 | <i>C11orf65</i>     | 4                 | 213682        | 108272729  | 108486410 |
| rs10891420  | 11:112703765 | <i>LOC105369496</i> | 1                 | 1             | 112703765  | 112703765 |
| rs2131371   | 12:46402739  | <i>SLC38A2</i>      | 68                | 73721         | 46389870   | 46463590  |
| rs11178393  | 12:70756878  | <i>PTPRR</i>        | 10                | 12875         | 70751752   | 70764626  |
| rs28583837  | 12:123379073 | <i>KMT5A</i>        | 110               | 1265069       | 123129018  | 124394086 |
| rs117245733 | 13:40149807  | <i>FOXO1</i>        | 1                 | 1             | 40149807   | 40149807  |
| rs12148374  | 15:67922458  | <i>SKOR1,PLASI</i>  | 38                | 445721        | 67890105   | 68335825  |
| rs12599260  | 16:50059327  | <i>HEATR3</i>       | 46                | 75529         | 50028661   | 50104189  |
| rs66998222  | 16:51447685  | <i>AC007344.1</i>   | 51                | 1425558       | 50028661   | 51454218  |
| rs78378222  | 17:7668434   | <i>TP53</i>         | 1                 | 1             | 7668434    | 7668434   |
| rs12601765  | 17:12652500  | <i>MYOCD</i>        | 7                 | 14865         | 12643623   | 12658487  |
| rs8105767   | 19:22032639  | <i>ZNF257</i>       | 173               | 538899        | 21938656   | 22477554  |
| rs16991615  | 20:5967581   | <i>MCM8</i>         | 1                 | 1             | 5967581    | 5967581   |
| rs13039273  | 20:57441016  | <i>CTCF</i>         | 4                 | 4528          | 57441016   | 57445543  |
| rs75691080  | 20:63638397  | <i>STMN3</i>        | 1                 | 1             | 63638397   | 63638397  |
| rs2834747   | 21:35072824  | <i>RUNX1</i>        | 7                 | 16610         | 35072753   | 35089362  |
| rs9610482   | 22:36287509  | <i>MYH9</i>         | 8                 | 28715         | 36287509   | 36316223  |
| rs112251865 | 22:40269221  | <i>TNRC6B</i>       | 18                | 186456        | 40135641   | 40322096  |
| rs5936604   | 23:70889039  | <i>SLC7A3</i>       | 6                 | 38152         | 70888397   | 70926548  |
| rs5930554   | 23:132178061 | <i>FRMD7</i>        | 16                | 80267         | 132117298  | 132197564 |

**Table S4. Fine-mapping results of META-2.**

We applied the FinnGen finemapping pipeline (available at <https://github.com/FINNGEN/finemapping-pipeline>, accessed on 2/2/2022) with default parameters. In brief, the pipeline calculates linkage disequilibrium within the regions of interest with LDstore2<sup>6</sup> using FinnGen samples, generates 99 % credible sets using the SUM of Single Effects (SuSiE)<sup>7</sup> and provides a summary for the results.

| rsid        | position     | nearest gene        | credible set size | interval (bp) | start (bp) | end (bp)  |
|-------------|--------------|---------------------|-------------------|---------------|------------|-----------|
| rs3820282   | 1:22141722   | <i>WNT4</i>         | 6                 | 45495         | 22096228   | 22141722  |
| rs61807787  | 1:172162145  | <i>DNM3</i>         | 73                | 215801        | 172002534  | 172218334 |
| rs4149909   | 1:241860596  | <i>EXO1</i>         | 2                 | 10366         | 241860596  | 241870961 |
| rs2183478   | 1:244151650  | <i>ZBTB18</i>       | 2                 | 93            | 244151558  | 244151650 |
| rs4335411   | 1:248897507  | <i>PGBD2</i>        | 4                 | 45077         | 248861710  | 248906786 |
| rs10929757  | 2:11562535   | <i>GREB1</i>        | 1                 | 1             | 11562535   | 11562535  |
| rs4637064   | 2:28213441   | <i>BABAM2</i>       | 61                | 1181058       | 27156503   | 28337560  |
| rs17631680  | 2:66863235   | <i>MEIS1</i>        | 1                 | 1             | 66863235   | 66863235  |
| rs1451246   | 2:99447821   | <i>REV1</i>         | 69                | 178093        | 99314447   | 99492539  |
| rs10804157  | 2:207258660  | <i>MYOSLID</i>      | 8                 | 8720          | 207257277  | 207265996 |
| rs6437284   | 2:241710378  | <i>ING5</i>         | 37                | 61383         | 241667096  | 241728478 |
| rs3804984   | 3:4674530    | <i>ITPR1</i>        | 1                 | 1             | 4674530    | 4674530   |
| rs2017200   | 3:24213261   | <i>THRB</i>         | 10                | 33694         | 24185179   | 24218872  |
| rs35701251  | 3:27488262   | <i>NEK10</i>        | 99                | 133939        | 27377371   | 27511309  |
| rs35446936  | 3:169768720  | <i>TERC</i>         | 26                | 51018         | 169759718  | 169810735 |
| rs66513933  | 3:185805582  | <i>IFG2BP2</i>      | 64                | 59017         | 185770515  | 185829531 |
| rs4864806   | 4:53634371   | <i>LNX1</i>         | 28                | 49637         | 53634371   | 53684007  |
| rs4694227   | 4:69658940   | <i>SULT1B1</i>      | 23                | 123121        | 69658940   | 69782060  |
| rs2452597   | 4:94572095   | <i>PDLIM5</i>       | 42                | 126001        | 94548157   | 94674157  |
| rs10069690  | 5:1279675    | <i>TERT</i>         | 1                 | 1             | 1279675    | 1279675   |
| rs2456181   | 5:177023836  | <i>ZNF346</i>       | 62                | 170805        | 176896297  | 177067101 |
| rs12196819  | 6:108976313  | <i>ARMC2</i>        | 160               | 98740         | 108956705  | 109055444 |
| rs58415480  | 6:152241136  | <i>SYNE1</i>        | 1                 | 1             | 152241136  | 152241136 |
| rs4730982   | 7:120807406  | <i>TSPAN12</i>      | 41                | 109929        | 120770147  | 120880075 |
| rs4545054   | 8:30444949   | <i>RBPMS</i>        | 24                | 107076        | 30443399   | 30550474  |
| rs11786929  | 8:129467485  | <i>GSDMC</i>        | 9                 | 18602         | 129448884  | 129467485 |
| rs10815466  | 9:680714     | <i>KANK1</i>        | 3                 | 2717          | 680714     | 683430    |
| rs1243192   | 10:21695031  | <i>MLLT10</i>       | 30                | 205612        | 21494705   | 21700316  |
| rs7090544   | 10:31666087  | <i>ZEB1</i>         | 36                | 61057         | 31624962   | 31686018  |
| rs2082415   | 10:76884502  | <i>KCNMA1</i>       | 4410              | 2999032       | 75385239   | 78384270  |
| rs189195982 | 10:101726828 | <i>FGF8</i>         | 12                | 433026        | 101726828  | 102159853 |
| rs75731980  | 10:102788270 | <i>WBP1L</i>        | 3                 | 160004        | 102788270  | 102948273 |
| rs182218101 | 10:103873824 | <i>OBFC1</i>        | 2                 | 29588         | 103844237  | 103873824 |
| rs17119191  | 10:105587387 | <i>SORCS3</i>       | 15                | 642130        | 105095632  | 105737761 |
| rs1336619   | 10:106822067 | <i>SORCS1</i>       | 24                | 582458        | 106329275  | 106911732 |
| rs7103852   | 11:197557    | <i>ODF3</i>         | 16                | 67925         | 197557     | 265481    |
| rs11031006  | 11:30204981  | <i>FSHB</i>         | 18                | 118370        | 30204809   | 30323178  |
| rs11031731  | 11:32343884  | <i>WT1</i>          | 2                 | 14004         | 32329881   | 32343884  |
| rs2553772   | 11:35063906  | <i>PDHX</i>         | 26                | 20058         | 35056662   | 35076719  |
| rs149934734 | 11:108444879 | <i>C11orf65</i>     | 4                 | 213682        | 108272729  | 108486410 |
| rs10891420  | 11:112703765 | <i>LOC105369496</i> | 28                | 29522         | 112693680  | 112723201 |
| rs1472178   | 12:46410392  | <i>SLC38A2</i>      | 79                | 73721         | 46389870   | 46463590  |
| rs142808358 | 12:68692314  | <i>NUP107</i>       | 3                 | 243755        | 68564481   | 68808235  |
| rs11178393  | 12:70756878  | <i>PTPRR</i>        | 18                | 27874         | 70751752   | 70779625  |
| rs28576953  | 12:123405729 | <i>KMT5A</i>        | 136               | 320052        | 123108835  | 123428886 |
| rs149775438 | 13:38939164  | <i>STOML3</i>       | 2                 | 399980        | 38939164   | 39339143  |
| rs117245733 | 13:40149807  | <i>FOXO1</i>        | 1                 | 1             | 40149807   | 40149807  |
| rs2306022   | 15:68335825  | <i>ITGAI1</i>       | 13                | 17113         | 68318713   | 68335825  |
| rs62033024  | 16:50056732  | <i>HEATR3</i>       | 67                | 112294        | 49991896   | 50104189  |
| rs66998222  | 16:51447685  | <i>AC007344.1</i>   | 9                 | 21780         | 51432439   | 51454218  |
| rs78378222  | 17:7668434   | <i>TP53</i>         | 1                 | 1             | 7668434    | 7668434   |
| rs74876186  | 17:8767403   | <i>SPDYE4</i>       | 2                 | 130623        | 8636781    | 8767403   |
| rs12449987  | 17:12656880  | <i>MYOCD</i>        | 27                | 15266         | 12643623   | 12658888  |
| rs8105767   | 19:22032639  | <i>ZNF257</i>       | 216               | 570782        | 21906773   | 22477554  |
| rs16991615  | 20:5967581   | <i>MCM8</i>         | 1                 | 1             | 5967581    | 5967581   |
| rs75691080  | 20:63638397  | <i>STMN3</i>        | 16                | 61305         | 63577093   | 63638397  |
| rs71758825  | 22:28779069  | <i>CCDC117</i>      | 124               | 874010        | 28224596   | 29098605  |
| rs9610482   | 22:36287509  | <i>MYH9</i>         | 8                 | 28715         | 36287509   | 36316223  |
| rs112251865 | 22:40269221  | <i>TNRC6B</i>       | 15                | 186456        | 40135641   | 40322096  |
| rs5936980   | X:70762863   | <i>TEX11</i>        | 8                 | 163686        | 70762863   | 70926548  |
| rs5930554   | X:132140742  | <i>FRMD7</i>        | 19                | 80267         | 132117298  | 132197564 |

cs\_size: the size of the credible set

**Table S5. Fine-mapping results of the secondary signals.**

We applied the FinnGen finemapping pipeline (available at <https://github.com/FINNGEN/finemapping-pipeline>, accessed on 2/2/2022) with default parameters. In brief, the pipeline calculates linkage disequilibrium within the regions of interest with LDstore2<sup>6</sup> using FinnGen samples, generates 99 % credible sets using the SUM of Single Effects (SuSiE)<sup>7</sup> and provides a summary for the results.

| cond. | rsid        | position     | nearest gene   | credible set size | interval (bp) | start (bp) | end (bp)  |
|-------|-------------|--------------|----------------|-------------------|---------------|------------|-----------|
| 1     | rs13407702  | 2:11515558   | <i>GREB1</i>   | 17                | 58841         | 11475067   | 11533908  |
| 1     | rs7584910   | 2:207848303  | <i>PLEKHM3</i> | 48                | 138584        | 207819617  | 207958200 |
| 1     | rs11735529  | 4:52992781   | <i>SCFD2</i>   | 16                | 35728         | 52957054   | 52992781  |
| 2     | rs188378292 | 4:53301527   | <i>SCFD2</i>   | 1                 | 1             | 53301527   | 53301527  |
| 1     | rs41292311  | 4:69750098   | <i>SULT1B1</i> | 3                 | 35313         | 69738255   | 69773567  |
| 1     | rs9397523   | 6:152551137  | <i>SYNE1</i>   | 1                 | 1             | 152551137  | 152551137 |
| 2     | rs6901631   | 6:152245912  | <i>SYNE1</i>   | 11                | 28999         | 152217850  | 152246848 |
| 1     | rs35469085  | 9:806912     | <i>DMRT1</i>   | 14                | 9155          | 804231     | 813385    |
| 2     | rs7856727   | 9:854375     | <i>DMRT1</i>   | 1                 | 1             | 854375     | 854375    |
| 1     | rs4387287   | 10:103918139 | <i>OBFC1</i>   | 6                 | 6351          | 103916188  | 103922538 |
| 2     | rs188848367 | 10:103895645 | <i>OBFC1</i>   | 16                | 1515494       | 102560691  | 104076184 |
| 1     | rs12222188  | 11:224063    | <i>SIRT3</i>   | 17                | 22829         | 202017     | 224845    |
| 2     | rs2038318   | 11:32325691  | <i>WT1</i>     | 1                 | 1             | 32325691   | 32325691  |
| 1     | rs2207548   | 11:32347198  | <i>WT1</i>     | 3                 | 8523          | 32338676   | 32347198  |
| 1     | rs1519074   | 11:108177255 | <i>NPAT</i>    | 27                | 382360        | 108112369  | 108494728 |
| 1     | rs7986407   | 13:40605661  | <i>FOXO1</i>   | 13                | 74954         | 40573021   | 40647975  |
| 2     | rs9548898   | 13:39726408  | <i>COG6</i>    | 68                | 116924        | 39661542   | 39778465  |
| 3     | rs6563799   | 13:40162152  | <i>FOXO1</i>   | 3                 | 4292          | 40160593   | 40164884  |
| 4     | rs9576914   | 13:39898446  | <i>COG6</i>    | 45                | 29226         | 39898446   | 39927671  |
| 1     | rs2058814   | 16:50048520  | <i>CNEPIR1</i> | 1                 | 1             | 50048520   | 50048520  |
| 1     | rs138420351 | 17:7796745   | <i>DNAH2</i>   | 1                 | 1             | 7796745    | 7796745   |

cond: the number of variants the signal is conditioned for

**Table S6. RegulomeDB annotation of the association lead variants near *MYOCD*.**

The RegulomeDB probability score is ranging from 0 to 1, with 1 being most likely to be a regulatory variant. ‘Ranking’ refers to following evidence: 1a, eQTL + TF binding + matched TF motif + matched DNase Footprint + DNase peak; 1b, eQTL + TF binding + any motif + DNase Footprint + DNase peak; 1c, eQTL + TF binding + matched TF motif + DNase peak; 1d, eQTL + TF binding + any motif + DNase peak; 1e, eQTL + TF binding + matched TF motif; 1f, eQTL + TF binding / DNase peak; 2a, TF binding + matched TF motif + matched DNase Footprint + DNase peak; 2b, TF binding + any motif + DNase Footprint + DNase peak; 2c, TF binding + matched TF motif + DNase peak; 3a, TF binding + any motif + DNase peak; 3b, TF binding + matched TF motif; 4, TF binding + DNase peak; 5, TF binding or DNase peak; 6, Motif hit; 7, Other. RegulomeDB ranking < 3 and/or probability score > 0.8 can be considered as evidence for altered regulatory consequences. Data was downloaded from RegulomeDB 02/10/2021.

| <u>Rsids</u> | <u>Probability</u> | <u>Ranking</u> |
|--------------|--------------------|----------------|
| rs11871444   | 0.60906            | 4              |
| rs12601765   | 0.0                | 5              |
| rs12601724   | 0.13454            | 5              |
| rs4792271    | 0.00167            | 6              |
| rs4792272    | 0.13454            | 5              |
| rs11870377   | 0.58955            | 5              |
| rs72811248   | 0.58955            | 5              |

**Table S7. RegulomeDB annotation of the association lead variants near *MYOSLID*.**

The RegulomeDB probability score is ranging from 0 to 1, with 1 being most likely to be a regulatory variant. ‘Ranking’ refers to following evidence: 1a, eQTL + TF binding + matched TF motif + matched DNase Footprint + DNase peak; 1b, eQTL + TF binding + any motif + DNase Footprint + DNase peak; 1c, eQTL + TF binding + matched TF motif + DNase peak; 1d, eQTL + TF binding + any motif + DNase peak; 1e, eQTL + TF binding + matched TF motif; 1f, eQTL + TF binding / DNase peak; 2a, TF binding + matched TF motif + matched DNase Footprint + DNase peak; 2b, TF binding + any motif + DNase Footprint + DNase peak; 2c, TF binding + matched TF motif + DNase peak; 3a, TF binding + any motif + DNase peak; 3b, TF binding + matched TF motif; 4, TF binding + DNase peak; 5, TF binding or DNase peak; 6, Motif hit; 7, Other. RegulomeDB ranking < 3 and/or probability score > 0.8 can be considered as evidence for altered regulatory consequences. Data was downloaded from RegulomeDB 02/10/2021.

| <b><u>Rsids</u></b> | <b><u>Probability</u></b> | <b><u>Ranking</u></b> |
|---------------------|---------------------------|-----------------------|
| rs6758102           | 0.60906                   | 4                     |
| rs10804157          | 1.0                       | 2b                    |
| rs6709320           | 0.18412                   | 7                     |
| rs2111595           | 0.60906                   | 4                     |
| rs11694764          | 0.18412                   | 7                     |
| rs56167178          | 0.13454                   | 5                     |



**Table S8. ChIP-seq data of rs10804157.**

The variant rs10804157 showed the highest probability (1.0) of being a regulatory variant among the variants showing genome-wide significant ( $p < 5 \times 10^{-8}$ ) association with UL at 2q33.3. ChIP-seq data for this variant was extracted from RegulomeDB on 02/10/2021.

| Method   | Peak location             | Biosample                          | Targets | Organ                                       | Dataset     | File        | Value            | Strand |
|----------|---------------------------|------------------------------------|---------|---|-------------|-------------|------------------|--------|
| ChIP-seq | chr2:208123084..208123749 | A549                               | SP1     | lung  | ENCSR000BPE | ENCFF348RKC | 326.58420        | -      |
| ChIP-seq | chr2:208123107..208123712 | A549                               | EP300   | lung  | ENCSR000BPW | ENCFF002CFV | 287.620948909819 | -      |
| ChIP-seq | chr2:208123262..208123522 | A549                               | NR3C1   | lung  | ENCSR000BHF | ENCFF648ZNE | 244.46238        | -      |
| ChIP-seq | chr2:208123094..208123709 | A549                               | TCF12   | lung  | ENCSR000BQQ | ENCFF672FQU | 221.07448        | -      |
| ChIP-seq | chr2:208123378..208123656 | MCF-7                              | FOS     | mammary gland                               | ENCSR569XNP | ENCFF965AIZ | 206.29520        | -      |
| ChIP-seq | chr2:208123332..208123669 | A549                               | FOSL2   | lung  | ENCSR000BQO | ENCFF374ZCG | 187.18388        | -      |
| ChIP-seq | chr2:208123364..208123572 | A549                               | FOXA1   | lung  | ENCSR000BRD | ENCFF755AXA | 170.22291        | -      |
| ChIP-seq | chr2:208123171..208123507 | MCF-7                              | ESRRA   | mammary gland                               | ENCSR954WVZ | ENCFF044NEB | 156.03072        | -      |
| ChIP-seq | chr2:208123287..208123667 | A549                               | MAFK    | lung  | ENCSR541WQI | ENCFF530ZTE | 139.13663        | -      |
| ChIP-seq | chr2:208123361..208123595 | HEK293                             | ZBTB17  | kidney                                      | ENCSR631WAA | ENCFF047LUI | 114.24409        | -      |
| ChIP-seq | chr2:208123179..208123669 | MCF-7                              | ZNF217  | mammary gland                               | ENCSR465XQW | ENCFF567MGV | 99.76437         | -      |
| ChIP-seq | chr2:208123231..208123661 | MCF-7                              | ZNF579  | mammary gland                               | ENCSR018MQH | ENCFF854CXA | 98.09751         | -      |
| ChIP-seq | chr2:208123265..208123545 | A549                               | NR3C1   | lung  | ENCSR000BHG | ENCFF913WFD | 97.82031         | -      |
| ChIP-seq | chr2:208123181..208123801 | A549                               | SIN3A   | lung  | ENCSR513XQX | ENCFF172VGB | 94.53579         | -      |
| ChIP-seq | chr2:208123210..208123666 | MCF-7                              | MNT     | mammary gland                               | ENCSR663ZZZ | ENCFF628SBD | 84.80959         | -      |
| ChIP-seq | chr2:208123135..208123675 | A549                               | BCL3    | lung  | ENCSR000BQH | ENCFF325WAV | 84.05348         | -      |
| ChIP-seq | chr2:208123311..208123581 | IMR-90                             | MAFK    | lung  | ENCSR000EFH | ENCFF593MEB | 83.58383         | -      |
| ChIP-seq | chr2:208123232..208123622 | MCF-7                              | FOXA1   | mammary gland                               | ENCSR126YEB | ENCFF596OJV | 82.25613         | -      |
| ChIP-seq | chr2:208123208..208123618 | MCF-7                              | CTBP1   | mammary gland                               | ENCSR636EYA | ENCFF785ZQF | 81.59685         | -      |
| ChIP-seq | chr2:208123147..208123591 | liver                              | RXRA    | liver                                       | ENCSR098XMN | ENCFF189HPG | 75.54675         | -      |
| ChIP-seq | chr2:208123227..208123697 | A549                               | ZBTB33  | lung  | ENCSR000BPZ | ENCFF639NGJ | 68.14892         | -      |
| ChIP-seq | chr2:208123237..208123541 | A549                               | NR3C1   | lung  | ENCSR000BJR | ENCFF080RMP | 63.97341         | -      |
| ChIP-seq | chr2:208123188..208123618 | HEK293                             | KLF1    | kidney                                      | ENCSR859BMR | ENCFF620ZDF | 61.18339         | -      |
| ChIP-seq | chr2:208123153..208123417 | A549                               | ESRRA   | lung  | ENCSR473SUA | ENCFF266ORV | 60.61061         | -      |
| ChIP-seq | chr2:208123318..208123702 | MCF-7                              | MAZ     | mammary gland                               | ENCSR288IJC | ENCFF492DZG | 58.62570         | -      |
| ChIP-seq | chr2:208123059..208123459 | endothelial cell of umbilical vein | FOS     | vein, vasculature, epithelium, blood vessel | ENCSR000EVU | ENCFF390MXI | 56.59256         | -      |
| ChIP-seq | chr2:208123235..208123645 | MCF-7                              | NFIB    | mammary gland                               | ENCSR702BYX | ENCFF817RST | 56.19887         | -      |
| ChIP-seq | chr2:208123294..208123578 | IMR-90                             | BHLHE40 | lung  | ENCSR957KYB | ENCFF942FBW | 53.93919         | -      |
| ChIP-seq | chr2:208122889..208123613 | K562                               | FOSL1   | blood, bodily fluid                         | ENCSR239ZLZ | ENCFF692PVV | 52.28088         | -      |
| ChIP-seq | chr2:208123124..208123544 | liver                              | NR2F2   | liver                                       | ENCSR338MMB | ENCFF266KLW | 50.28680         | -      |
| ChIP-seq | chr2:208123248..208123738 | A549                               | REST    | lung  | ENCSR000BQP | ENCFF136RBA | 49.93059         | -      |
| ChIP-seq | chr2:208123340..208123630 | A549                               | ZFP36   | lung  | ENCSR294JWV | ENCFF418DRY | 49.62579         | -      |
| ChIP-seq | chr2:208123096..208123416 | SK-N-SH                            | JUND    | brain                                       | ENCSR000BSK | ENCFF598ZLV | 49.00620         | -      |
| ChIP-seq | chr2:208123233..208123757 | A549                               | YY1     | lung  | ENCSR000BPM | ENCFF713ISJ | 48.03768         | -      |
| ChIP-seq | chr2:208123332..208124008 | 22Rv1                              | CTCF    | prostate gland                              | ENCSR857PBV | ENCFF030BPR | 44.66346         | -      |
| ChIP-seq | chr2:208123056..208123476 | liver                              | JUND    | liver                                       | ENCSR837GTK | ENCFF804UDG | 44.66249         | -      |
| ChIP-seq | chr2:208123048..208123638 | MCF-7                              | FOSL2   | mammary gland                               | ENCSR546KCN | ENCFF331KNS | 43.40140         | -      |
| ChIP-seq | chr2:208123246..208123730 | A549                               | ATF3    | lung  | ENCSR000BPS | ENCFF913MUA | 43.04867         | -      |

| Method   | Peak location             | Biosample                          | Targets | Organ                                       | Dataset     | File        | Value            | Strand |
|----------|---------------------------|------------------------------------|---------|---|-------------|-------------|------------------|--------|
| ChIP-seq | chr2:208123340..208124040 | 22Rv1                              | CTCF    | prostate gland                              | ENCSR847XGE | ENCFF259XYR | 41.50506         | -      |
| ChIP-seq | chr2:208123167..208123671 | liver                              | SP1     | liver                                       | ENCSR386YIH | ENCFF017YUI | 41.36437         | -      |
| ChIP-seq | chr2:208123257..208123587 | T47D                               | EP300   | mammary gland                               | ENCSR000BLM | ENCFF002CNZ | 39.636132175516  | -      |
| ChIP-seq | chr2:208123176..208123640 | liver                              | RXRA    | liver                                       | ENCSR352QSB | ENCFF651LIG | 39.78583         | -      |
| ChIP-seq | chr2:208123138..208123628 | liver                              | NR2F2   | liver                                       | ENCSR168SMX | ENCFF168INE | 38.88749         | -      |
| ChIP-seq | chr2:208123233..208123877 | HEK293                             | TRIM28  | kidney                                      | ENCSR618HNF | ENCFF034GYQ | 37.81934         | -      |
| ChIP-seq | chr2:208123305..208123735 | MCF-7                              | ZNF687  | mammary gland                               | ENCSR899BKM | ENCFF955YVT | 37.18623         | -      |
| ChIP-seq | chr2:208123250..208123560 | MCF-7                              | MYC     | mammary gland                               | ENCSR000DMQ | ENCFF695IQU | 37.15063         | -      |
| ChIP-seq | chr2:208123277..208123697 | A549                               | ELF1    | lung  | ENCSR000BPT | ENCFF533NIV | 37.00036         | -      |
| ChIP-seq | chr2:208122967..208123727 | MCF-7                              | KLF4    | mammary gland                               | ENCSR265WJC | ENCFF463ZWH | 34.95441         | -      |
| ChIP-seq | chr2:208123205..208123815 | IMR-90                             | POLR2A  | lung  | ENCSR000EFK | ENCFF002CVJ | 33.0223703871219 | -      |
| ChIP-seq | chr2:208123269..208123669 | endothelial cell of umbilical vein | FOS     | vein, vasculature, epithelium, blood vessel | ENCSR000EVU | ENCFF390MXI | 32.41105         | -      |
| ChIP-seq | chr2:208123383..208123623 | IMR-90                             | NFE2L2  | lung  | ENCSR197WGI | ENCFF641RNZ | 31.19285         | -      |
| ChIP-seq | chr2:208123247..208123678 | Caco-2                             | HNF4A   | intestine, large intestine                  | TSTR342350  | TSTFF265946 | 30               | -      |
| ChIP-seq | chr2:208123293..208123583 | T47D                               | GATA3   | mammary gland                               | ENCSR000BMX | ENCFF058XAD | 29.56353         | -      |
| ChIP-seq | chr2:208123281..208123601 | A549                               | NR3C1   | lung  | ENCSR000BJT | ENCFF495YRW | 29.31897         | -      |
| ChIP-seq | chr2:208123261..208123531 | A549                               | NR3C1   | lung  | ENCSR000BHE | ENCFF841IFL | 29.14627         | -      |
| ChIP-seq | chr2:208123248..208123838 | MCF-7                              | FOSL2   | mammary gland                               | ENCSR546KCN | ENCFF331KNS | 29.01817         | -      |
| ChIP-seq | chr2:208123298..208123598 | MCF 10A                            | MYC     | mammary gland                               | ENCSR000DOM | ENCFF002CZA | 24.1612783298454 | -      |
| ChIP-seq | chr2:208123121..208123685 | IMR-90                             | CHD1    | lung  | ENCSR000EFC | ENCFF441IFB | 24.73066         | -      |
| ChIP-seq | chr2:208123247..208123517 | A549                               | USF1    | lung  | ENCSR000BHX | ENCFF002CGC | 23.8430557308026 | -      |
| ChIP-seq | chr2:208123084..208123749 | A549                               | SP1     | lung  | ENCSR000BPE | ENCFF348RKC | 23.40951         | -      |
| ChIP-seq | chr2:208123079..208123399 | HeLa-S3                            | JUND    | uterus                                      | ENCSR000EDH | ENCFF002CSP | 22.3246370112007 | -      |
| ChIP-seq | chr2:208123359..208123703 | GM12878                            | BCL3    | blood, bodily fluid                         | ENCSR000BNQ | ENCFF625SHY | 20.58068         | -      |
| ChIP-seq | chr2:208123138..208123394 | HeLa-S3                            | FOS     | uterus                                      | ENCSR000EZE | ENCFF002CSB | 19.8552135147245 | -      |
| ChIP-seq | chr2:208123318..208123638 | SK-N-SH                            | JUND    | brain                                       | ENCSR000BSK | ENCFF598ZLV | 19.05498         | -      |
| ChIP-seq | chr2:208123375..208123631 | A549                               | USF1    | lung  | ENCSR000BJB | ENCFF002CGD | 18.2821813113775 | -      |
| ChIP-seq | chr2:208123323..208123739 | Caco-2                             | CDX2    | intestine, large intestine                  | TSTR586454  | TSTFF910843 | 18               | -      |
| ChIP-seq | chr2:208123114..208123530 | liver                              | ATF3    | liver                                       | ENCSR480LIS | ENCFF975PTM | 17.59478         | -      |
| ChIP-seq | chr2:208122865..208123405 | MCF 10A                            | POLR2A  | mammary gland                               | ENCSR000DPA | ENCFF755ZCF | 17.14568         | -      |
| ChIP-seq | chr2:208123302..208123558 | MCF 10A                            | STAT3   | mammary gland                               | ENCSR000DOZ | ENCFF807JAC | 14.95877         | -      |
| ChIP-seq | chr2:208123094..208123714 | A549                               | TCF12   | lung  | ENCSR000BQQ | ENCFF672FQU | 11.69204         | -      |
| ChIP-seq | chr2:208123257..208123677 | liver                              | JUND    | liver                                       | ENCSR837GTK | ENCFF804UDG | 10.18840         | -      |

**Table S9. RegulomeDB annotation of the association lead variants near *CDKN1A*.**

The RegulomeDB probability score is ranging from 0 to 1, with 1 being most likely to be a regulatory variant. ‘Ranking’ refers to following evidence: 1a, eQTL + TF binding + matched TF motif + matched DNase Footprint + DNase peak; 1b, eQTL + TF binding + any motif + DNase Footprint + DNase peak; 1c, eQTL + TF binding + matched TF motif + DNase peak; 1d, eQTL + TF binding + any motif + DNase peak; 1e, eQTL + TF binding + matched TF motif; 1f, eQTL + TF binding / DNase peak; 2a, TF binding + matched TF motif + matched DNase Footprint + DNase peak; 2b, TF binding + any motif + DNase Footprint + DNase peak; 2c, TF binding + matched TF motif + DNase peak; 3a, TF binding + any motif + DNase peak; 3b, TF binding + matched TF motif; 4, TF binding + DNase peak; 5, TF binding or DNase peak; 6, Motif hit; 7, Other. RegulomeDB ranking < 3 and/or probability score > 0.8 can be considered as evidence for altered regulatory consequences. Data was downloaded from RegulomeDB 02/10/2021.

| <u>Rsids</u> | <u>Probability</u> | <u>Ranking</u> |
|--------------|--------------------|----------------|
| rs6457932    | 0.60906            | 4              |
| rs9349003    | 0.49417            | 3a             |
| rs9366912    | 0.55436            | 1f             |
| rs112297876  | 0.58955            | 5              |
| rs12524435   | 0.38284            | 5              |
| rs10947616   | 0.58955            | 5              |
| rs4713993    | 0.13454            | 5              |
| rs6915170    | 0.30943            | 6              |
| rs4464789    | 0.6893             | 3a             |
| rs10456441   | 0.49737            | 3a             |
| rs10456442   | 0.60906            | 4              |
| rs10456443   | 0.61652            | 2b             |
| rs12210094   | 0.60906            | 4              |
| rs12528913   | 0.08               | 5              |
| rs12530170   | 0.84573            | 2b             |
| rs12203953   | 0.96944            | 1a             |
| rs6920453    | 0.60906            | 4              |
| rs75420281   | 0.60906            | 4              |
| rs3176348    | 0.86655            | 2b             |
| rs150499251  | 0.58955            | 5              |
| rs9357241    | 0.04578            | 5              |
| rs6921165    | 0.60906            | 4              |
| rs9394413    | 0.98162            | 5              |
| rs7741267    | 0.60906            | 4              |
| rs7751412    | 0.30476            | 3a             |

**Table S10. Results of MAGMA enrichment analysis.**

We conducted MAGMA<sup>4</sup> gene-set enrichment analysis as implemented in FUMA<sup>5</sup> using genome-wide summary statistics from META-2. Gene-based p-values were computed for protein-coding genes by mapping variants to genes with default parameters, 1000 Genomes European population, and SNP-wide mean model, and subsequent enrichment analyses were performed for the significant genes using 4728 curated gene sets and 6166 GO terms as reported in MsigDB<sup>8</sup>. The table shows the results for the gene sets significant after false discovery rate (FDR) correction ( $p_{\text{FDR}} < 0.05$ ).

| Gene_set  | Ngenes | BETA | SE   | P        | P <sub>FDR</sub> |
|---|--------|------|------|----------|------------------|
| GO_bp:go_regulation_of_male_gonad_development   | 8      | 2.34 | 0.35 | 1.15E-11 | 1.78E-07         |
| GO_cc:go_telomere_cap_complex   | 13     | 1.43 | 0.26 | 1.39E-08 | 0.00011          |
| GO_bp:go_regulation_of_nuclear_transcribed_mrna_catabolic_process_deadenylation_dependent_decay | 20     | 1.15 | 0.22 | 1.03E-07 | 0.00053          |
| GO_bp:go_regulation_of_gonad_development  | 18     | 1.10 | 0.22 | 4.52E-07 | 0.0017           |
| GO_bp:go_sex_determination  | 21     | 0.86 | 0.18 | 1.73E-06 | 0.0048           |
| Curated_gene_sets:pid_angiopoietin_receptor_pathway   | 49     | 0.60 | 0.13 | 1.85E-06 | 0.0048           |
| GO_bp:go_positive_regulation_of_heart_growth  | 37     | 0.74 | 0.16 | 2.33E-06 | 0.0052           |
| GO_mf:go_translation_regulator_activity   | 132    | 0.32 | 0.07 | 3.48E-06 | 0.0063           |
| Curated_gene_sets:nikolsky_breast_cancer_5p15_amplicon  | 26     | 1.08 | 0.24 | 3.80E-06 | 0.0063           |
| Curated_gene_sets:pid_telomerase_pathway  | 68     | 0.49 | 0.11 | 4.57E-06 | 0.0063           |
| GO_bp:go_respiratory_system_development   | 195    | 0.31 | 0.07 | 4.87E-06 | 0.0063           |
| GO_bp:go_kidney_mesenchyme_development  | 19     | 1.06 | 0.24 | 4.91E-06 | 0.0063           |
| GO_bp:go_metanephric_mesenchyme_development   | 15     | 1.18 | 0.27 | 5.81E-06 | 0.0065           |
| GO_bp:go_positive_regulation_of_gonad_development   | 10     | 1.50 | 0.34 | 5.89E-06 | 0.0065           |
| GO_bp:go_posttranscriptional_regulation_of_gene_expression                                      | 581    | 0.16 | 0.04 | 1.03E-05 | 0.0097           |
| GO_bp:go_type_i_pneumocyte_differentiation  | 5      | 2.09 | 0.49 | 1.04E-05 | 0.0097           |
| GO_bp:go_diaphragm_development  | 9      | 1.43 | 0.34 | 1.06E-05 | 0.0097           |
| Curated_gene_sets:wu_hbx_targets_3_dn   | 13     | 1.05 | 0.25 | 1.58E-05 | 0.013            |
| Curated_gene_sets:tsai_dnajb4_targets_dn  | 6      | 1.72 | 0.41 | 1.60E-05 | 0.013            |
| GO_bp:go_regulation_of_cell_cycle   | 1151   | 0.10 | 0.03 | 3.82E-05 | 0.028            |
| GO_bp:go_positive_regulation_of_organ_growth  | 48     | 0.55 | 0.14 | 3.91E-05 | 0.028            |
| Curated_gene_sets:pid_plk1_pathway  | 44     | 0.53 | 0.13 | 3.99E-05 | 0.028            |
| GO_bp:go_cell_proliferation_involved_in_metanephros_development                                 | 10     | 1.34 | 0.34 | 4.28E-05 | 0.028            |
| Curated_gene_sets:lindvall_immortalized_by_tert_up  | 65     | 0.46 | 0.12 | 4.32E-05 | 0.028            |
| GO_bp:go_connective_tissue_development  | 266    | 0.22 | 0.06 | 4.81E-05 | 0.030            |
| Curated_gene_sets:reactome_cellular_senescence  | 171    | 0.27 | 0.07 | 5.20E-05 | 0.031            |
| GO_bp:go_chondroblast_differentiation   | 5      | 1.44 | 0.37 | 5.45E-05 | 0.031            |
| GO_bp:go_regulation_of_biominerale_tissue_development   | 86     | 0.40 | 0.10 | 5.60E-05 | 0.031            |
| Curated_gene_sets:biocarta_egfr_smrte_pathway   | 11     | 1.17 | 0.30 | 5.75E-05 | 0.031            |
| GO_bp:go_regulation_of_nuclear_transcribed_mrna_poly_a_tail_shortening                          | 14     | 1.06 | 0.28 | 5.95E-05 | 0.031            |
| Curated_gene_sets:pilon_klf1_targets_dn   | 1980   | 0.08 | 0.02 | 6.12E-05 | 0.031            |
| GO_bp:go_positive_regulation_of_cell_cycle  | 380    | 0.17 | 0.04 | 7.11E-05 | 0.034            |
| GO_bp:go_cellular_response_to_starvation  | 146    | 0.27 | 0.07 | 7.71E-05 | 0.036            |
| GO_bp:go_regulation_of_epidermis_development  | 82     | 0.41 | 0.11 | 8.89E-05 | 0.040            |
| GO_bp:go_regulation_of_heart_growth   | 63     | 0.44 | 0.12 | 9.49E-05 | 0.041            |
| GO_bp:go_regulation_of_cellular_amide_metabolic_process   | 375    | 0.17 | 0.04 | 9.65E-05 | 0.041            |
| GO_bp:go_positive_regulation_of_mrna_catabolic_process  | 47     | 0.47 | 0.13 | 9.82E-05 | 0.041            |
| GO_bp:go_negative_regulation_of_gonad_development   | 6      | 1.38 | 0.37 | 0.00010  | 0.042            |
| Curated_gene_sets:biocarta_rna_pathway  | 9      | 0.84 | 0.23 | 0.00011  | 0.042            |
| GO_bp:go_cellular_response_to_extracellular_stimulus  | 259    | 0.20 | 0.05 | 0.00012  | 0.047            |
| GO_bp:go_cell_cycle   | 1766   | 0.08 | 0.02 | 0.00013  | 0.048            |
| Curated_gene_sets:abdelmohsen_elavl4_targets  | 16     | 0.79 | 0.22 | 0.00013  | 0.049            |
| Curated_gene_sets:reactome_runx3_regulates_cdkn1a_transcription                                 | 7      | 1.45 | 0.40 | 0.00014  | 0.049            |
| GO_bp:go_adrenal_gland_development  | 24     | 0.74 | 0.20 | 0.00014  | 0.049            |
| GO_bp:go_negative_regulation_of_telomere_maintenance_via_telomerase                             | 20     | 0.78 | 0.21 | 0.00014  | 0.049            |
| GO_mf:go_dna_binding_transcription_factor_activity  | 1661   | 0.09 | 0.02 | 0.00015  | 0.049            |
| GO_bp:go_male_sex_determination   | 13     | 0.89 | 0.25 | 0.00015  | 0.049            |
| GO_bp:go_positive_regulation_of_cardiac_muscle_cell_proliferation                               | 25     | 0.72 | 0.20 | 0.00015  | 0.049            |
| GO_bp:go_stress_induced_premature_senescence  | 8      | 1.06 | 0.29 | 0.00016  | 0.049            |
| GO_bp:go_organ_growth   | 176    | 0.25 | 0.07 | 0.00016  | 0.049            |

**Table S11. Genetic correlations of UL with 20 metabolic and anthropometric traits.**

We used LDSC software<sup>2</sup> to estimate genetic correlations ( $r_g$ ) of UL with 20 metabolic and anthropometric traits extracted from the GWAS database provided by the MRC Integrative Epidemiology Unit (<https://gwas.mrcieu.ac.uk/>). For UL, genome-wide data from META-2 was used in the  $r_g$  estimation. We run LDSC using standard settings described at <https://github.com/bulik/ldsc/wiki/Heritability-and-Genetic-Correlation>. Genetic correlations passing false discovery rate (fdr) correction were deemed significant ( $p_{fdr} < 0.05$ ).

| Trait                                  | Trait ID         | Sample size | N SNPs   | $r_g$   | se     | p        | $p_{fdr}$ |
|--|------------------|-------------|----------|---------|--------|----------|-----------|
| Triglycerides                          | ieu-b-111        | 441016      | 12321875 | 0.1609  | 0.0276 | 5.52E-09 | 1.10E-07  |
| Waist circumference                    | ukb-b-9405       | 462166      | 9851867  | 0.1012  | 0.0243 | 3.08E-05 | 1.23E-04  |
| Diastolic blood pressure               | ieu-b-39         | 757601      | 7160619  | 0.0978  | 0.0248 | 8.27E-05 | 2.76E-04  |
| Waist-to-hip ratio                     | ieu-a-72         | 224459      | 2562516  | 0.0953  | 0.0381 | 0.012    | 0.020     |
| Body mass index (BMI)                  | ukb-b-19953      | 461460      | 9851867  | 0.0912  | 0.0250 | 0.0003   | 7.63E-04  |
| Basal metabolic rate                   | ukb-b-16446      | 454874      | 9851867  | 0.0841  | 0.0251 | 0.0008   | 0.002     |
| Whole body water mass                  | ukb-b-14540      | 454888      | 9851867  | 0.0832  | 0.0253 | 0.001    | 0.002     |
| Whole body fat-free mass               | ukb-b-13354      | 454850      | 9851867  | 0.0810  | 0.0252 | 0.001    | 0.003     |
| Systolic blood pressure                | ieu-b-38         | 757601      | 7088083  | 0.0605  | 0.0239 | 0.011    | 0.020     |
| Whole body fat mass                    | ukb-b-19393      | 454137      | 9851867  | 0.0566  | 0.0238 | 0.017    | 0.026     |
| Hip circumference                      | ukb-b-15590      | 462117      | 9851867  | 0.0513  | 0.0242 | 0.034    | 0.048     |
| Total cholesterol                      | ieu-a-301        | 187365      | 2446982  | 0.0416  | 0.0399 | 0.297    | 0.371     |
| Body fat percentage                    | ukb-b-8909       | 454633      | 9851867  | 0.0346  | 0.0242 | 0.153    | 0.204     |
| Apolipoprotein B                       | ieu-b-108        | 439214      | 12321875 | 0.0126  | 0.0332 | 0.705    | 0.720     |
| LDL cholesterol                        | ieu-b-110        | 440546      | 12321875 | -0.0201 | 0.0367 | 0.584    | 0.649     |
| C-reactive protein                     | bbj-a-14         | 75391       | 6108953  | -0.0445 | 0.1240 | 0.720    | 0.720     |
| Fasting blood glucose adjusted for BMI | ebi-a-GCST007858 | 33231       | 105585   | -0.0882 | 0.1187 | 0.457    | 0.538     |
| Apolipoprotein A-I                     | ieu-b-107        | 393193      | 12321875 | -0.1100 | 0.0260 | 2.26E-05 | 1.13E-04  |
| Impedance of whole body                | ukb-b-19921      | 454840      | 9851867  | -0.1299 | 0.0270 | 1.56E-06 | 1.04E-05  |
| HDL cholesterol                        | ieu-b-109        | 403943      | 12321875 | -0.1386 | 0.0245 | 1.48E-08 | 1.48E-07  |

**Table S12. Results of the bi-directional two-sample Mendelian randomization.**

Bi-directional two-sample Mendelian randomization of UL risk and 20 metabolic and anthropometric traits was completed using TwoSampleMR R library<sup>12</sup>. To avoid possible bias from overlapping samples, we extracted genetic instruments for UL from the GWAS results obtained in FinnGen, and for other, mostly UKBB-based traits, from the GWAS database provided by the MRC IEU and integrated in TwoSampleMR. LD pruning was completed using European population reference, threshold of  $r^2=0.001$ , and clumping window of 10 kb. We considered inverse variance weighted (IVW) method as the primary analysis for which false discovery rate (fdr) correction was applied to adjust for multiple comparisons. MR Egger analysis was considered exploratory and multiple testing correction was not applied.

| Direction   | Trait                                   | Method   | N <sub>SNP</sub> | Causal estimate scale | Causal estimate | CI95L   | CI95U   | P      | P <sub>FDR</sub> | P <sub>heterogeneity</sub> | Egger intercept | P <sub>pleiotropy</sub> |
|-------------|---|----------|------------------|-----------------------|-----------------|---------|---------|--------|------------------|----------------------------|-----------------|-------------------------|
| Trait -> UL | apolipoprotein A-I    id:ieu-b-107      | IVW      | 250              | OR                    | 0.97            | 0.89    | 1.05    | 0.4178 | 0.6693           | 3.70E-11                   |                 |                         |
| Trait -> UL | apolipoprotein A-I    id:ieu-b-107      | MR Egger | 250              | OR                    | 1.00            | 0.88    | 1.15    | 0.9580 |                  | 3.40E-11                   | -0.0015         | 0.4731                  |
| UL -> Trait | apolipoprotein A-I    id:ieu-b-107      | IVW      | 26               | beta                  | -0.0192         | -0.0348 | -0.0036 | 0.0156 | 0.0626           | 1.04E-10                   |                 |                         |
| UL -> Trait | apolipoprotein A-I    id:ieu-b-107      | MR Egger | 26               | beta                  | -0.0379         | -0.0647 | -0.0110 | 0.0107 |                  | 2.40E-09                   | 0.0031          | 0.1124                  |
| Trait -> UL | apolipoprotein B    id:ieu-b-108        | IVW      | 167              | OR                    | 1.03            | 0.96    | 1.12    | 0.3912 | 0.6693           | 8.15E-05                   |                 |                         |
| Trait -> UL | apolipoprotein B    id:ieu-b-108        | MR Egger | 167              | OR                    | 1.08            | 0.97    | 1.19    | 0.1758 |                  | 8.87E-05                   | -0.0023         | 0.2829                  |
| UL -> Trait | apolipoprotein B    id:ieu-b-108        | IVW      | 26               | beta                  | -0.0036         | -0.0169 | 0.0097  | 0.5970 | 0.7701           | 2.89E-05                   |                 |                         |
| UL -> Trait | apolipoprotein B    id:ieu-b-108        | MR Egger | 26               | beta                  | -0.0035         | -0.0275 | 0.0206  | 0.7810 |                  | 1.71E-05                   | -2.07E-05       | 0.9904                  |
| Trait -> UL | Basal metabolic rate    id:ukb-b-16446  | IVW      | 487              | OR                    | 1.24            | 1.08    | 1.43    | 0.0022 | 0.0205           | 2.00E-39                   |                 |                         |
| Trait -> UL | Basal metabolic rate    id:ukb-b-16446  | MR Egger | 487              | OR                    | 1.36            | 0.98    | 1.89    | 0.0673 |                  | 1.67E-39                   | -0.0014         | 0.5563                  |
| UL -> Trait | Basal metabolic rate    id:ukb-b-16446  | IVW      | 26               | beta                  | 0.0198          | 0.0009  | 0.0388  | 0.0401 | 0.1070           | 5.49E-55                   |                 |                         |
| UL -> Trait | Basal metabolic rate    id:ukb-b-16446  | MR Egger | 26               | beta                  | 0.0386          | 0.0055  | 0.0717  | 0.0316 |                  | 6.66E-51                   | -0.0031         | 0.1921                  |
| Trait -> UL | Body fat percentage    id:ukb-b-8909    | IVW      | 351              | OR                    | 0.99            | 0.88    | 1.13    | 0.9379 | 0.9619           | 0.00066                    |                 |                         |
| Trait -> UL | Body fat percentage    id:ukb-b-8909    | MR Egger | 351              | OR                    | 1.07            | 0.71    | 1.63    | 0.7370 |                  | 0.00060                    | -0.0011         | 0.7052                  |
| UL -> Trait | Body fat percentage    id:ukb-b-8909    | IVW      | 26               | beta                  | -0.0041         | -0.0139 | 0.0058  | 0.4183 | 0.6693           | 2.86E-05                   |                 |                         |
| UL -> Trait | Body fat percentage    id:ukb-b-8909    | MR Egger | 26               | beta                  | 0.0042          | -0.0132 | 0.0216  | 0.6369 |                  | 4.97E-05                   | -0.0014         | 0.2686                  |
| Trait -> UL | Body mass index (BMI)    id:ukb-b-19953 | IVW      | 399              | OR                    | 1.13            | 1.03    | 1.24    | 0.0084 | 0.0373           | 3.42E-06                   |                 |                         |
| Trait -> UL | Body mass index (BMI)    id:ukb-b-19953 | MR Egger | 399              | OR                    | 1.14            | 0.89    | 1.46    | 0.3014 |                  | 2.92E-06                   | -0.00011        | 0.9615                  |
| UL -> Trait | Body mass index (BMI)    id:ukb-b-19953 | IVW      | 26               | beta                  | 0.0038          | -0.0171 | 0.0246  | 0.7217 | 0.8248           | 2.15E-24                   |                 |                         |
| UL -> Trait | Body mass index (BMI)    id:ukb-b-19953 | MR Egger | 26               | beta                  | 0.0253          | -0.0111 | 0.0617  | 0.1852 |                  | 2.49E-22                   | -0.0036         | 0.1734                  |

| Direction   | Trait   | Method   | N <sub>SNP</sub> | Causal estimate scale | Causal estimate | CI95L   | CI95U   | P      | P <sub>FDR</sub> | P <sub>heterogeneity</sub> | Egger intercept | P <sub>pleiotropy</sub> |
|-------------|---|----------|------------------|-----------------------|-----------------|---------|---------|--------|------------------|----------------------------|-----------------|-------------------------|
| Trait -> UL | C-Reactive protein level    id:ieu-b-35                       | IVW      | 52               | OR                    | 1.01            | 0.93    | 1.10    | 0.8251 | 0.9168           | 0.0024                     |                 |                         |
| Trait -> UL | C-Reactive protein level    id:ieu-b-35                       | MR Egger | 52               | OR                    | 0.99            | 0.87    | 1.11    | 0.8305 |                  | 0.0020                     | 0.0019          | 0.6141                  |
| UL -> Trait | C-Reactive protein level    id:ieu-b-35                       | IVW      | 19               | beta                  | 0.0090          | -0.0173 | 0.0354  | 0.5016 | 0.7166           | 0.0275                     |                 |                         |
| UL -> Trait | C-Reactive protein level    id:ieu-b-35                       | MR Egger | 19               | beta                  | 0.0076          | -0.1014 | 0.1166  | 0.8932 |                  | 0.0190                     | 0.0002          | 0.9786                  |
| Trait -> UL | diastolic blood pressure    id:ieu-b-39                       | IVW      | 415              | OR                    | 1.02            | 1.01    | 1.03    | 0.0026 | 0.0205           | 4.75E-21                   |                 |                         |
| Trait -> UL | diastolic blood pressure    id:ieu-b-39                       | MR Egger | 415              | OR                    | 1.01            | 0.99    | 1.04    | 0.3482 |                  | 3.70E-21                   | 0.00081         | 0.7317                  |
| UL -> Trait | diastolic blood pressure    id:ieu-b-39                       | IVW      | 24               | beta                  | 0.3687          | 0.1493  | 0.5882  | 0.0010 | 0.0205           | 2.08E-30                   |                 |                         |
| UL -> Trait | diastolic blood pressure    id:ieu-b-39                       | MR Egger | 24               | beta                  | 0.6254          | 0.2022  | 1.0486  | 0.0084 |                  | 9.05E-28                   | -0.0386         | 0.1813                  |
| Trait -> UL | Fasting blood glucose adjusted for BMI    id:ebi-a-GCST007858 | IVW      | 9                | OR                    | 0.91            | 0.62    | 1.34    | 0.6353 | 0.7701           | 0.019                      |                 |                         |
| Trait -> UL | Fasting blood glucose adjusted for BMI    id:ebi-a-GCST007858 | MR Egger | 9                | OR                    | 0.88            | 0.34    | 2.28    | 0.8067 |                  | 0.010                      | 0.0011          | 0.9490                  |
| UL -> Trait | Fasting blood glucose adjusted for BMI    id:ebi-a-GCST007858 | IVW      | 6                | beta                  | 0.0014          | -0.0322 | 0.0349  | 0.9371 | 0.9619           | 0.4507                     |                 |                         |
| UL -> Trait | Fasting blood glucose adjusted for BMI    id:ebi-a-GCST007858 | MR Egger | 6                | beta                  | -0.0686         | -0.1656 | 0.0284  | 0.2381 |                  | 0.6528                     | 0.0091          | 0.2065                  |
| Trait -> UL | HDL cholesterol    id:ieu-b-109                               | IVW      | 298              | OR                    | 0.89            | 0.82    | 0.97    | 0.0075 | 0.0373           | 3.21E-18                   |                 |                         |
| Trait -> UL | HDL cholesterol    id:ieu-b-109                               | MR Egger | 298              | OR                    | 0.99            | 0.86    | 1.13    | 0.8460 |                  | 1.46E-17                   | -0.0040         | 0.0420                  |
| UL -> Trait | HDL cholesterol    id:ieu-b-109                               | IVW      | 26               | beta                  | -0.0152         | -0.0310 | 0.0005  | 0.0584 | 0.1461           | 3.85E-12                   |                 |                         |
| UL -> Trait | HDL cholesterol    id:ieu-b-109                               | MR Egger | 26               | beta                  | -0.0389         | -0.0652 | -0.0126 | 0.0078 |                  | 1.43E-09                   | 0.0039          | 0.0431                  |
| Trait -> UL | Hip circumference    id:ukb-b-15590                           | IVW      | 377              | OR                    | 1.05            | 0.96    | 1.16    | 0.2888 | 0.5624           | 1.31E-07                   |                 |                         |
| Trait -> UL | Hip circumference    id:ukb-b-15590                           | MR Egger | 377              | OR                    | 0.97            | 0.75    | 1.26    | 0.8429 |                  | 1.19E-07                   | 0.0016          | 0.5255                  |
| UL -> Trait | Hip circumference    id:ukb-b-15590                           | IVW      | 26               | beta                  | 0.0114          | -0.0106 | 0.0334  | 0.3093 | 0.5624           | 1.35E-27                   |                 |                         |
| UL -> Trait | Hip circumference    id:ukb-b-15590                           | MR Egger | 26               | beta                  | 0.0336          | -0.0048 | 0.0721  | 0.0994 |                  | 2.14E-25                   | -0.0037         | 0.1836                  |
| Trait -> UL | Impedance of whole body    id:ukb-b-19921                     | IVW      | 463              | OR                    | 0.79            | 0.69    | 0.91    | 0.0010 | 0.0205           | 3.80E-44                   |                 |                         |
| Trait -> UL | Impedance of whole body    id:ukb-b-19921                     | MR Egger | 463              | OR                    | 0.58            | 0.41    | 0.84    | 0.0034 |                  | 1.89E-43                   | 0.0049          | 0.0691                  |
| UL -> Trait | Impedance of whole body    id:ukb-b-19921                     | IVW      | 26               | beta                  | -0.0135         | -0.0389 | 0.0119  | 0.2970 | 0.5624           | 1.62E-77                   |                 |                         |
| UL -> Trait | Impedance of whole body    id:ukb-b-19921                     | MR Egger | 26               | beta                  | -0.0342         | -0.0791 | 0.0107  | 0.1487 |                  | 7.37E-74                   | 0.0034          | 0.2856                  |
| Trait -> UL | LDL cholesterol    id:ieu-b-110                               | IVW      | 144              | OR                    | 0.99            | 0.90    | 1.09    | 0.9099 | 0.9619           | 3.25E-06                   |                 |                         |
| Trait -> UL | LDL cholesterol    id:ieu-b-110                               | MR Egger | 144              | OR                    | 1.06            | 0.92    | 1.22    | 0.4124 |                  | 4.13E-06                   | -0.0031         | 0.2217                  |

| Direction   | Trait                                   | Method   | N <sub>SNP</sub> | Causal estimate scale | Causal estimate | CI95L   | CI95U  | P      | P <sub>FDR</sub> | P <sub>heterogeneity</sub> | Egger intercept | P <sub>pleiotropy</sub> |
|-------------|---|----------|------------------|-----------------------|-----------------|---------|--------|--------|------------------|----------------------------|-----------------|-------------------------|
| UL -> Trait | LDL cholesterol    id:i eu-b-110        | IVW      | 26               | beta                  | -0.0029         | -0.0149 | 0.0090 | 0.6296 | 0.7701           | 0.0013                     |                 |                         |
| UL -> Trait | LDL cholesterol    id:i eu-b-110        | MR Egger | 26               | beta                  | -0.0061         | -0.0278 | 0.0155 | 0.5831 |                  | 0.0009                     | 0.0005          | 0.7289                  |
| Trait -> UL | systolic blood pressure    id:i eu-b-38 | IVW      | 405              | OR                    | 1.01            | 1.00    | 1.01   | 0.0261 | 0.0948           | 1.34E-14                   |                 |                         |
| Trait -> UL | systolic blood pressure    id:i eu-b-38 | MR Egger | 405              | OR                    | 1.01            | 1.00    | 1.03   | 0.0543 |                  | 1.58E-14                   | -0.0027         | 0.2574                  |
| UL -> Trait | systolic blood pressure    id:i eu-b-38 | IVW      | 23               | beta                  | 0.3458          | -0.0854 | 0.7771 | 0.1160 | 0.2578           | 1.41E-38                   |                 |                         |
| UL -> Trait | systolic blood pressure    id:i eu-b-38 | MR Egger | 23               | beta                  | -0.0863         | -0.9173 | 0.7446 | 0.8406 |                  | 4.29E-36                   | 0.0653          | 0.2479                  |
| Trait -> UL | Total cholesterol    id:i eu-a-301      | IVW      | 79               | OR                    | 1.01            | 0.94    | 1.09   | 0.7106 | 0.8248           | 0.015                      |                 |                         |
| Trait -> UL | Total cholesterol    id:i eu-a-301      | MR Egger | 79               | OR                    | 1.07            | 0.96    | 1.20   | 0.2351 |                  | 0.018                      | -0.0041         | 0.2204                  |
| UL -> Trait | Total cholesterol    id:i eu-a-301      | IVW      | 17               | beta                  | 0.0111          | -0.0238 | 0.0460 | 0.5333 | 0.7356           | 0.1610                     |                 |                         |
| UL -> Trait | Total cholesterol    id:i eu-a-301      | MR Egger | 17               | beta                  | -0.0145         | -0.1602 | 0.1312 | 0.8477 |                  | 0.1276                     | 0.0027          | 0.7272                  |
| Trait -> UL | Triglycerides    id:i eu-a-302          | IVW      | 53               | OR                    | 1.09            | 0.97    | 1.22   | 0.1395 | 0.2936           | 2.17E-05                   |                 |                         |
| Trait -> UL | Triglycerides    id:i eu-a-302          | MR Egger | 53               | OR                    | 1.12            | 0.94    | 1.34   | 0.2214 |                  | 1.63E-05                   | -0.0018         | 0.6903                  |
| UL -> Trait | Triglycerides    id:i eu-a-302          | IVW      | 17               | beta                  | 0.0078          | -0.0234 | 0.0390 | 0.6239 | 0.7701           | 0.2008                     |                 |                         |
| UL -> Trait | Triglycerides    id:i eu-a-302          | MR Egger | 17               | beta                  | 0.0628          | -0.0637 | 0.1894 | 0.3460 |                  | 0.1944                     | -0.0058         | 0.3929                  |
| Trait -> UL | Waist circumference    id:ukb-b-9405    | IVW      | 326              | OR                    | 1.19            | 1.05    | 1.35   | 0.0052 | 0.0334           | 2.61E-09                   |                 |                         |
| Trait -> UL | Waist circumference    id:ukb-b-9405    | MR Egger | 326              | OR                    | 1.25            | 0.88    | 1.77   | 0.2118 |                  | 2.14E-09                   | -0.00077        | 0.7821                  |
| UL -> Trait | Waist circumference    id:ukb-b-9405    | IVW      | 26               | beta                  | 0.0127          | -0.0028 | 0.0282 | 0.1085 | 0.2554           | 4.49E-14                   |                 |                         |
| UL -> Trait | Waist circumference    id:ukb-b-9405    | MR Egger | 26               | beta                  | 0.0287          | 0.0016  | 0.0558 | 0.0486 |                  | 7.41E-13                   | -0.0027         | 0.1741                  |
| Trait -> UL | Waist-to-hip ratio    id:i eu-a-72      | IVW      | 29               | OR                    | 1.26            | 1.01    | 1.57   | 0.0388 | 0.1070           | 0.320                      |                 |                         |
| Trait -> UL | Waist-to-hip ratio    id:i eu-a-72      | MR Egger | 29               | OR                    | 1.42            | 0.52    | 3.89   | 0.4966 |                  | 0.277                      | -0.0031         | 0.8070                  |
| UL -> Trait | Waist-to-hip ratio    id:i eu-a-72      | IVW      | 19               | beta                  | -0.0001         | -0.0344 | 0.0342 | 0.9946 | 0.9946           | 0.0016                     |                 |                         |
| UL -> Trait | Waist-to-hip ratio    id:i eu-a-72      | MR Egger | 19               | beta                  | -0.0695         | -0.2096 | 0.0705 | 0.3443 |                  | 0.0021                     | 0.0075          | 0.3306                  |
| Trait -> UL | Whole body fat mass    id:ukb-b-19393   | IVW      | 387              | OR                    | 1.04            | 0.94    | 1.14   | 0.4634 | 0.7120           | 5.68E-05                   |                 |                         |
| Trait -> UL | Whole body fat mass    id:ukb-b-19393   | MR Egger | 387              | OR                    | 1.17            | 0.90    | 1.52   | 0.2382 |                  | 5.77E-05                   | -0.0023         | 0.3258                  |
| UL -> Trait | Whole body fat mass    id:ukb-b-19393   | IVW      | 26               | beta                  | 0.0056          | -0.0099 | 0.0210 | 0.4806 | 0.7120           | 1.41E-10                   |                 |                         |
| UL -> Trait | Whole body fat mass    id:ukb-b-19393   | MR Egger | 26               | beta                  | 0.0242          | -0.0023 | 0.0507 | 0.0862 |                  | 3.41E-09                   | -0.0031         | 0.1084                  |



| <b>Direction</b> | <b>Trait</b>                               | <b>Method</b> | <b>N<sub>SNP</sub></b> | <b>Causal estimate scale</b> | <b>Causal estimate</b> | <b>CI95L</b> | <b>CI95U</b> | <b>P</b> | <b>P<sub>FDR</sub></b> | <b>P<sub>heterogeneity</sub></b> | <b>Egger intercept</b> | <b>P<sub>pleiotropy</sub></b> |
|------------------|--|---------------|------------------------|------------------------------|------------------------|--------------|--------------|----------|------------------------|----------------------------------|------------------------|-------------------------------|
| Trait -> UL      | Whole body fat-free mass    id:ukb-b-13354 | IVW           | 486                    | OR                           | 1.24                   | 1.08         | 1.42         | 0.0024   | 0.0205                 | 6.68E-33                         |                        |                               |
| Trait -> UL      | Whole body fat-free mass    id:ukb-b-13354 | MR Egger      | 486                    | OR                           | 1.40                   | 1.01         | 1.93         | 0.0422   |                        | 6.53E-33                         | -0.0018                | 0.4187                        |
| UL -> Trait      | Whole body fat-free mass    id:ukb-b-13354 | IVW           | 26                     | beta                         | 0.0203                 | 0.0014       | 0.0392       | 0.0353   | 0.1070                 | 7.97E-62                         |                        |                               |
| UL -> Trait      | Whole body fat-free mass    id:ukb-b-13354 | MR Egger      | 26                     | beta                         | 0.0383                 | 0.0052       | 0.0715       | 0.0328   |                        | 1.26E-57                         | -0.0030                | 0.2097                        |
| Trait -> UL      | Whole body water mass    id:ukb-b-14540    | IVW           | 500                    | OR                           | 1.22                   | 1.06         | 1.40         | 0.0058   | 0.0334                 | 3.19E-35                         |                        |                               |
| Trait -> UL      | Whole body water mass    id:ukb-b-14540    | MR Egger      | 500                    | OR                           | 1.33                   | 0.97         | 1.84         | 0.0814   |                        | 2.74E-35                         | -0.0014                | 0.5321                        |
| UL -> Trait      | Whole body water mass    id:ukb-b-14540    | IVW           | 26                     | beta                         | 0.0204                 | 0.0013       | 0.0396       | 0.0367   | 0.1070                 | 1.13E-63                         |                        |                               |
| UL -> Trait      | Whole body water mass    id:ukb-b-14540    | MR Egger      | 26                     | beta                         | 0.0387                 | 0.0050       | 0.0723       | 0.0336   |                        | 2.24E-59                         | -0.0030                | 0.2108                        |

**Table S13. Results of multivariable MR.**

The multivariable effects of whole-body fat-free mass, whole-body fat mass, and estradiol level on the risk of uterine leiomyomata (UL) were evaluated using TwoSampleMR R library<sup>12</sup>. We extracted genetic instruments for UL from the GWAS results obtained in FinnGen, for whole-body fat-free mass and fat mass from the UKBB as provided by the MRC IEU and integrated in TwoSampleMR, and for estradiol from a study by Ruth *et al*<sup>13</sup>. LD pruning was completed using European population reference, threshold of  $r^2=0.001$ , and clumping window of 10 kb.

| <b>exposure</b>                            | <b>outcome</b>      | <b>n<sub>snp</sub></b> | <b>b</b> | <b>se</b> | <b>pval</b> |
|--|---------------------|------------------------|----------|-----------|-------------|
| Estradiol                                  | Uterine leiomyomata | 13                     | 0.616    | 0.520     | 0.235       |
| Whole body fat-free mass    id:ukb-b-13354 | Uterine leiomyomata | 415                    | 0.271    | 0.114     | 0.018       |
| Whole body fat mass    id:ukb-b-19393      | Uterine leiomyomata | 207                    | -0.061   | 0.106     | 0.567       |

**Table S14. Results of outlier-corrected MR-PRESSO.**

We derived causal estimates using outlier-corrected MR-PRESSO<sup>14</sup> for the traits showing a significant IVW-based causal effect on the risk of uterine leiomyomata. As in the primary analyses, we extracted genetic instruments from the GWAS completed in FinnGen and for other traits from the MRC-IEU database. Also, to ensure comparability and the usage of the same genetic instruments, LD pruning was completed as previously, *i.e.*, using European population reference, threshold of  $r^2=0.001$ , and clumping window of 10 kb. The analysis was considered exploratory and no multiple testing correction was applied.

| <b>Causal Estimate</b> | <b>Sd</b> | <b>T-stat</b> | <b>P-value</b> | <b>pheno</b>         | <b>id.exposure</b> |
|------------------------|-----------|---------------|----------------|----------------------|--------------------|
| 0.1634                 | 0.0548    | 2.9802        | 0.0030         | Basal metabolic rate | ukb-b-16446        |
| 0.1143                 | 0.0430    | 2.6599        | 0.0081         | BMI                  | ukb-b-19953        |
| 0.0112                 | 0.0045    | 2.5060        | 0.0126         | Diastolic BP         | ieu-b-39           |
| 0.1685                 | 0.0553    | 3.0460        | 0.0024         | Fat-free mass        | ukb-b-13354        |
| -0.1244                | 0.0394    | -3.1564       | 0.0018         | HDL-C                | ieu-b-109          |
| -0.1610                | 0.0524    | -3.0729       | 0.0022         | Impedance            | ukb-b-19921        |
| 0.1870                 | 0.0581    | 3.2209        | 0.0014         | Waist circumference  | ukb-b-9405         |
| 0.1409                 | 0.0562    | 2.5085        | 0.0124         | Water mass           | ukb-b-14540        |

**Table S15. Results of MRMix.**

We derived causal estimates using MRMix<sup>15</sup> method for the traits showing a significant IVW-based causal effect on the risk of uterine leiomyomata. As in the primary analyses, we extracted genetic instruments from the GWAS completed in FinnGen and for other traits from the MRC-IEU database. Also, to ensure comparability and the usage of the same genetic instruments, LD pruning was completed as previously, *i.e.*, using European population reference, threshold of  $r^2=0.001$ , and clumping window of 10 kb. The analysis was considered exploratory and no multiple testing correction was applied.

| <b>theta</b> | <b>setheta</b> | <b>p</b> | <b>trait</b>         | <b>Id.exposure</b> |
|--------------|----------------|----------|----------------------|--------------------|
| 0.11         | 0.089          | 0.217    | Basal metabolic rate | ukb-b-16446        |
| 0.11         | 0.067          | 0.101    | BMI                  | ukb-b-19953        |
| 0.08         | 0.110          | 0.468    | Diastolic BP         | ieu-b-39           |
| 0.13         | 0.111          | 0.240    | Fat-free mass        | ukb-b-13354        |
| -0.12        | 0.054          | 0.027    | HDL-C                | ieu-b-109          |
| -0.13        | 0.108          | 0.227    | Impedance            | ukb-b-19921        |
| 0.12         | 0.094          | 0.200    | Waist circumference  | ukb-b-9405         |
| 0.13         | 0.090          | 0.149    | Water mass           | ukb-b-14540        |

## Supplementary References

1. Gallagher, C. S. *et al.* Genome-wide association and epidemiological analyses reveal common genetic origins between uterine leiomyomata and endometriosis. *Nat. Commun.* **10**, 1–11 (2019).
2. Bulik-Sullivan, B. *et al.* LD score regression distinguishes confounding from polygenicity in genome-wide association studies. *Nat. Genet.* **47**, 291–295 (2015).
3. Lonsdale, J. *et al.* The Genotype-Tissue Expression (GTEx) project. *Nat. Genet.* **45**, 580–5 (2013).
4. de Leeuw, C. A., Mooij, J. M., Heskes, T. & Posthuma, D. MAGMA: Generalized Gene-Set Analysis of GWAS Data. *PLoS Comput. Biol.* **11**, 1–19 (2015).
5. Watanabe, K., Taskesen, E., Van Bochoven, A. & Posthuma, D. Functional mapping and annotation of genetic associations with FUMA. *Nat. Commun.* **8**, 1–11 (2017).
6. Benner, C. *et al.* Prospects of Fine-Mapping Trait-Associated Genomic Regions by Using Summary Statistics from Genome-wide Association Studies. *Am. J. Hum. Genet.* **101**, 539–551 (2017).
7. Wang, G., Sarkar, A., Carbonetto, P. & Stephens, M. A simple new approach to variable selection in regression, with application to genetic fine mapping. *J. R. Stat. Soc. Ser. B Stat. Methodol.* **82**, 1273–1300 (2020).
8. Liberzon, A. *et al.* Molecular signatures database (MSigDB) 3.0. *Bioinformatics* **27**, 1739–1740 (2011).
9. Giambartolomei, C. *et al.* Bayesian Test for Colocalisation between Pairs of Genetic Association Studies Using Summary Statistics. *PLoS Genet.* **10**, (2014).
10. Zhu, Z. *et al.* Integration of summary data from GWAS and eQTL studies predicts complex trait gene targets. *Nat. Genet.* **48**, 481–487 (2016).
11. Cuellar-Partida, G. *et al.* Complex-Traits Genetics Virtual Lab: A community-driven web platform for post-GWAS analyses. *bioRxiv* 518027 (2019). doi:10.1101/518027
12. Hemani, G. *et al.* The MR-base platform supports systematic causal inference across the human phenome. *Elife* **7**, 1–29 (2018).
13. Ruth, K. S. *et al.* Using human genetics to understand the disease impacts of testosterone in men and women. *Nat. Med.* **26**, 252–258 (2020).
14. Verbanck, M., Chen, C. Y., Neale, B. & Do, R. Detection of widespread horizontal pleiotropy in causal relationships inferred from Mendelian randomization between complex traits and diseases. *Nat. Genet.* **50**, 693–698 (2018).
15. Qi, G. & Chatterjee, N. Mendelian randomization analysis using mixture models for robust and efficient estimation of causal effects. *Nat. Commun.* **10**, 1–10 (2019).